OFFICE OF CIVILIAN RADIOACTIVE WASTE MANAGEMENT
SPECIAL INSTRUCTION SHEET

1. QA: QA

Complete Only Applicable Items

This is a placeholder page for records that cannot be scanned.

2. Record Date	3. Accession Number
09/28/2001	MOL.20011017.0092
4. Author Name(s)	**5. Author Organization**
HORIA R. RADULESCU	N/A

6. Title/Description
EVALUATION OF CODISPOSAL VIABILITY FOR TH/U CARBIDE (FORT SAINT VRAIN HTGR) DOE-OWNED FUEL

7. Document Number(s)	8. Version Designator
TDR-EDC-NU-000007	REV. 00
9. Document Type	**10. Medium**
REPORT	OPTIC/PAPER

11. Access Control Code
PUB

12. Traceability Designator
DC# 28745

13. Comments
THIS IS A ONE-OF-A-KIND DOCUMENT DUE TO THE COLORED GRAPHS ENCLOSED AND CAN BE LOCATED THROUGH THE RPC.

QA: QA

TDR-EDC-NU-000007 REV 00

September 2001

Evaluation of Codisposal Viability for Th/U Carbide (Fort Saint Vrain HTGR) DOE-Owned Fuel

By

Horia R. Radulescu

Prepared for:
U.S. Department of Energy
Yucca Mountain Site Characterization Office
P.O. Box 30307
North Las Vegas, Nevada 89036-0307

Prepared by:
Bechtel SAIC Company, LLC
1180 Town Center Drive
Las Vegas, Nevada 89144

Under Contract Number
DE-AC08-01RW12101

DISCLAIMER

This report was prepared as an account of work sponsored by an agency of the United States Government. Neither the United States Government nor any agency thereof, nor any of their employees, nor any of their contractors, subcontractors or their employees, makes any warranty, express or implied, or assumes any legal liability or responsibility for the accuracy, completeness, or any third party's use or the results of such use of any information, apparatus, product, or process disclosed, or represents that its use would not infringe privately owned rights. Reference herein to any specific commercial product, process, or service by trade name, trademark, manufacturer, or otherwise, does not necessarily constitute or imply its endorsement, recommendation, or favoring by the United States Government or any agency thereof or its contractors or subcontractors. The views and opinions of authors expressed herein do not necessarily state or reflect those of the United States Government or any agency thereof.

Bechtel SAIC Company, LLC

Evaluation of Codisposal Viability for Th/U Carbide (Fort Saint Vrain HTGR) DOE-Owned Fuel

TDR-EDC-NU-000007 REV 00

September 2001

Prepared by:

Horia R. Radulescu — Date 09/28/2001

Horia R. Radulescu
Waste Package Criticality

Checked by:

S.F. Alex Deng (Technical Checker) — Date 09/28/01
Waste Package Criticality

John M. Scaglione (Compliance Checker) — Date 9/28/01
Waste Package Criticality

Approved by:

Abdelhalim A. Alsaed, Lead — Date 9/28/2001
Waste Package Criticality

Daniel Thomas, Manager — Date 09/28/2001
Waste Package Criticality

David Rhodes, Manager — Date 9/29/01
DOE SNF

HISTORY OF CHANGE

Revision Number	Description of Change
00	Initial Issue

INTENTIONALLY LEFT BLANK

EXECUTIVE SUMMARY

INTRODUCTION

There are more than 250 forms of U.S. Department of Energy (DOE)-owned spent nuclear fuel (SNF). Due to the variety of the spent nuclear fuel, the National Spent Nuclear Fuel Program has designated nine representative fuel groups for disposal criticality analyses based on fuel matrix, primary fissile isotope, and enrichment. The Fort Saint Vrain reactor (FSVR) SNF has been designated as the representative fuel for the Th/U carbide fuel group. The FSVR SNF consists of small particles (spheres of the order of 0.5-mm diameter) of thorium carbide or thorium and high-enriched uranium carbide mixture, coated with multiple, thin layers of pyrolytic carbon and silicon carbide, which serve as miniature pressure vessels to contain fission products and the U/Th carbide matrix. The coated particles are bound in a carbonized matrix, which forms fuel rods or "compacts" that are loaded into large hexagonal graphite prisms. The graphite prisms (or blocks) are the physical forms that are handled in reactor loading and unloading operations, and which will be loaded into the DOE standardized SNF canisters. The results of the analyses performed will be used to develop waste acceptance criteria. The items that are important to criticality control are identified based on the analysis needs and result sensitivities. Prior to acceptance of fuel from the Th/U carbide fuel group for disposal, the important items for the fuel types that are being considered for disposal under the Th/U carbide fuel group must be demonstrated to satisfy the conditions determined in this report.

The analyses have been performed by following the methodology documented in the *Disposal Criticality Analysis Methodology Topical Report* and submitted to the U.S. Nuclear Regulatory Commission for approval. The methodology includes analyzing the geochemical and environmental processes that can breach the waste package (WP) and degrade the waste forms and other internal components, as well as the structural, thermal, shielding, and intact and degraded component criticality analyses. One or more addenda (validation reports) to the topical report will be required to establish the critical limit for DOE SNF once sufficient critical benchmarks are identified and verified. The WP design for FSVR SNF holds one 18-in.-outer diameter DOE standardized SNF canister containing the FSVR SNF, and five defense high-level radioactive waste (DHLW) glass canisters.

The DOE SNF canisters will be available in two lengths (internal cavity lengths of 2.540 m and 4.115 m) and two outer diameters (45.72 cm [18.0 in.] and 60.96 cm [24.0 in.]). Canisters of the smaller diameter are just large enough to accommodate the FSVR hexagonal fuel elements and, still provide a radial gap of approximately 1.1 cm. This characteristic recommends the 45.72-cm- (18-in.-) outer diameter DOE SNF canisters as the appropriate choice for the disposal of FSVR SNF. The 2.54-m-long (known also as 10-ft total length) DOE SNF canister can accommodate three stacked FSVR SNF blocks, whereas the 4.115-m-long (15-ft total length) canister can accommodate five stacked blocks. The use and modeling of the longer DOE SNF canister is bounding for all analyses, therefore this design is used in all analyses presented in this document. The 5-DHLW/DOE SNF-long WP is the design option that can accommodate the 4.115-m-long DOE SNF canister, and is therefore used in this document.

The 5-DHLW/DOE SNF-long WP design consists of two concentric cylindrical shells in which the waste forms will be placed. The outer shell is made of a corrosion resistant nickel-based

alloy (Alloy 22). The inner shell is composed of stainless steel (SS) 316 NG (nuclear grade). The WP design incorporates three lids at the one end of the WP (one for the inner shell and two for the outer shell) and two lids at the other end of the WP (one for each shell). This configuration represents the Site Recommendation design for WPs.

The DOE SNF canister containing five FSVR fuel elements is placed in a carbon steel support tube that becomes the center of the WP (see Figure ES-1). The DOE SNF canister is surrounded by five 4.5-meter-long Hanford DHLW glass canisters. The five DHLW glass canisters are evenly spaced around the DOE SNF canister.

This report presents the results of analyzing the 5-DHLW/DOE SNF-long WP (Figure ES-1) against various design criteria. Section 2.2 provides the criteria, and Section 2.3 provides the key assumptions for the various analyses.

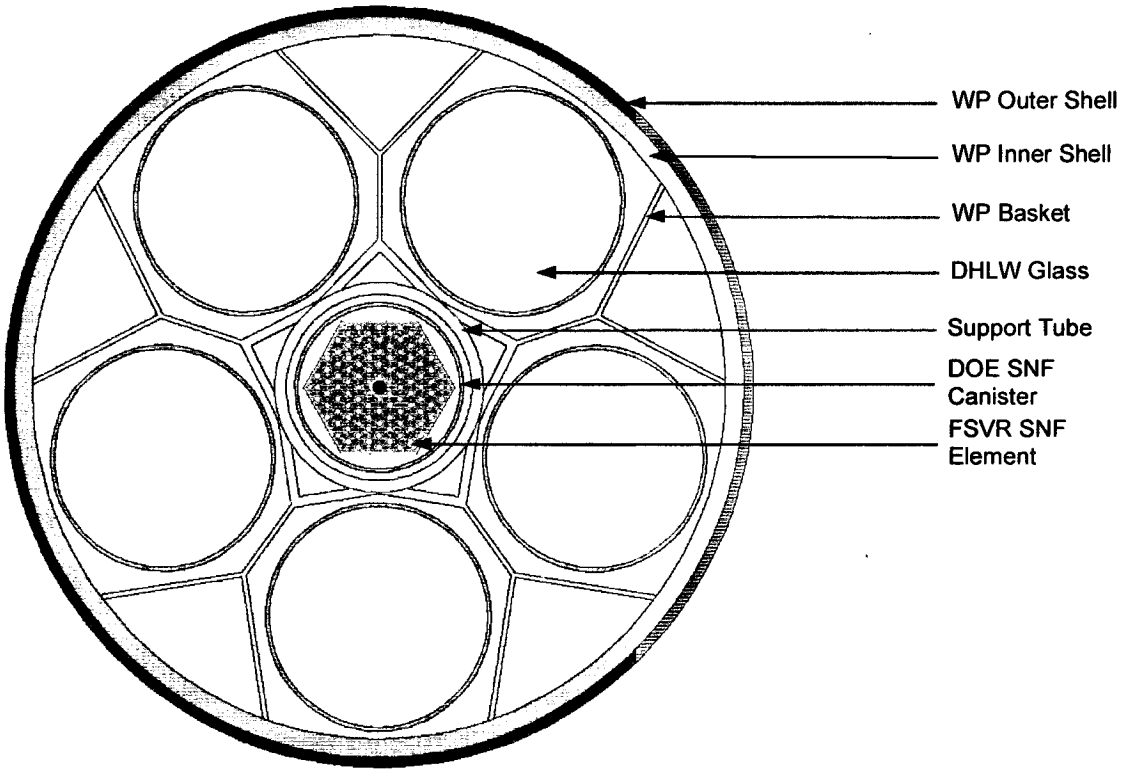

Figure ES-1. Cross-section View of the 5-DHLW/DOE SNF-long WP in an as-Loaded Condition

STRUCTURAL ANALYSIS

ANSYS Version 5.6.2 and LS-DYNA V950 – finite element analysis computer codes – were used for the structural analysis of the 5-DHLW/DOE SNF-long WP. A three-dimensional (3-D) finite element representation of this 5-DHLW/DOE-long WP was developed to determine the effects of loads on the WP structural components (inner and outer shells) due to a WP tip over design-basis event. The analysis considered the DOE SNF canister loaded with five FSVR standard fuel elements (which is the configuration with the maximum total mass of the DOE SNF canister loaded with FSVR fuel), and the maximum total mass for each DHLW glass canister (4,200 kg). The tip over event is known to be bounding for all WP handling accident

scenarios. The calculated stress intensities in both the inner and outer WP shells is less than the containment structure allowable stress limit. Hence, there would be no failure of the WP shells in the event of a tip over.

THERMAL ANALYSIS

The solution method employed was finite element analysis. A two-dimensional (2-D) finite element representation of a 5-DHLW/DOE-long WP in the repository was developed and solved using the thermal analysis capabilities of ANSYS Version 5.4. Version 5.4 was used because Version 5.6.2 could not be used for times past 60 years from WP emplacement in the monitored geologic repository.

The results indicate that the maximum DHLW glass temperature for the 5-DHLW/DOE SNF-long WP containing FSVR SNF is 167.4 °C (reached 59 years after emplacement), which is less than the System Description Document (SDD) criterion of 400 °C. The maximum temperature in the FSVR SNF element is 173.8 °C, reached at 59 years after emplacement. The maximum thermal output of the 5-DHLW/DOE SNF-long WP loaded with FSVR SNF is 1,037 W, which is less than the SDD criterion of 11,800 W.

SHIELDING ANALYSIS

The Monte Carlo particle transport code, MCNP Version 4B2LV, was used to calculate the average dose rates on the surfaces of the WP. Dose rate calculations were performed for a WP that contains five 4.5-m-long DHLW glass canisters and one DOE SNF canister loaded with FSVR SNF.

The maximum dose rate at the external surfaces of the WP is 101.97 rem/h (99.30 + two standard deviations). This value has been obtained on a segment of the radial surface adjacent to a DHLW glass canister. The maximum dose rate on the outer surfaces of the WP is more than one order of magnitude lower than the imposed limit of 1,450 rem/h. The neutron dose rates represent less than 0.2% of the gamma dose rates. Therefore, the gamma dose rates dominate the total dose rates.

DEGRADATION AND GEOCHEMISTRY ANALYSIS

The degradation analyses follow the general methodology developed for application to all waste forms containing fissile material. This methodology evaluates potential critical configurations from the intact WP (geometrically intact components in a breached WP assumed to be flooded with water as a moderator) through the completely degraded WP. The WP design is used as the starting point for the intact configuration. Sequences of events and/or processes of component degradation were developed. Standard scenarios from the master scenario list in the *Disposal Criticality Analysis Methodology Topical Report* were refined to develop degraded configurations using unique fuel characteristics. Potentially critical configurations were identified for further analysis.

The report titled *Generic Degradation Scenario and Configuration Analysis for DOE Codisposal Waste Package* serves as the basis for the specific degraded WP criticality analysis to be

performed for any type of DOE SNF that will be codisposed with the high-level radioactive waste in a codisposal WP. Starting from these guidelines, a set of degradation scenarios and resultant configurations has been developed for the codisposal WP with a DOE standardized SNF canister containing FSVR SNF.

The geochemistry analyses were performed using the EQ3/6 Version 7.2bLV geochemistry software package in the solid-centered flow-through mode. A principle objective of the geochemistry analysis was to estimate the chemical composition of the degradation products remaining in a WP containing FSVR SNF and DHLW glass. Particular emphasis was placed on the determination of the concentration of fissile material. The fissile material of concern was primarily U-235, and all the cases considered had only fresh fuel composition, which has the highest concentration of this isotope. Another objective was the assessment of the chemical circumstances that could lead to removal of Th, which is the main neutron absorber material, from the WP, while the fissile material (U-235) remains behind. Such circumstances could increase the potential of a nuclear criticality occurrence within the WP. Water with the composition of J-13 well water is assumed to drip in through an opening at the top of the WP, pooling inside and eventually overflowing, allowing soluble components to be removed through continual dilution. Twenty-seven EQ6 reaction path calculations were carried out to span the range of possible system behavior and to assess the specific and coupled effects of SNF degradation, steel corrosion, DHLW glass degradation, and fluid influx rate on U and Th mobilization. Corrosion product accumulation was examined as well. The results were used as inputs to the criticality calculations.

INTACT AND DEGRADED COMPONENT CRITICALITY ANALYSES

The criticality analyses considered all aspects of intact and degraded configurations of the codisposal WP containing FSVR SNF, including optimum moderation conditions, optimum reflection, geometry, and composition. The results of the 3-D Monte Carlo criticality calculations for all anticipated intact- and degraded-mode configurations developed through the degradation analysis, and which are physically possible, show that the requirement of $k_{eff}+2\sigma$ values less than or equal to the interim critical limit of 0.93 is satisfied. No neutron absorber material is required as long as the U-235 mass for codisposal is within the specified limit.

The highest k_{eff} values resulted from the configurations assuming that approximately 10% of the fuel contained in the compacts inside the FSVR fuel elements is degraded and leaves the compacts, while the DOE SNF canister is still intact. However, these configurations are not credible due to the fact that the carbonaceous matrix of the fuel compacts is similar to graphite with respect to degradation, therefore chemically inert, and there is no known degradation mechanism that can remove 10% or more of the fuel particles from the compacts.

CONCLUSIONS

The structural, thermal and shielding design criteria are met for a WP containing five DHLW glass canisters and one DOE SNF canister loaded with FSVR SNF. Each WP falls below the interim critical limit of 0.93 without any neutron absorber present in the DOE SNF canister. With this design, there will be approximately 442 DOE SNF canisters that will be loaded with FSVR SNF, which corresponds to 442 WPs.

CONTENTS

CONTENTS (Continued)

Page

CONTENTS (Continued)

Page

INTENTIONALLY LEFT BLANK

FIGURES

Page

FIGURES (Continued)

Page

TABLES

TABLES (Continued)

Page

ACRONYMS AND ABBREVIATIONS

AP	administrative procedure
ASME	American Society of Mechanical Engineers
ASTM	American Society for Testing and Materials
BPVC	Boiler and Pressure Vessel Code
BSC	Bechtel SAIC Company, LLC
BOL	beginning of life
CRWMS	Civilian Radioactive Waste Management System
DHLW	defense high-level radioactive waste
DOE	U.S. Department of Energy
DTN	Data Tracking Number
EOL	end of life
FSVR	Fort Saint Vrain Reactor
HTGR	High Temperature Gas Reactor
k_{eff}	effective neutron multiplication factor
M&O	Management and Operating Contractor
NG	nuclear grade
OIC	other internal components
OD	outer diameter
QARD	Quality Assurance Requirements and Description
SDD	System Description Document
SNF	spent nuclear fuel
SRS	Savannah River Site
SS	stainless steel
UNS	Unified Numbering System
vol%	volume %
WP	waste package
wt%	weight %
YMP	Yucca Mountain Project

INTENTIONALLY LEFT BLANK

1. INTRODUCTION AND BACKGROUND

There are more than 250 forms of U.S. Department of Energy (DOE)-owned spent nuclear fuels (SNF). Due to the variety of the spent nuclear fuel, the National Spent Nuclear Fuel Program has designated nine representative fuel groups for disposal criticality analyses based on fuel matrix, primary fissile isotope, and enrichment. The Fort Saint Vrain reactor (FSVR) fuel form has been designated as the representative fuel (DOE 2000b, Section 6.6.6) for the Th/U carbide fuel group. Demonstration that other fuels in this group are bounded by the FSVR SNF analysis remains to be completed before acceptance of these fuel forms. As part of the criticality licensing strategy, the National Spent Nuclear Fuel Program has provided a data report (DOE 2001) for the representative fuel type. The results of the analyses performed by using the information from this data report will be used to develop waste acceptance criteria which must be met by all fuel forms within the Th/U carbide fuel group. The items that are important to criticality control are identified based on analysis needs and result sensitivities. Prior to acceptance of the fuel from the Th/U carbide fuel group for disposal, the important items of the fuel types that are being considered for disposal under the Th/U carbide fuel group must be demonstrated to satisfy the conditions set in Section 8.6, Items Important to Criticality Control and Acceptance.

The Atomic Energy Commission, the predecessor of the Department of Energy (DOE), contracted with power companies and with Gulf General Atomics to jointly develop the commercial high temperature gas reactors (HTGR). These HTGRs were based on the thorium fuel cycle in which fissile U-233 is produced from Th-232 "fertile" material. Most of the stored carbide fuels came from two reactors, Peach Bottom 1 and Fort Saint Vrain. All spent fuel discharged prior to December 31, 1988, is located at Idaho Nuclear Technology and Engineering Center. Fuel removed from the FSVR core in 1989 and 1990 remains on-site at Fort Saint Vrain in temporary storage.

The Fort Saint Vrain HTGR (located in Platteville, Colorado) operated from 1974 to 1989, and was the nation's only commercial reactor of this type. The coolant gas was helium. The reactor had a rated power of 842 MW(t), but ran well below that rating for much of its lifetime. The plant had a net capacity of 330 MW. The core consisted of 1,482 hexagonal fuel elements stacked in six layers. The initial core contained 774 kg of uranium at 93.5 % enrichment and 15,905 kg of thorium (Taylor 2001, p. 8).

The criticality analyses have been performed according to the *Disposal Criticality Analysis Methodology Topical Report* (YMP 2000), which has been submitted to the U.S. Nuclear Regulatory Commission for approval. The methodology includes analyzing the geochemical and environmental processes that can breach the WP and degrade the waste forms as well as the intact and degraded component criticality analyses. Addenda to the topical report will be required to establish the critical limit for the DOE SNF types once sufficient critical benchmarks are identified and verified. In this report, a conservative and simplified bounding approach is employed to designate an interim critical limit.

This report also provides the bounding structural, thermal, and shielding analyses of the WP to ensure that the repository waste acceptance criteria have been met.

In this technical report, there are numerous references to "codisposal container" and "waste package." Since the use of these two terms may be confusing, a definition of the terms is included here:

"Codisposal container" is defined as the container shells, spacing structures and baskets, shielding integral to the container, packing contained within the container, and other absorbent materials designed to be placed internal to the container or immediately surrounding the disposal container (i.e., attached to the outer surface of the disposal container). The disposal container is designed to contain SNF and high-level radioactive waste, but exists only until the outer weld is complete and accepted. The disposal container does not include the waste form or the encasing containers or canisters (e.g., DHLW glass pour canisters, DOE SNF codisposal canisters, multi-canister overpacks, etc.).

"Waste package" is defined as the waste form and any containers (i.e., disposal container shells and other canisters), spacing structures or baskets, shielding integral to the container, packing contained within the container, and other absorbent materials immediately surrounding an individual waste container placed internally to the container or attached to the outer surface of the disposal container. The WP begins its existence when the outer lid weld of the disposal container is complete and accepted.

1.1 OBJECTIVE

The objective of this technical report is to provide sufficient detail in the areas of structural, thermal, shielding and criticality to establish the technical viability for disposing of Th/U carbide (FSVR) SNF in the potential monitored geologic repository at Yucca Mountain. This report sets limits and establishes values that a specific fuel type under the Th/U carbide fuel group must meet to be bounded by the results reported in this technical report.

1.2 SCOPE

This technical report summarizes and analyzes the results of the detailed calculations that were performed in evaluating the codisposal viability of Th/U carbide (FSVR) SNF. These calculation documents and the sections of this technical report in which they are summarized and analyzed are shown in Table 1-1. The information provided by the sketches appended to this technical report (Appendix A) is that of the potential design for the type of WP considered in the detailed calculations supporting this technical report.

Table 1-1. List of Supporting Documents

Discipline	Document Title	Summarized/ Analyzed in	Reference
Structural	*Tip-Over of the 5 DHLW/DOE SNF - Long Waste Package Containing Fort Saint Vrain HTGR Fuel onto an Unyielding Surface*	Section 3	BSC (2001a)
Thermal	*Thermal Evaluation of the Fort Saint Vrain Codisposal Waste Package*	Section 4	BSC (2001b)
Shielding	*Dose Rate Calculation for the Codisposal Waste Package of HLW Glass and the FSVR Fuel*	Section 5	BSC (2001c)
Degradation and Geochemistry	*EQ6 Calculation for Chemical Degradation of Fort St. Vrain (Th/U carbide) Waste Packages*	Section 6	BSC (2001d)
Intact and Degraded Mode Criticality	*Intact and Degraded Mode Criticality Calculations for the Codisposal of Fort Saint Vrain Spent Nuclear Fuel in a Waste Package*	Section 7	BSC (2001e)

1.3 QUALITY ASSURANCE

The activity evaluation (Addendum A of the *Technical Work Plan,* CRWMS M&O 2000i) concluded that the development of this report is subject to the United States Department of Energy OCRWM *Quality Assurance Requirements and Description* (QARD) (DOE 2000a) controls. The information provided in this report is to be indirectly used in the evaluation of the codisposal viability of Th/U carbide fuel.

Although scientific and engineering software or computational software was used for the input calculations, none was directly used in the development of this report. Electronic management of data was accomplished in accordance with the controls specified in the *Technical Work Plan* (CRWMS M&O 2000i).

The work that is to be performed to support the License Application using this information will be performed in accordance with the then current versions of the QARD and NRC regulations. All information used for the License Application will be developed in accordance with the QARD and NRC regulations, or will be from acceptable sources.

This technical report is based in part on unqualified data. However, the unqualified data is only used to determine the bounding values and items that are important to criticality control for the fuel group by establishing the limits based on the representative fuel type (FSVR SNF) for this group (Th/U carbide). Hence, the input values used for evaluation of codisposal viability of Th/U carbide (FSVR) SNF do not constitute data that have to be qualified in this application. They merely establish the bounds for acceptance (Assumption 2.3.6.1). Since the input values are not relied upon directly to address safety and waste isolation issues, and since the design inputs do not affect a system characteristic that is critical for satisfactory performance, according to the governing administrative procedure (AP-3.11Q, *Technical Reports*), the data do not need to be controlled as to-be-verified (AP-3.15Q, *Managing Technical Product Inputs*). However, prior to acceptance of the fuel for disposal, the items that are identified as important to criticality control and acceptance in Section 8.6 must be qualified by any means identified in the *Quality Assurance Requirements and Description* document (DOE 2000a) (e.g., experiment, non-destructive test, chemical assay, qualification under a program subject to the QARD requirements).

INTENTIONALLY LEFT BLANK

2. DESIGN INPUTS

The number of digits in the values cited herein may be the result of a calculation or may reflect the input from another source; consequently, the number of digits should not be interpreted as an indication of accuracy. In the following tables, three to four digits after the decimal place have been retained to reduce the round-off errors in subsequent calculations.

2.1 DESIGN PARAMETERS

Each of the following subsections either describes the design of the WP or identifies the basis of major parameters.

2.1.1 Codisposal WP

The codisposal WP for FSVR SNF contains five DHLW glass canisters and one DOE SNF canister loaded with five FSVR SNF elements. The 5-DHLW/DOE SNF-long WP design that is referred to as the Site Recommendation design (CRWMS M&O 2000b, p. 29 and Attachment V; see Appendix A). The shell materials of the WP are typical of those used for commercial SNF WP. The WP design consists of two concentric cylindrical shells. The inner shell is a 50.0-mm-thick cylinder of stainless steel (SS) 316 NG (nuclear grade; identified as SA-240 in Appendix A). The outer shell is composed of 25.0-mm-thick high-nickel alloy ASTM B 575 (Alloy 22) and its outer diameter (OD) is 2,030.0 mm. The length of WP's inside cavity is 4,617.0 mm (Appendix A, p. A-1), which is designed to accommodate five 4.5-m- (15-ft-) long Hanford DHLW glass canisters. The lid of the inner shell is 105.0-mm thick. The outer shell flat bottom lid is 25.0-mm thick and the outer shell flat closure lid is 10.0-mm thick. Table 2-1 summarizes the dimensions and materials of the WP.

Table 2-1. Codisposal WP Dimensions and Material Specifications

Component	Material	Parameter	Dimension (mm)
Outer barrier shell	ASTM B 575 (Alloy 22)	Thickness	25.0
		Outer diameter	2,030.0
Inner barrier shell	SS 316 NG (SA-240)	Thickness	50.0
		Inner length	4,617.0
Top and bottom outer barrier lids	ASTM B 575 (Alloy 22)	Thickness	25.0
Closure lid (only at the top)	ASTM B 575 (Alloy 22)	Thickness	10.0
Top and bottom inner barrier lids	SS 316 NG (SA-240)	Thickness	105.0
Gap between the top inner and closure lids	Air	Thickness	30.0
Gap between the top outer and closure lids	Air	Thickness	30.0
Gap between the bottom inner and outer lids	Air	Thickness	70.0
Support tube	ASTM A 516 Grade 70	Outer diameter	565.0
		Inner diameter	501.5
		Length	4,607.0

Source: CRWMS M&O 2000b, Attachment V.

The DOE SNF canister is placed in a 31.8-mm-thick carbon steel (ASTM A 516 Grade 70) support tube with a nominal outer diameter of 565.0 mm. The support tube is connected to the inside wall of the WP by a web-like structure of carbon steel (ASTM A 516 Grade 70) basket

plates to support five long DHLW glass canisters, as shown in Figure 2-1. The support tube and the plates are 4,607.0-mm long.

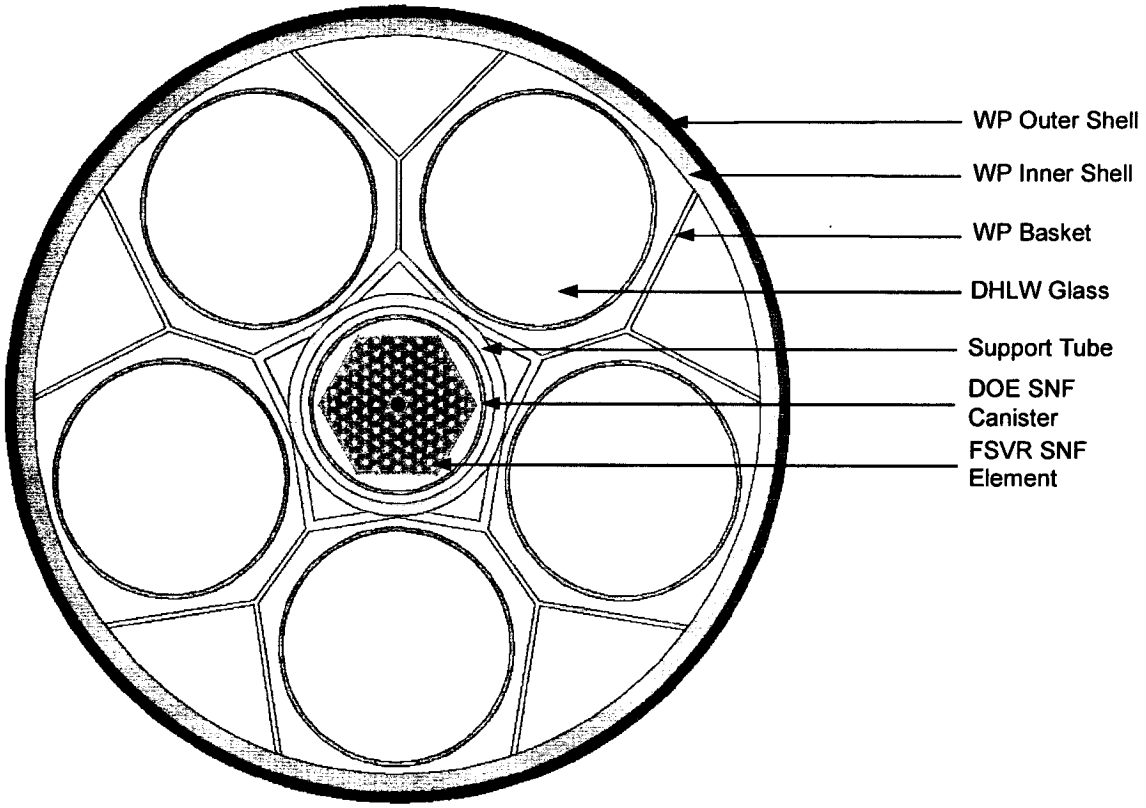

Figure 2-1. Cross-section View of the 5-DHLW/DOE WP in an as-Loaded Condition

2.1.2 High-Level Radioactive Waste Glass Pour Canisters

There is no long Savannah River Site (SRS) DHLW glass canister. Therefore, the Hanford 4.5-m- (15-ft-) long DHLW glass canister (Figure 2-2) is used in the FSVR WP. Since the composition of the Hanford DHLW glass has not yet been specified, it has been assumed to be the same as the SRS DHLW glass (see Assumption 2.3.6.2). The Hanford DHLW glass canister is a 4,572.0-mm-long cylindrical SS (Type 304L) shell with an OD of 610.0 mm (24.0 in.) (BSC 2001f, Table 1) and a wall thickness of 10.5 mm (Taylor 1997). The maximum loaded canister mass is 4,200 kg (BSC 2001f, Table 1) and the fill volume is 87% (Taylor 1997). The nominal dimensions of the canister were used for the analyses. The geometry and material specifications for DHLW glass canisters are given in Table 2-2.

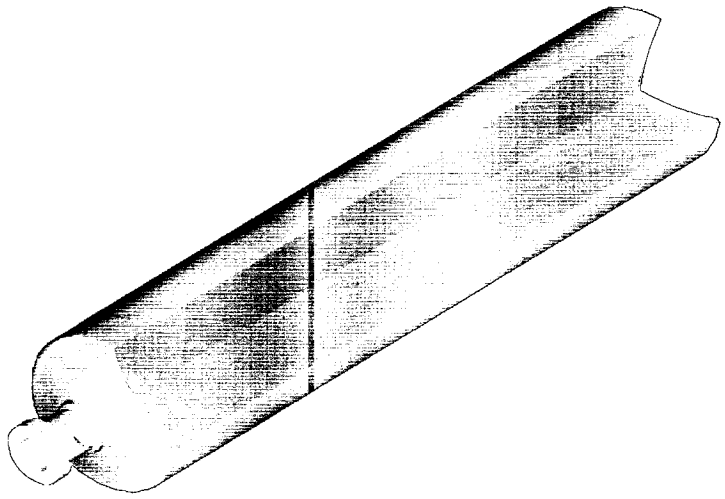

Figure 2-2. High-Level Radioactive Waste Glass Pour Canister

Table 2-2. Geometry and Material Specifications for DHLW Glass Canisters

Component	Material	Parameter	Value
Hanford 4.5-m (15-ft) Canister	SS 304L	Outer diameter	610.0 mm[a]
		Total weight of canister and glass	4,200 kg[a]
		Fill volume of glass in canister	87%[b]
		Wall thickness	10.5 mm[b]
		Length	4,572.0 mm[a]

Sources: [a]BSC 2001f, Table 1.
[b]Taylor 1997.

2.1.3 DOE Standardized SNF Canister

The conceptual design for the standardized 18-in.-OD DOE SNF canister is taken from DOE (1999b, pp. 5 and A-2). The canister is a right circular cylinder of SS 316L with an outer diameter of 457.2 mm (18.0 in.) and a wall thickness of 9.5 mm (0.375 in.). The minimum internal length of the canister is 4,115.0 mm and the nominal overall length is 4,569.0 mm. There is a curved carbon-steel impact plate, 50.8-mm (2.0-in.) thick, at the top and bottom boundaries of the canister. The maximum loaded mass of the canister is 2,721 kg (DOE 1999b, Table 3.2). A representation of the canister is shown in Figure 2-3.

The DOE standardized SNF canister will contain up to five FSVR SNF elements. No internal basket structure and no neutron absorber intended to prevent criticality will be present inside the DOE SNF canister loaded with FSVR SNF.

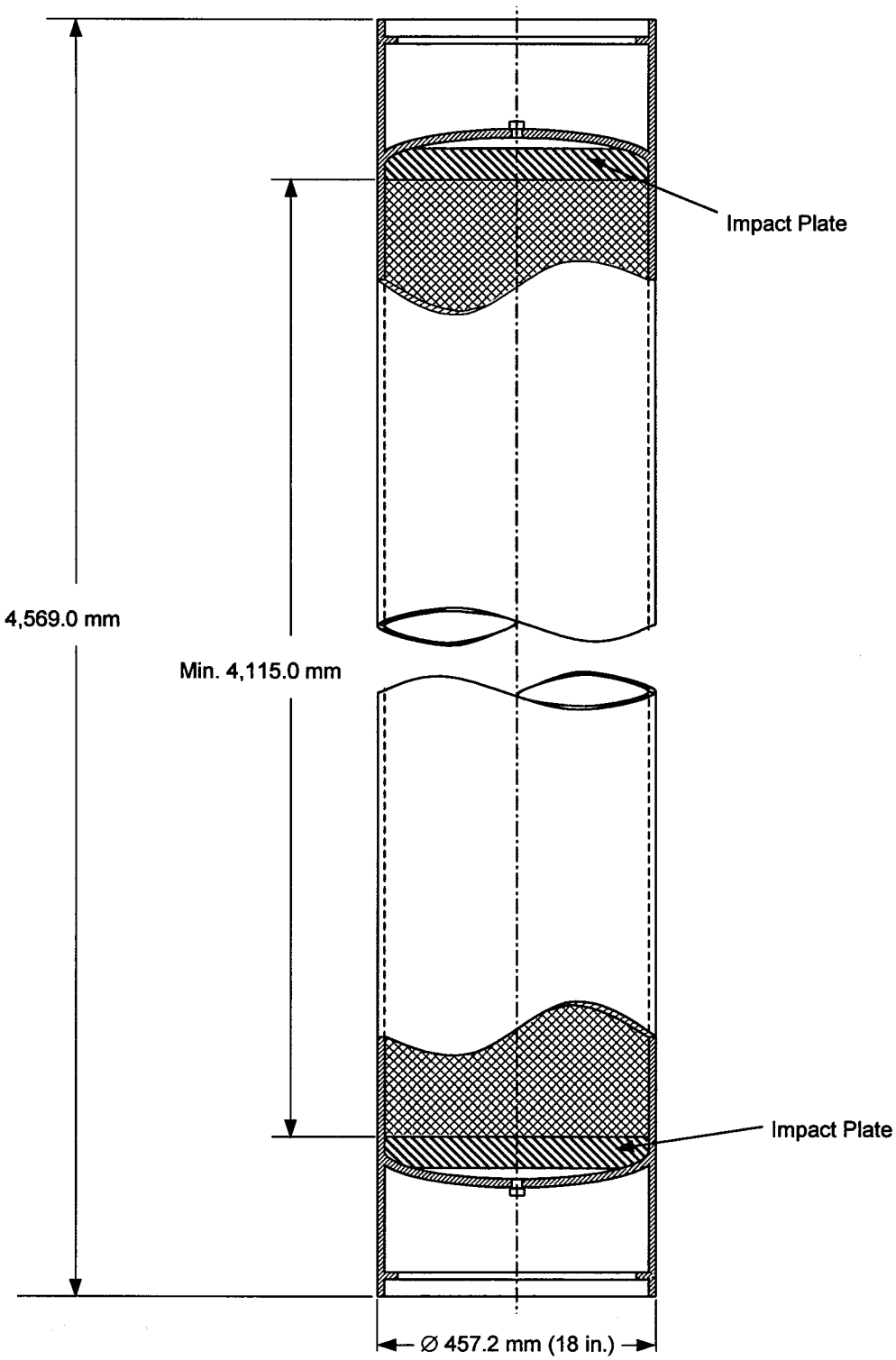

NOTE: Figure not to scale.

Source: DOE 1999b, p. A-2.

Figure 2-3. Plan View of the 18-in.-OD DOE Standardized SNF Canister

2.1.4 Fort Saint Vrain SNF

The information on FSVR SNF used in this section was obtained from the National Spent Nuclear Fuel Program and is documented in the report, *Fort Saint Vrain HTGR (Th/U carbide) Fuel Characteristics for Disposal Criticality Analysis* (Taylor 2001).

2.1.4.1 Fuel Element Characteristics

There are four main types of FSVR fuel elements: standard elements, control elements, bottom control elements, and neutron source elements with the neutron sources removed. All four types are made of graphite and have the same external dimensions, but differ in weight, number of coolant holes, reactivity holes, and neutron source holes. No metallic components are present in the fuel elements. Descriptions of the physical characteristics of each element are shown in Table 2-3.

Table 2-3. Physical Characteristics of FSVR Fuel Elements

Characteristic	Control Element	Bottom Control Element	Standard Element
Approximate Mass (with fuel compacts/matrix, kg)	109	111	128
Graphite Body Mass (kg)	85	94	86
Number of Coolant Holes (12.7 mm and 15.9 mm dia.)	57	57	108
Number of Fuel Holes (12.7 mm dia.)	120	120	210
Fuel Hole Pitch (mm)	18.8	18.8	18.8
Number of Control Rod Drive Holes (101.6 mm dia.)	2	2	0
Number of Reserve Shutdown Holes (95.3 mm)	1	1	0

NOTE: The characteristics of the standard fuel elements are also applicable to the neutron source fuel elements.

The FSVR graphite blocks for the initial core were machined from H-327 graphite cylinders. The graphite was produced from needle coke filler material, pitch blend, and additives processed to minimize impurity content.

The FSVR fuel element (Figure 2-4) is hexagonal in cross section with dimensions of 360.0 mm (14.172 in.) across flats by 793.0 mm (31.22 in.) high. The active fuel is contained in an array of small-diameter holes, which are parallel with the coolant channels, and occupy alternating positions in a triangular array within the graphite structure. The fuel holes are drilled from the top face of the element to within approximately 7.6 mm (0.3 in.) of the bottom face. A cemented graphite plug that is 12.7 mm (0.5 in.) long closes the top of each fuel channel after the fuel compacts were installed. The fuel holes in all elements are 12.7 mm (0.5 in.) in diameter. The bonded rods (also referred to as "fuel compacts") of coated fuel particles are stacked within the hole. These rods had a nominal dimension of 12.5 mm (0.49 in.) in diameter. At least one standard fuel block used 3130 compacts (which is the maximum number of compacts in a fuel block) to distribute the Th and U throughout the block. A representative layout of how compacts might be stacked in any given fuel channel is shown in Figure 2-5. The fuel holes and coolant channels are distributed on a triangular array with a pitch of approximately 18.8 mm (0.74 in.).

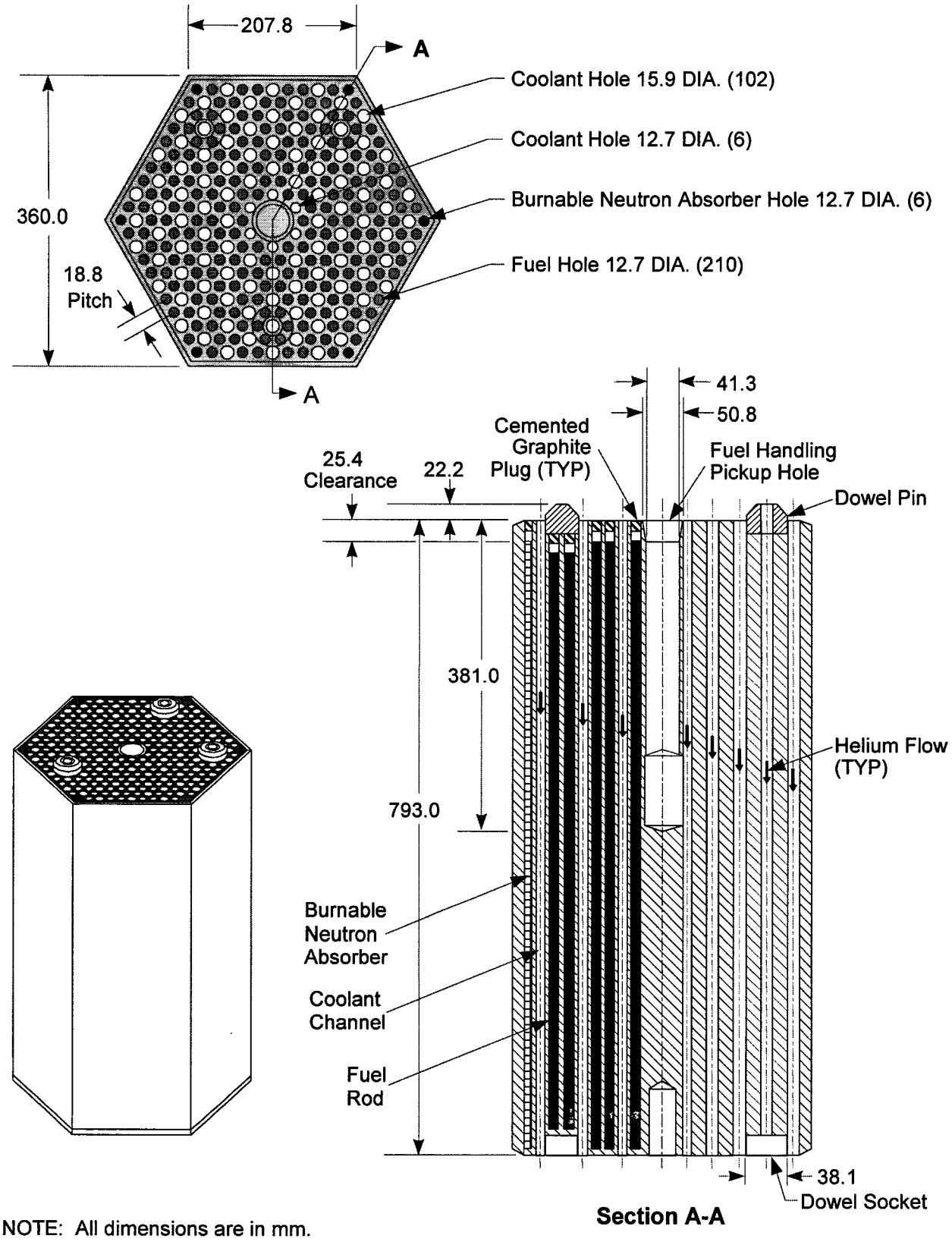

Figure 2-4. Standard FSVR Fuel Element

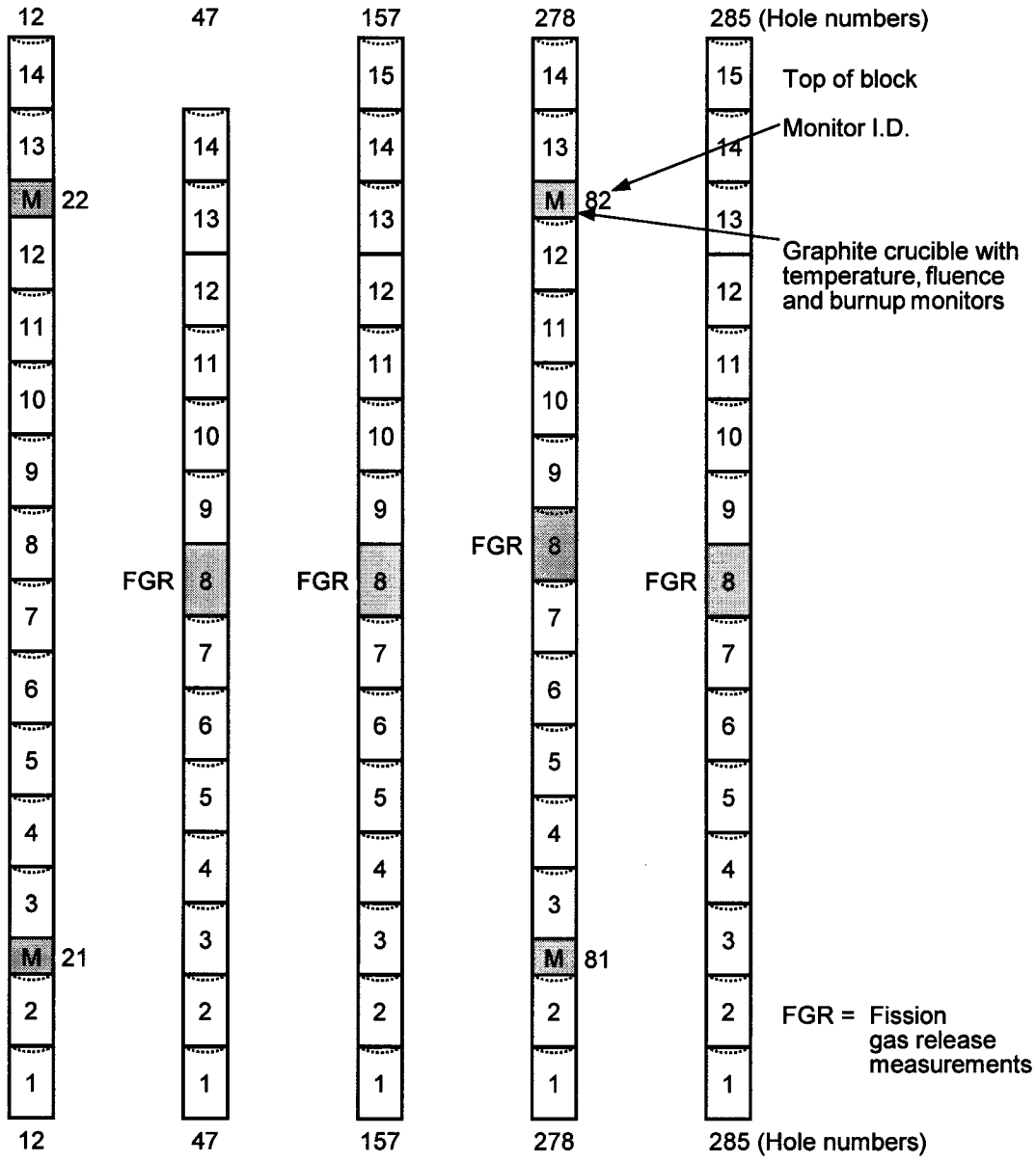

Figure 2-5. Fuel Compact Positioning for Selected Fuel Channels within a FSVR Fuel Block

The control element is similar to the standard fuel elements, but contains enlarged channels for the two control rods and the reserve shutdown absorber material. The control rod channels have a 246.9 mm (9.72 in.) centerline spacing and a diameter of 101.6 mm (4.0 in.). The reserve shutdown channel has a diameter of 95.3 mm (3.75 in.).

All of the standard elements have 12.7-mm (0.5-in.) diameter holes in each of their six corners for possible insertion of burnable neutron absorber rods. All of the control and bottom control elements have similar holes on four corners for burnable neutron absorber rods. The burnable neutron absorber rods are 50.8-mm (2.0-in) long and 11.43 mm (0.45 in.) in diameter, and are made of boron carbide particles in a carbon matrix. They are added as required and did not always fill the complete hole.

The lateral alignment of the six-layered fuel element column in the core is maintained by a system of three graphite dowels located on the top face of each element. A normal coolant channel passes through the center of each dowel. The dowels are threaded into the graphite structure and affixed with carbonaceous cement. Height of the dowels measured from the block surface is 22.2 mm (0.875 in.). The bottom side of all fuel blocks have three dowel sockets for interlocking with the block underneath (Figure 2-4).

The fuel blocks are made of nuclear grade graphite, type H-327 (needle-coke graphite) or type H-451 (near-isotropic graphite). Dowels and plugs used in the fuel element are of the same type of graphite as the element. Some physical characteristics of H-327 and H-451 types are shown in Table 2-4.

Table 2-4. Physical Characteristics of Graphite Types H-327 and H-451

Characteristic		H-327	H-451
Maximum Grain Size (mm)		1.65 (0.065 in.)	1.65 (0.065 in.)
Apparent Density (g/cm^3)		1.72	1.75
Tensile Strength (MPa)	Axial	11.238 (940 psi)	13.583 (1,970 psi)
	Radial	6.481 (1,630 psi)	10.756 (1,560 psi)

Based on the apparent (production) densities reported in Table 2-4 and a reported amorphous carbon density (maximum) of 2.1 g/cm^3, there is a corresponding calculated porosity of the fuel block of 16.67% and 18.10% for H-451 and H-327 materials, respectively. The 18.10% porosity was used to calculate the maximum water uptake in a block for criticality modeling. Calculating void space within the fuel channels must also account for the interstitial gap between the fuel compacts and fuel channels, as well as the porosity of the compacts. As a simplifying and conservative assumption (see Assumption 2.3.5.2), the irregularities in the flat surfaces and the cusp on the top end of each compact were accounted for by modeling a fuel channel that was bored completely through and neglecting the graphite filler plug installed in the top of each fuel channel. The interstitial gap used to calculate void space between the compacts of 12.5 mm (0.49 in.) diameter and the fuel channel of 12.7 mm (0.5 in.) diameter represents a maximum gap. The fabrication techniques used materials similar to the graphite blocks, but the allowable macroporosity was specified to less than 45% for the compacts. The calculation for the displaced volume of the compacts also assumed a fuel column length of 15 compacts per fuel channel. In combination, these additive voids yield a calculated "porosity" or void volume of 50.76% within each fuel channel. While irradiation may have altered the properties of the compacts, the original displaced volume would remain the same within each sealed fuel channel.

2.1.4.2 Fuel Particles Characteristics

The fissile and fertile fuel particles are coated microspheres of uranium and thorium dicarbide. As shown in Figure 2-6, each fuel particle consists of a spherical kernel covered with four main layers of coating material plus a thin intermediate seal coating, which is not represented.

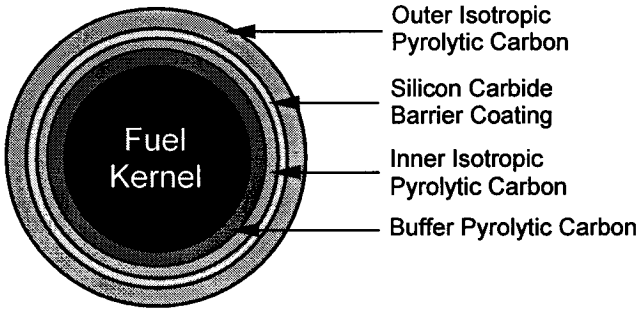

Figure 2-6. Cross-sectional View of Fertile and Fissile Fuel Particles Used in FSVR

The maximum uranium load per FSVR fuel element at beginning of life (BOL) was 1,485 g with a specified 93.15±0.15 wt% enrichment in U-235, which results in a nominal 1,383.3 g of U-235.

The graphite reactors are generally considered to be "converter" reactors, where a near-equivalent quantity of fissile atoms is produced as it is consumed. In the case of FSVR, this conversion resulted from the production of U-233 from Th-232. U-233 is known to be more reactive than an equivalent gram quantity of U-235, therefore it is reasonable to account for U-233 end of life (EOL) values in addition to any U-235 BOL values (since the DOE SNF is not taking burnup credits).

The average content of fertile and fissile species at BOL was 11.3 kg Th-232 per fuel block and 0.5 kg U-235 per fuel block. Specific data, on a block by block basis, indicates a BOL range of U-235 fissile loading values of 131.4 to 1,256.61 g, with a computed average of 574.4 g (Taylor 2001, Section 2.1.2.2 and Appendix B). The maximum uranium (total U with 93.15 wt% U-235 enrichment) was 1,485 g per fuel block.

Selection of the appropriate fissile loading is paramount to criticality analysis, both for fissile material accountability and storage/transportation issues for FSVR SNF. The production of U-233 is proportional to the ThO_2 loading and burnup, and inversely proportional to the UO_2 loading in a given element, i.e. lower U-233 production associated with higher U-235 loading.

For purposes of criticality safety evaluations, it is always the goal to describe and analyze the most reactive configuration. To this end, it will be necessary to identify the most reactive isotopic mixture given the blended quantities of U-233 and U-235 in the FSVR SNF. To establish a base-case fissile load limit per fuel element, there are three apparent combinations and one hypothetical set of values that should be analyzed for reactivity. The first three combinations are derived from the BOL U-235 load (maximum) and EOL U-233 load (associated maximum) and a similar construct reported in the FSVR fuel database (Taylor 2001, Appendix B). The following four isotopic combinations were evaluated and compared for maximum k_{eff} in the same MCNP representation (the load values are reported per fuel element).

1. BOL U-235 load of 1,256.61 g, EOL U-233 load of 135.79 g.

2. BOL U-235 load of 1,172.0 g, EOL U-233 load of 239.63 g; there should be a "defacto" U-238 composition of at least 73.8 g (from adjacent U group loading in database) since U-235 was never available in the 100% enrichments inferred in the database.

3. BOL U-235 load of 1,168 g, EOL U-233 load of 248.95 g; use a "defacto" U-238 composition of at least 73.8 g.

4. Total U load of 1,485.0 g with 93.15 wt% enrichment (from FSVR fuel specification); use 1,485.0 g BOL U-235 load as maximum case and EOL U-233+U-238 load of 0.0 g.

The kernel dimensions, coating designations, and coating thickness for the fissile and fertile particles are listed in Table 2-5.

Table 2-5. FSVR Fuel Particle Characteristics (all dimensions are in μm)

Parameter	Fissile		Fertile	
Th:U	3.6:1, 4.25:1		All Th	
Kernel Composition	$(Th:U)C_2$		ThC_2	
	Small	Large	Small	Large
Average fuel kernel diameter	140	225	375	525
	100-275		300-500	
	220		490	
Seal layer	<5		<5	
Buffer carbon layer	50	50	50	50
	45-110		45-65	
	50		50	
Isotropic carbon layer	20	20	20	20
	20-30		20-40	
	20		20	
SiC layer	20	20	20	20
	20-30		20-30	
	20		20	
Isotropic carbon layer	30	40	40	50
	≥25		≥30	
	30		30	
Average coated fuel diameter	380	485	635	805
	460		730	
	460		730	

The various coatings applied to the outside of the fuel matrix are installed using vapor deposition from some combination of carbon-based gases in a heated fluidized bed. In the case of the application of SiC on a pyrolyticly-coated fuel particle, methyltrichlorosilane (CH_3SiCl_3) is fed into the fluidized-bed reactor at temperatures ≥ 1450 °C and ≤ 1700 °C. Coating thicknesses are controlled for a sample mean value of 20-30 μm, and the target density layer is ≥ 3.18 g/cm^3; theoretical density of SiC is 3.217 g/cm^3.

The theoretical density of ThC_2 is 8.96 g/cm^3, and that of UC_2 is 11.28 g/cm^3 with production (fuel particle kernels) densities being ≥8.8 g/cm^3.

The porosity of the fuel matrix material can be calculated using the following expression:

$$\text{Porosity (\%)} = (TD-PD)\cdot 100/TD$$

where

TD = theoretical density
PD = production density of the respective U and Th materials.

For example, using the Th/U ratio equal to 3.6, TD = (3.6·8.96+1.0·11.28)/(3.6+1.0) = 9.464 g/cm^3 and maximum porosity is 7.016%. For the Th/U ratio equal to 4.25, TD = 9.402 g/cm^3 and porosity is 6.403%.

2.1.4.3 Fuel Rod Characteristics

A fuel rod is a column of coated fuel particles bonded together by a binder matrix. Fuel rods are cylinders 12.45 mm (0.49 in.) in diameter and 49.276-mm (1.94-in.) long. The chemical characteristics can be varied considerably depending upon blending ratios of the fuel kernels. For initial core loading, and the first reload segment, the FSVR fuel rod design utilized a homogeneous mixture of a graphite filler material and carbonized coal tar pitch as the binder. Beginning with the second reload (segment 8), petroleum-derived pitch was used as the binder, and isotropic shim particles, nominally 800 μm in diameter, were used to accommodate differences in heavy metal loading within the compacts. Hot injection molding process is the reference process for FSVR fuel rod fabrication.

The fuel rods and their individual fissile gram loading of U-235 were controlled by the fuel blend number used during the extrusion process. Similarly, the fissile distributions within the individual fuel blocks were used to adjust the fuel block loading to effect reactor core flux leveling.

The individual fuel compact fissile loading in a fuel block may have incorporated either a single or binary fuel mix number as shown in the following table. The data in Table 2-6 incorporates prescribed fissile loading from the General Atomics FSVR fuel specification (for the first core).

Table 2-6. Fuel Compact Composition Used

Element		Compact Composition (g)	Comments
Thorium (as ThC_2)		3.447	Based on 10789.97 g Th (EOL), and 3130 compacts per fuel element
Uranium (as $^{235}UC_2$)		0.474	Based on 1485 g maximum total U (BOL) and 100% U-235 enrichment (combination 4 at page 2-10)
Silicon (as SiC)		0.800	Based on assumption of uniform coating on particles
Carbon	Pyrolytic Coating	4.100	Based on assumption of uniform coating on particles
	Compact Matrix	3.858	Calculated based on mass differences between loaded fuel elements (Table 2-3) and components
	Fuel Matrix	0.399	Calculated from ThC_2 and UC_2 masses (per compact)
	SiC Layer	0.341	Calculated as a percentage of SiC from reported pure Si mass

Post-irradiation destructive examination was conducted on selected fuel compacts from a single fuel element, 1-0743. The fuel element experienced a burnup of 6.2% fissile and 0.3% fertile (from U-233 during the transmutation of Th-232). The analysis reported that approximately

0.3% of the fissile and 0.2% of the fertile microspheres were failed. These failures were due to manufacturing defects such as no coating, cracks, thin coatings, etc. Approximately 3% of the compacts were broken; most of them were likely broken by the disassembly process involved by pushing them out from the bottom of the fuel block. These data were used in the criticality safety evaluations for cases where the FSVR was considered to be degraded (Sections 7.4.1, 7.4.2.2.3, and 7.4.3).

2.1.5 Structural

A full three-dimensional (3-D) finite element representation of the 5-DHLW/DOE SNF-long WP was developed to determine the effects of loads on the structural components due to a tip over design basis event. Calculations of maximum stress intensity for each WP handling accident scenario (horizontal drop, vertical drop, and tip over design basis event) showed that the bounding dynamic load is obtained from a tip over case in which the rotating end of the WP experiences the highest impact load. Therefore, the structural evaluations presented in this technical report are bounding for all handling-accident scenarios. The finite element representation was developed using the dimensions provided in Taylor (2001).

2.1.6 Thermal

Table 2-7 lists the average heat output history of the DHLW glass inside the Hanford 4.5-m-(15-ft-) long canister.

Table 2-7. Average Heat Output History of DHLW Glass

Time after emplacement (years)	Heat Output (W/m^3)	Time after emplacement (years)	Heat Output (W/m^3)	Time after emplacement (years)	Heat Output (W/m^3)	Time after emplacement (years)	Heat Output (W/m^3)
0	52.21	45	17.94	90	6.29	5500	0.09
1	51.00	46	17.57	91	6.15	6000	0.08
2	49.80	47	17.11	92	6.01	6500	0.08
3	48.60	48	16.74	93	5.87	7000	0.08
4	47.48	49	16.36	94	5.74	7500	0.08
5	46.37	50	15.99	95	5.61	8000	0.08
6	45.26	51	15.62	96	5.48	8500	0.08
7	44.15	52	15.25	97	5.36	9000	0.08
8	43.13	53	14.88	98	5.24	9500	0.08
9	42.11	54	14.51	99	5.12	10000	0.08
10	41.10	55	14.23	100	5.01	15000	0.07
11	40.17	56	13.86	110	3.99	20000	0.06
12	39.24	57	13.58	120	3.20	25000	0.05
13	38.32	58	13.21	130	2.57	30000	0.05
14	37.39	59	12.94	140	2.07	35000	0.04
15	36.56	60	12.66	150	1.68	40000	0.04
16	35.63	61	12.29	160	1.38	45000	0.03
17	34.80	62	12.01	170	1.13	50000	0.03
18	34.06	63	11.73	180	0.93	55000	0.03
19	33.22	64	11.45	190	0.78	60000	0.03
20	32.39	65	11.27	200	0.66	65000	0.02
21	31.65	66	10.99	250	0.35	70000	0.02
22	30.91	67	10.71	300	0.24	75000	0.02
23	30.17	68	10.43	350	0.21	80000	0.02
24	29.52	69	10.25	400	0.19	85000	0.02
25	28.78	70	9.97	450	0.18	90000	0.02
26	28.13	71	9.78	500	0.17	95000	0.02
27	27.48	72	9.51	550	0.17	100000	0.02
28	26.83	73	9.32	600	0.16	150000	0.01
29	26.18	74	9.11	650	0.16	200000	0.01
30	25.63	75	8.89	700	0.15	250000	0.01
31	24.98	76	8.69	750	0.15	300000	0.01
32	24.42	77	8.49	800	0.15	350000	0.01
33	23.87	78	8.29	850	0.14	400000	0.01
34	23.31	79	8.11	900	0.14	450000	0.01
35	22.76	80	7.92	950	0.13	500000	0.01
36	22.20	81	7.74	1000	0.13	550000	0.01
37	21.64	82	7.56	1500	0.11	600000	0.01
38	21.18	83	7.39	2000	0.10	650000	0.01
39	20.72	84	7.23	2500	0.10	700000	0.01
40	20.16	85	7.06	3000	0.09	750000	0.01
41	19.70	86	6.89	3500	0.09	800000	0.01
42	19.24	87	6.73	4000	0.09	850000	0.01
43	18.87	88	6.59	4500	0.09	900000	0.01
44	18.40	89	6.44	5000	0.09	1000000	0.01

Source: BSC 2001b, Table 5.3-1.

Table 2-8 lists the maximum heat output history of the FSVR SNF as total Watts per WP.

Table 2-8. Maximum Heat Output History of the FSVR Fuel

Year	Heat Output (Watts per WP)
2010	776
2020	620
2030	496
2040	398
2050	320
2060	258
2070	209
2080	170
2090	138
2100	113
2200	21.7
2300	8.15
2400	4.55
2500	3.08
2600	2.37
2700	1.99
2800	1.77
2900	1.63
3000	1.52
4000	1.13
5000	1.05
6000	1.02
7000	1.00
8000	0.986
9000	0.937
10000	0.960

Source: BSC 2001b, Table 5.3-2.

The surface temperature of the WP was taken from Table 6-18 in CRWMS M&O (2000a) under the heading "Waste Package 1". "Waste Package 1" was chosen because it most closely matches 5-DHLW/DOE SNF-long WP with FSVR fuel output in terms of total heat generation (W) and is bounding. This choice is conservative since "Waste Package 1" column is based on a heat source approximately three times than that of 5-DHLW/DOE SNF-long WP with FSVR fuel, and the volume where the heat is generated is smaller. The temperatures used are listed in Table 2-9. The sudden increase in temperature at 50 years is due to the end of forced ventilation.

The boundary conditions for the thermal analysis are:

- The spacing between the WPs will be 0.1 m (Curry 2001, p. 2-17).
- The repository will be ventilated for 50 years after initial emplacement (Curry 2001, p. 2-21).
- There will be no backfill in the emplacement drift (Stroupe 2000, Attachment I).

Table 2-9. WP Boundary Conditions

Time after emplacement (years)	Temperature (°C)	Time after emplacement (years)	Temperature (°C)
0	36	50.6	126
0.1	56	50.7	128
0.2	62	50.8	129
0.3	65	50.9	130
0.4	67	51	131
0.5	69	52	141
0.6	71	53	148
0.7	72	54	152
0.8	74	55	155
0.9	75	56	158
1	76	57	161
2	83	58	162
3	86	59	163
4	88	60	163
5	90	70	163
6	91	80	163
7	92	90	159
8	92	100	155
9	92	110	152
10	93	120	150
15	92	130	147
20	91	140	144
25	89	150	141
30	87	250	128
35	85	350	123
40	83	450	119
45	82	550	116
50	80	650	113
50.01	87	750	110
50.02	95	850	109
50.03	100	950	107
50.04	103	1050	106
50.05	105	2050	93
50.06	107	3050	87
50.07	108	4050	83
50.08	110	5050	80
50.09	110	6050	77
50.1	111	7050	75
50.2	116	8050	73
50.3	119	9050	71
50.4	121	10050	69
50.5	124		

Source: CRWMS M&O 2000a, Table 6-18.

2.1.7 Shielding Source Term

The gamma and neutron source terms of the FSVR SNF are presented in Table 2-10. The radiation source terms, which are provided per FSVR fuel element, have been calculated for a fuel element with maximum burnup. A bounding peaking factor has been applied to the calculations to conservatively consider the variation of the fuel irradiation flux during the fuel cycles (Taylor 2001, pp. 32 and 35). The dose rate evaluations used the radiation source terms at the time of fuel discharge, which conservatively bound all expected shipments of FSVR SNF to the monitored geologic repository.

Table 2-10. Gamma and Neutron Sources per FSVR Fuel Element

Photon Mean Energy[a] (MeV)	Gamma Intensity[a] (photons/s)	Neutron Energy Group Boundaries[a] (MeV)	Neutron Intensity[a] (neutrons/s)
3.00E-01	3.27E+13	0.00-0.10	0.000E+00
6.50E-01	4.68E+14	0.10-0.40	7.931E+03
1.13E+00	9.15E+12	0.40-0.90	4.067E+04
1.57E+00	4.22E+12	0.90-1.40	3.961E+04
2.00E+00	3.11E+12	1.40-1.85	3.274E+04
2.40E+00	5.58E+10	1.85-3.00	7.086E+04
2.80E+00	6.86E+09	3.00-6.43	5.263E+04
3.25E+00	7.81E+08	6.43-20.00	3.812E+03
3.75E+00	3.44E+05		
4.25E+00	7.70E-07		
4.75E+00	3.86E-07		
5.50E+00[b]	2.86E-07		
Total	5.17E+14	**Total**	2.483E+05

Sources: [a]Taylor 2001, pp. 35 and 36.
[b]ORNL 1997, p. M6.3.1. The value of the photon mean energy for this last energy group is mistakenly represented in Taylor (2001), therefore the value from ORNL (1997, p. M6.3.1) was used.

It is assumed that the high-level radioactive waste glass that fills the 4.5-m-long Hanford glass pour canisters is the SRS Design-Basis DHLW glass (Assumption 2.3.6.2). Table 2-11 presents the gamma and neutron source terms per 4.5-m-long Hanford DHLW glass canister at year 2010.1. The values in Table 2-11 were obtained by multiplying the gamma and neutron source terms of the 3-m-long SRS DHLW glass canister (CRWMS M&O 2000c, pp. V-1 and VI-1) with the scale up factor given in Taylor (1997), which is 3.67/2.17=1.69.

Table 2-11. Gamma and Neutron Sources per 4.5-m-long Hanford DHLW Glass Canister[a]

Gamma Source		Neutron Source	
Photon Upper Energy Boundary (MeV)	Intensity (photons/s)	Neutron Upper Energy Boundary (MeV)	Intensity (neutrons/s)
0.05	2.18E+15	0.10	2.60E+05
0.10	6.58E+14	0.40	2.71E+06
0.20	5.11E+14	0.90	9.44E+06
0.30	1.45E+14	1.40	1.01E+07
0.40	1.06E+14	1.85	8.81E+06
0.60	1.45E+14	3.00	3.59E+07
0.80	2.27E+15	6.43	4.63E+07
1.00	3.52E+13	20.00	5.06E+05
1.33	4.92E+13		
1.66	1.05E+13		
2.00	8.22E+11		
2.50	4.57E+12		
3.00	3.23E+10		
4.00	3.64E+09		
5.00	8.79E+05		
6.50	3.53E+05		
8.00	6.92E+04		
10.00	1.47E+04		
Total	6.11E+15	**Total**	1.14E+08

NOTE: [a]Calculated by multiplying the gamma and neutron source terms of the 3-m-long SRS DHLW glass canister provided in CRWMS M&O (2000c, pp. V-1 and VI-1) with the scale up factor given in Taylor (1997), which is 3.67/2.17=1.69.

2.1.8 Material Compositions

The chemical compositions of the materials used in the analyses are given in Tables 2-12 through 2-16.

Table 2-12. Chemical Composition of ASTM B 575 (Alloy 22) (Universal Numbering System [UNS] N06022)

Element	Composition (wt%)	Value Used (wt%)
Carbon (C)	0.015 (max)	0.015
Manganese (Mn)	0.50 (max)	0.50
Silicon (Si)	0.08 (max)	0.08
Chromium (Cr)	20.0 - 22.5	21.25
Molybdenum (Mo)	12.5 - 14.5	13.5
Cobalt (Co)	2.50 (max)	2.50
Tungsten (W)	2.5 - 3.5	3.00
Vanadium (V)	0.35 (max)	0.35
Iron (Fe)	2.0 - 6.0	4.00
Phosphorus (P)	0.02 (max)	0.02
Sulfur (S)	0.02 (max)	0.02
Nickel (Ni)	Balance	54.765
Density = 8.69 g/cm^3		

Source: ASTM B 575-97, p. 2.

Table 2-13. Chemical Composition of ASTM A 516 Grade 70 Carbon Steel (UNS K02700)

Element	Composition[a] (wt%)	Value Used (wt%)
Carbon (C)	0.28 (max)	0.28
Manganese (Mn)	0.79-1.30	1.045
Phosphorus (P)	0.035 (max)	0.035
Sulfur (S)	0.035 (max)	0.035
Silicon (Si)	0.13-0.45	0.29
Iron (Fe)	Balance	98.325
Density[b] = 7.85 g/cm^3		

Sources: [a] ASTM A 516/A 516M – 90, Table 1.
[b] ASTM A 20/A 20M-99a, p. 9.

Table 2-14. Chemical Composition of SS Type 304L (UNS S30403)

Element	Composition[a] (wt%)	Value Used (wt%)
Carbon (C)	0.03 (max)	0.03
Manganese (Mn)	2.00 (max)	2.00
Phosphorus (P)	0.045 (max)	0.045
Sulfur (S)	0.03 (max)	0.03
Silicon (Si)	0.75 (max)	0.75
Chromium (Cr)	18.00 - 20.00	19.00
Nickel (Ni)	8.00 - 12.00	10.00
Nitrogen (N)	0.10	0.10
Iron (Fe)	Balance	68.045
Density[b] = 7.94 g/cm^3		

Sources: [a] ASTM A 240/A 240M-99b, p. 3.
[b] ASTM G 1-90, Table X1.

Table 2-15. Chemical Composition of SS Type 316L (UNS S31603)

Element	Composition[a] (wt%)	Value Used (wt%)
Carbon (C)	0.03 (max)	0.03
Manganese (Mn)	2.00 (max)	2.00
Phosphorus (P)	0.045 (max)	0.045
Sulfur (S)	0.03 (max)	0.03
Silicon (Si)	1.00 (max)	1.00
Chromium (Cr)	16.00 - 18.00	17.00
Nickel (Ni)	10.00 - 14.00	12.00
Molybdenum (Mo)	2.00 - 3.00	2.50
Nitrogen (N)	0.00	0.10[c]
Iron (Fe)	Balance	65.295
Density[b] = 7.98 g/cm^3		

Sources: [a] ASTM A 276-00, p.2.
[b] ASTM G 1-90, Table X1.
[c] This value is consistent with previous releases of ASTM A 276-00. However, the amount is negligible and does not affect the results of the calculations.

Table 2-16. Chemical Composition of SRS DHLW Glass

Element/Isotope	Composition[a] (wt %)	Element/Isotope	Composition[a] (wt %)
O	4.4770E+01	Ni	7.3490E-01
U-234	3.2794E-04	Pb	6.0961E-02
U-235	4.3514E-03	Si	2.1888E+01
U-236	1.0415E-03	Th	1.8559E-01
U-238	1.8666E+00	Ti	5.9676E-01
Pu-238	5.1819E-03	Zn	6.4636E-02
Pu-239	1.2412E-02	B-10	5.9176E-01
Pu-240	2.2773E-03	B-11	2.6189E+00
Pu-241	9.6857E-04	Li-6	9.5955E-02
Pu-242	1.9168E-04	Li-7	1.3804E+00
Cs-133	4.0948E-02	F	3.1852E-02
Cs-135	5.1615E-03	Cu	1.5264E-01
Ba-137	1.1267E-01	Fe	7.3907E+00
Al	2.3318E+00	K	2.9887E+00
S	1.2945E-01	Mg	8.2475E-01
Ca	6.6188E-01	Mn	1.5577E+00
P	1.4059E-02	Na	8.6284E+00
Cr	8.2567E-02	Cl	1.1591E-01
Ag	5.0282E-02		
Density[b] at 25 °C = 2.85 g/cm^3			

Sources: [a] CRWMS 1999a, p. 7.
[b] The average glass density is 2.65 g/cm^3 (CRWMS M&O 2000b). Stout and Leider (1991, p. 2.2.1.1-4) gives an upper limit of the glass density of 2.85 g/cm^3. The upper limit is the value used unless otherwise noted.

2.1.9 Degradation and Geochemistry

This section identifies the degradation rates of the principal alloys, the chemical composition of J-13 well water, and the drip rate of J-13 well water into a WP. These rates are used in Section 6, Degradation and Geochemistry Analyses.

2.1.9.1 Physical and Chemical Form of FSVR WP

It is convenient to consider the FSVR WP as several structural components, specifically:

- The outer shell constructed of corrosion resistant material (Alloy 22).
- The inner shell (also called liner) constructed of SS 316NG.
- The "outer web", a carbon steel (A516) structural basket designed to hold the DHLW glass canisters in place.
- Impact plates constructed of A516 carbon steel.
- The 5 DHLW glass canisters, constructed of SS 304L and filled with solidified DHLW glass.
- The 18-in.-outer diameter DOE SNF canister, constructed of SS 316L, which holds the FSVR fuel elements (maximum five per canister).

- The fuel compacts containing the fuel kernels. A maximum of 3130 fuel compacts fit into a FSVR fuel element.

Table 2-17 gives the composition of the DHLW glass used in the calculations. Several minor changes were made to these basic compositions to increase the efficiency of the calculations and to decrease the EQ6 run time. Principally, minor elements in the DHLW glass composition were removed or merged with chemically similar elements (e.g., Li was merged with Na in the glass composition). If the DHLW glass composition is simplified, it can be entered as a pseudo-mineral, "GlassSRL," in the database. Entering the glass as a pseudo-mineral reactant allows EQ6 to apply a pH dependent degradation rate using the Transition State Theory formalism (Wolery and Daveler 1992, Sec 3.3.3). Since Np and Pu made up only 1.1% of the total actinide content of the DHLW glass, they were combined with U to further simplify the composition.

Table 2-17. Simplified DHLW Glass Composition and Degradation Rate Constants

Element	Composition[a] (wt%)	Comments
O	4.2605E+01	-
U	1.8612E+00	-
Ba	1.4718E-01	-
Al	2.3285E+00	-
S	1.2849E-01	-
Ca	6.5021E-01	-
P	1.5136E-02	-
Si	2.1808E+01	-
B	3.1486E+00	-
F	3.1565E-02	-
Fe	9.6172E+00	-
K	2.9347E+00	-
Mg	8.1001E-01	-
Na	1.3259E+01	-
Np	0	Merged with U (~0.1% of actinides)
Pu	0	Merged with U (Pu ~1% actinides)
Cr	0	Merged with Al (overwhelmed by Cr in steel; Cr_2O_3 similar to Al_2O_3)
Cu, Mn, Ni	0	Merged with Fe
Pb	0	Merged with Ba (both form insoluble $CrO_4^=$ compounds in EQ6 runs)
Ti	0	Merged with Si (TiO_2 similar to SiO_2)
Li	0	Merged with Na
Cl	0	Removed (overwhelmed by Cl in in-dripping water)
Total	1.0000E+02	
Total Degradation Rate[b] = $k_1[H+]^{-0.4} + k_2[H+]^{0.6}$ (moles/cm^2·s)[c]		
Moderate Rate Constant (k_1)		8.858E-19 liters/cm^2·s
High Rate Constant (k_1)		1.076E-17 liters/cm^2·s
Moderate Rate Constant (k_2)		7.976E-13 liters/cm^2·s
High Rate Constant (k_2)		4.874E-12 liters/cm^2·s

NOTES: [a]Composition based on CRWMS M&O (1999a, p. 7) as simplified in CRWMS M&O (2001a, Table 3).
[b]Rates based on CRWMS M&O (2001b, Section 6.2.3.3, Eq. 7 and 8), checked against CRWMS M&O (2000f, Eq. 3.6-4 and 3.6-5); as simplified in CRWMS M&O (2001a, Table 3).
[c]One Mole = 100 g DHLW glass. The molecular mass of all WP components was set to 100 g to simplify EQ6 inputs.

A pH-dependent rate for DHLW glass degradation was derived from CRWMS M&O (2001b, Sec. 6.2.3.3, Eq. 7 and 8), and normalized in CRWMS M&O (2001a, Attachment III). The first rate mechanism (described with k_1) in Table 2-17 is dominant at pH values above 7, whereas the second rate mechanism (described with k_2) is dominant at pH values below 7. The high glass degradation rate constants in Table 2-17 are those predicted at 50°C, while the moderate rate constants are those derived for degradation at 25°C (CRWMS M&O 2001b, Section 6.2.3.3, Eq. 7 and 8).

As was shown in Sections 5.3.2 and 5.3.3 of CRWMS M&O (1999b), EQ6 (which is part of EQ3/6 geochemistry software package) estimates of U loss from the WP are not greatly affected by substantial variations in the composition of the DHLW glass. The actual DHLW glass composition used in the glass pour canister may vary significantly from these values, since the sources of the DHLW glass and melting processes are not currently fixed. For example, compositions proposed for SRS DHLW glass vary by a factor of ~6 in U_3O_8 content, from 0.53 to 3.16 wt% (DOE 1992, p. 3.3-15, Table 3.3.8.). The Si and alkali metal contents (Na, Li, and K) of the DHLW glass have perhaps the most significant bearing on EQ6 calculations. The amount of Si in the DHLW glass strongly controls the amount of clay that forms in the WP, and the Si activity controls the presence of insoluble uranium phases such as soddyite ($[UO_2]_2SiO_4 \cdot 2H_2O$), sodium boltwoodite ($NaUO_2SiO_3OH \cdot 1.5H_2O$), or α-uranophane ($Ca[UO_2SiO_3OH]_2 \cdot 5H_2O$). As the DHLW glass degrades in an EQ6 run, the alkali metal content of the corrosion products increases and the pH rises. The Si and alkali metal contents in Table 2-17 are typical for proposed DOE high-level radioactive waste glasses (CRWMS M&O 1999a).

Table 2-18 shows the reaction rates of the various components. The data are taken from the geochemistry calculations for the FSVR WPs (BSC 2001d). The reaction rate for the DHLW glass is pH dependent and the values given are the upper and lower bounds used in the geochemistry calculations.

Table 2-18. Properties of Materials in FSVR Codisposal WP

Reactant	*rk*			*sk*
	Reaction Rate[a] (moles/cm^2·s)			Surface Area[b] (cm^2)
	Low	Average	High	
DHLW Glass	rk1=8.858E-19 cdac1= -0.4 rk2=7.976E-13 cdac2= 0.6	rk1=1.076E-17 cdac1= -0.4 rk2=4.874E-12 cdac2= 0.6	Not Applicable (N/A)	1340.60
Fuel Compacts	See Table 2-19			58.76
Graphite Block	Considered inert, therefore not included in EQ6 calculations (Assumption 2.3.4.11)			
304L Glass Pour Canister	2.52E-14	2.52E-13	8.656E-12	150.80
A516 Outer Web	Same as average	1.79E-11	Same as average	128.30
A516 Impact Plates	Same as average	1.79E-11	Same as average	1.28
316L DOE SNF Canister	2.53E-14	2.53E-13	5.056E-13	23.22
316NG Inner Shell	2.53E-14	2.53E-13	5.056E-13	56.52

Source: [a]BSC 2001c, Table 5-2.
[b]BSC 2001c, Table 5-1.

The degradation rates in Table 2-18 range from low to high (indicated by "1" to "3"). The true reaction rate is obtained by multiplying the reaction rate (***rk***) by the surface area (***sk***) to get moles/s. Inspection of the rates show that for a comparable surface area, the A516 carbon steel is expected to degrade much more rapidly than the stainless steels (316L, 316NG, and 304L).

The outer web is composed of A-516 carbon steel, and serves two purposes: it centers, holds in place, and separates the DOE SNF canister and the DHLW canisters; and prevents them from transmitting undue stress to each other in the event of a fall (tip over) of the entire WP. In a breach scenario, the A516 WP components will be exposed to water and corrode before the rest of the WP, and are expected to degrade within a few hundred to a few thousand years.

Table 2-19 presents the degradation rates of the FSVR fuel.

Table 2-19. Degradation Rates of FSVR Fuel

Rate	moles/(cm^2·s)	Comments
inert	N/A	Based on SiC rate found in Weast and Astle 1979 (p. B-121) and Opila 1999.
low	6.00E-16	Based on SiC degradation in BSC 2001g (Section 6.3.5).
high	2.78E-10	Based on UC_2 degradation, 10X U-metal at 25°C, in BSC 2001g (Section 6.3.7).
very high	1.50E-08	Based on UC_2 degradation, 10X U-metal at 50°C, in BSC 2001g (Section 6.3.7) (not used for FSVR fuel).

2.1.9.2 Chemical Composition of Incoming Water

It was assumed that the water composition entering the WP would be the same as for water from well J-13 (Assumption 2.3.4.1). The composition of J-13 well water as used in this report has been adjusted slightly (see Assumption 2.3.4.8). Tables 2-20 and 2-21 contain the EQ3NR (which is part of EQ3/6 geochemistry software package) input file constraints for J-13 well water composition and the EQ6 input file elemental molal composition used for J-13 well water.

The "Basis Species" column of Table 2-20 lists the chemical species names recognized by EQ3NR and EQ6. Since some of the components of J-13 well water, as analyzed (Data Tracking Number [DTN]: MO0006J13WTRCM.000) are in a different chemical form than the species listed in this column, these components must be substituted or "switched" with the basis species for input into EQ6 and are listed in the "Basis Switch" column. Basis species listed as "Trace" in the "Basis Switch" column are not found in J-13 well water, as analyzed (DTN: MO0006J13WTRCM.000), but are in the composition of other WP components and must be input at a minimum concentration for numerical stability in EQ6 calculations.

Table 2-20. EQ3NR Input File Constraints for J-13 Well Water Composition

Basis Species	Basis Switch	Concentration	Units
redox		-0.7[d]	log fO_2
Na+		45.8	mg/L
SiO_2(aq)		60.97	mg/L
Ca++		13.0	mg/L
K+		5.04	mg/L
Mg++		2.01	mg/L

Table 2-20. EQ3NR Input File Constraints for J-13 Well Water Composition (Continued)

H+		8.1[b]	pH
HCO_3-	CO_2(g)	-3[d]	log fCO_2
O_2(aq)		5.6[c]	mg/L
F-		2.18	mg/L
Cl-		7.14	mg/L
NO_3-	NH_3(aq)	8.78	mg/L
SO_4--		18.4	mg/L
Al+++	Trace	1.000E-16[a]	Molality
Mn++	Trace	1.000E-16[a]	Molality
Fe++	Trace	1.000E-16[a]	Molality
$B(OH)_3$(aq)	Trace	1.000E-16[a]	Molality
HPO_4--	Trace	1.000E-16[a]	Molality
Ba++	Trace	1.000E-16[a]	Molality
CrO_4--	Trace	1.000E-16[a]	Molality
Gd+++	Trace	1.000E-16[a]	Molality
MoO_4--	Trace	1.000E-16[a]	Molality
Ni++	Trace	1.000E-16[a]	Molality
Pu++++	Trace	1.000E-16[a]	Molality
Th++++	Trace	1.000E-16[a]	Molality
UO_2++	Trace	1.000E-16[a]	Molality

DTN: MO0006J13WTRCM.000

NOTES: [a] A trace concentration (1.000E-16 molal) is added for elements that are not in J-13 well water as analyzed, but are in the composition of the WP components to ensure numerical stability in EQ3/6 runs.
[b] If log(fCO_2) = –3, then EQ3NR calculates pH = 8.1.
[c] From Harrar et al. (1990, Table 4.2).
[d] See assumption 2.3.4.8.

Table 2-21. EQ6 Input File Elemental Molal Composition for J-13 Well Water

Element	Moles/kg	Element	Moles/kg
O	5.55E+01	P	1.26E-06[a]
Al	1.00E-16	K	1.29E-04
B	1.00E-16	Mg	8.27E-05[a]
Ba	1.00E-16	Mn	1.00E-16
Ca	3.24E-04	Mo	1.00E-16
Cl	2.01E-04	N	1.42E-04
Cr	1.00E-16	Na	1.99E-03
F	1.15E-04	Ni	1.00E-16
Fe	1.00E-16	S	1.92E-04
Gd	1.00E-16	Si	1.02E-03
H	1.11E+02	U	1.00E-16
C	2.07E-03		

DTN: MO0006J13WTRCM.000

NOTE: [a] From Harrar et al. (1990, Table 4.2).

2.1.9.3 Drip Rate of Incoming Water

It was assumed (Assumption 2.3.4.7) that the drip rate onto a WP is the same as the rate at which water flows through the WP. The drip rate is taken from a correlation between percolation flux and drip rate, also called mean seep flow rate (CRWMS M&O 2000h, Figure 3.2-15). A range of drip rates was chosen. Specifically, values of 0.0015, 0.015, and 0.15 m^3/year were used for most cases, corresponding to percolation fluxes ranging from about 10 mm/year to 80 mm/year. The value of 10 mm/year corresponds to a high infiltration rate for the present-day climate and 80 mm/year corresponds to about twice the high infiltration rate for the glacial-transition climate (CRWMS M&O 2000h, Table 3.2-2). Table 3.2-2 of CRWMS M&O (2000h) gives values of net infiltration rate, rather than percolation flux; however, they are equal at the potential repository level (CRWMS M&O 2000h, Section 3.2.3.4, p. 3-33). For a few cases, the range of allowed drip rates included an upper value of 0.5 m^3/yr, which represents approximately 100 mm/year percolation flux.

2.2 FUNCTIONS AND DESIGN CRITERIA

The design criteria are based on the *Defense High Level Waste Disposal Container System Description Document* (BSC 2001f), hereafter referred to as the SDD. In this subsection, the key WP design criteria from the SDD are identified for the following areas: structural, thermal, shielding, criticality within a breached but otherwise intact WP, degradation and geochemistry, and criticality of a degraded WP and waste form. These criteria are subject to verification. SDD paragraph numbers are identified below as SDD X.X.X.X. or SDD X.X.X.X.X.

The disposal container accommodates five Hanford 4.5-m- (15-ft-) long DHLW canisters and one DOE SNF canister containing FSVR SNF as required by SDDs 1.2.1.1 and 1.2.1.2.

The disposal container consists of two cylinders; an inner cylinder that is stainless steel (alloy 316 NG) with a minimal thickness of 5 cm, and an outer cylinder that is alloy 22 material with a minimal thickness of 2 cm (SDD 1.2.1.4).

2.2.1 Structural Criteria

2.2.1.1 The disposal container/WP shall prevent the breach of the waste form canister during normal handling operations (SDD 1.2.1.8).

2.2.1.2 During the preclosure period (i.e., the time period before the monitored geologic repository is permanently closed), the disposal container/WP, shall be designed to withstand (while in a vertical orientation) a drop from a height of 2 m (6.6 ft) onto a flat, unyielding surface without breaching (SDD 1.2.2.1.3).

2.2.1.3 During the preclosure period, the disposal container/WP, shall be designed to withstand (while in a horizontal orientation) a drop from a height of 2.4 m (7.9 ft) onto a flat, unyielding surface without breaching (SDD 1.2.2.1.4).

2.2.1.4 During the preclosure period, the WP shall be designed to withstand a tip over from a vertical position with slap down onto a flat, unyielding surface without breaching (SDD 1.2.2.1.6).

2.2.1.5 The WP shall be designed to withstand transfer, emplacement, and retrieval operations without breaching (SDD 1.2.1.18).

2.2.1.6 The disposal container shall be designed in accordance with the applicable sections of "1995 ASME Boiler and Pressure Vessel Code" (Section III, Division 1, Subsection NB-1995) (SDD 1.2.6.2).

Calculations of maximum potential energy for each handling accident scenario (horizontal drop, vertical drop, and tip over design-basis events) show that the bounding dynamic load is obtained from a tip over case in which the WP experiences the highest impact load with maximum rotational velocity of 1.89 rad/s (CRWMS M&O 2000b, p. 14). This equates to a maximum velocity of the rotating top end of the WP of 9.86 m/s ($v = r \cdot \omega$, where r is the length of the WP and ω is the rotational velocity in rad/s). The maximum velocities of the WP for 2.4-m horizontal and 2.0-m vertical drops are approximately 6.86 m/s ($v = \sqrt{2 \cdot g \cdot h}$, where g is the gravitational acceleration and h is drop height) and 6.26 m/s, respectively. Therefore, tip over structural evaluations are bounding for all WP handling accident scenarios.

The tip over design-basis event may only take place during a WP transfer operation from vertical to horizontal position (just after WP closure) or horizontal to vertical position (upon retrieval). Section 3, Structural Analysis, demonstrates that the WP will not breach under such a handling-accident scenario.

2.2.2 Thermal Criteria

2.2.2.1 The WP shall maintain the temperature of high-level radioactive waste glass below 400 °C (752 °F) under normal conditions, and below 460 °C (860 °F) for short-term exposure to fire, as specified by Criterion 1.2.2.1.11 (BSC 2001f) (SDD 1.2.1.6).

2.2.2.2 The WP shall be designed to have a maximum thermal output of 11,800 W (SDD 1.2.4.2).

2.2.3 Shielding Criteria

WP design shall reduce the dose rate at all external surfaces of a WP to 1,450 rem/h or less. This criterion identifies a disposal container interface with the Disposal Container Handling System, the Waste Emplacement/Retrieval System, and the Performance Confirmation Emplacement Drift Monitoring System (SDD 1.2.4.1).

2.2.4 Degradation and Geochemistry Criteria

There are no degradation and geochemistry criteria in the SDD to address.

2.2.5 Intact and Degraded Criticality Criteria

During the preclosure period, the disposal container/waste package shall be designed such that the effective neutron multiplication factor (k_{eff}) is less than or equal to 0.95 under assumed accident conditions considering allowance for the bias in the method of calculation and the uncertainty in the experiments used to validate the method of calculation (SDD 1.2.2.1.12).

SDD 1.2.2.1.13 and 1.2.2.1.14 are not considered because the frequency of criticality occurrence and the associated consequence are not within the scope of this report.

2.3 ASSUMPTIONS

In the course of developing this report, assumptions were made regarding the WP structural, thermal, shielding, intact criticality, degradation and geochemistry, and degraded component criticality analyses. A listing of assumptions that are essential to this technical report is provided below.

2.3.1 Structural

The assumptions in this section are used throughout Section 3.

2.3.1.1 The target surface was conservatively assumed to be unyielding with a large elastic modulus for the target surface material compared to the WP materials. The rationale for this assumption was that a bounding set of results was required in terms of stresses, and it was known that the use of an unyielding surface with high stiffness ensures slightly higher stresses in the WP.

2.3.1.2 The exact geometry of the FSVR fuel element is simplified in such a way that its total maximum mass, 128 kg, is assumed to be distributed within a hexagonal prism with uniform mass density and constructed of H-327 graphite. The rationale for this assumption is that the FSVR fuel geometry is anticipated to be similar to a hexagonal prism and have a center of gravity at or near that of a hexagonal prism with uniform mass density. This assumption provides a set of bounding results, while simplifying the finite element representation.

2.3.1.3 The exact geometry of the DHLW glass canister was simplified for the purpose of the calculation in such a way that its total mass, 4,200 kg (DOE 1999, p. 18), was assumed to be distributed within a cylinder with uniform mass density. The rationale for this conservative assumption was to provide the set of bounding results, while simplifying the finite element representation.

2.3.2 Thermal

The assumptions in this section are used throughout Section 4.

2.3.2.1 It is assumed that the DHLW glass filling the Hanford 4.5-m- (15-ft-) long canister has an age of zero. The rationale is that there is no criterion for minimum aging time of the DHLW glass. This assumption may result in conservative temperature results.

2.3.2.2 It is assumed that a 2-D finite element representation of a cross section of the WP will be representative of the hottest portion of the WP. The rationale for this assumption is that axial heat transfer does not significantly affect the solution (i.e., the flow of heat in the radial direction is assumed to dominate the solution since the WP internal components have uniform heat generation and material properties along the WP axis, and the WP is a cylinder with a length approximately 2.5 times larger than its diameter).

2.3.2.3 The thermal conductivity of helium at atmospheric pressure is assumed to be representative of the conditions which helium will experience in the WP. The rationale of this assumption is the fact that one atmosphere fill pressure at ambient temperature is representative of the industry standard for storage casks. CRWMS M&O (1995, p. 10) states the highest pressure to which storage casks may be filled is approximately 1.5 atmospheres. Also, most industry vendors use substantially lower pressure in their designs. Although the internal pressure of the WP will increase due to the temperature rise, according to Bird (1960, p. 255) the thermal conductivity of most gasses is pressure independent. Thus, using the thermal conductivity at atmospheric pressure is reasonable.

2.3.2.4 Modeling only conduction and radiation heat transfer is assumed to provide conservative results. The rationale for this assumption is that although the fill gas in the WP will allow a convective heat transfer path to exist, the natural convective heat transfer will have a small or negligible impact on the total heat transfer. CRWMS M&O (1997a, Attachment X) estimates the effect of the convective heat transfer inside the 5-DHLW WP. The analysis indicates a potential for convection cells to develop in the larger cavities near the top and sides of the WP internals. Convection will likely not play a role in transferring heat near the bottom of the WP where heat transfer will be clearly dominated by conduction and thermal radiation. The total impact of convection on heat transfer within the WP is estimated to be less than 10%. Thus, the problem may be modeled with only the dominant heat transfer modes with a slightly conservative impact upon the results.

2.3.2.5 The equations for unirradiated graphite are used to calculate the thermal conductivity of the graphite block. The rationale for this assumption is that for the time frame considered (1 to 10^6 years) the thermal conductivity of the DOE SNF canister internal components has a negligible effect on the DHLW glass temperature.

2.3.2.6 The volume of glass contained in the Hanford 4.5-m- (15-ft-) long canister is assumed to be 1.08 m^3. The rationale for this assumption is the glass volume information taken from Picha (1997, Table RL-3). The difference between this value and the actual value is anticipated to have a negligible effect on any results reported.

2.3.2.7 The fill gas used in the DOE SNF canister is assumed to be air. In DOE (1999b, p. 6) it is indicated that the DOE SNF canister shall be backfilled with an inert cover gas (e.g., helium). The rationale for this assumption is that for the time frame considered (1 to 10^6 years) the thermal conductivity of the DOE SNF canister internal components has a negligible effect on the DHLW glass temperature.

2.3.3 Shielding

The assumptions in this section are used throughout Section 5.

2.3.3.1 It is assumed that the density of the SRS DHLW glass (which is assumed to fill the Hanford DHLW glass canisters; see Assumption 2.3.6.2) is 2.56 g/cm^3. The density of the SRS DHLW glass may vary between 2.56 and 2.75 g/cm^3 according to Plodinec and Marra (1994, p. 22). Stout and Leider (1991, p. 2.2.1.1-4) gives an upper limit for the glass density of 2.85 g/cm^3. The rationale for this assumption is a lower glass density provides conservative (higher) gamma dose rates.

2.3.3.2 It is assumed that the 4.5-m-long DHLW glass canisters are cylinders of nominal length, wall thickness, and outer diameter. Thus, the head and neck of the canisters are neglected. The rationale for this assumption is that radiation transport in the upper part of the canister is not affected because this portion of the canister is empty and the wall thickness is maintained.

2.3.3.3 It is assumed that the components of a FSVR fuel element are homogeneously mixed inside each element volume. The rationale for this assumption is that the homogenization of the components inside the element volume statistically gives the same WP surface dose rate as does the heterogeneous representation (as demonstrated in CRWMS M&O 1998e, pp. 22-23).

2.3.4 Degradation and Geochemistry

The assumptions in this section are used throughout Sections 6.

2.3.4.1 It is assumed that the solutions that drip into the WP will have the major ion composition of J-13 well water as given in DTN: MO0006J13WTRCM.000. The rationale for this assumption is that the groundwater composition is controlled largely by transport through the host rock, over pathways of hundreds of meters, and the host rock composition is not expected to change substantially over 10^6 years. The assumption that the water entering the WP can be approximated by the J-13 well water implicitly assumes that any effects of contact with the engineered materials in the drift will be minimal after a few thousand years. For a few thousand years after emplacement, the composition may differ because of perturbations resulting from reactions with engineered materials and from the thermal pulse. These are not taken into account in the geochemistry calculation because the outer shell and inner liner are not expected to breach until after that perturbed period. Therefore, the early perturbation is not relevant to the calculations reported in this document. This assumption is justified by previous evaluations of codisposal WPs (CRWMS M&O 1998a) which show that degradation of the WP materials (specifically, DHLW glass and steel) overwhelms the native chemistry of the incoming water (Figures 5-2 through 5-20 of CRWMS M&O 1998a show pH variations of 3 to 10 in the WP).

2.3.4.2 It is assumed that an aqueous solution fills all voids within the WP. The rationale for this assumption is that it provides the maximum degradation rates of WP components

with the potential for precipitation of radionuclides within the WP or the flushing of radionuclides from the WP, and is therefore conservative.

2.3.4.3 It is assumed that water may circulate freely enough in the partially degraded WP that all degraded solid products will react with each other through the aqueous solution medium. The rationale for this assumption is that it provides the most rapid aqueous degradation and is, therefore, conservative with respect to criticality.

2.3.4.4 It is assumed that data in the 25°C thermodynamic database can be used for the calculation. The rationale for this assumption is that even though the initial breach of the WP may occur when the WP contents are at temperatures ~ 50°C (DOE 1998a, Figures 3-20 through 3-22), at times > 25,000 years the WP temperatures are likely to be close to 25°C. It is further assumed that the changes made to the thermodynamic database ("data0.ymp.R0", DTN: MO0009THRMODYN.001) effectively predict the local equilibrium state of the system during the reaction-path calculation and minor adjustments made to the database do not negatively impact the calculations.

2.3.4.5 In general, it is assumed that chromium and molybdenum will oxidize fully to chromate (or dichromate) and molybdate, respectively. This assumption is based on the available thermodynamic data (DTN: MO0009THRMODYN.001), which indicate that in the presence of air, the chromium and molybdenum would both oxidize to the VI valence state. The rationale for this assumption is that by allowing the Cr and Mo to oxidize, the pH of the system will be lowered allowing most of the U to remain in the WP. This is conservative for internal criticality.

2.3.4.6 It is assumed that sufficient decay heat is retained within the WP over times of interest to cause convective circulation and mixing of the water inside the WP. The rationale for this assumption is based on CRWMS M&O (1996, Attachment VI). This assumption is conservative for internal criticality since the increased circulation and mixing of water inside the WP increases the reaction rates, therefore the degradation processes that lead to potentially critical configurations will occur faster.

2.3.4.7 It is assumed that the rate of entry of water into, as well as the rate of egress from, a WP is equal to the rate at which water drips onto the WP. The rationale for this assumption is that for most of the time frame of interest, i.e., long after the outer barriers become largely degraded, it is more reasonable to assume that all or most of the dripping water will enter the degraded WP than to assume that a significant portion will instead be diverted around the remains. However, the calculations include scenarios with very low drip rates, which effectively simulate diversion of the bulk of the water striking the WP.

2.3.4.8 It is assumed that gases in the WP solution remain in equilibrium with the ambient atmosphere outside the WP. In other words, contact of WP fluids with the gas phase in the repository is envisioned to be sufficient to maintain equilibrium with the CO_2 and O_2 present, whether or not this gas phase is the normal atmosphere in open air or rock, which seeps out of the adjacent tuff. Moreover, the specific partial pressures of CO_2 and O_2 of the ambient repository atmosphere are set to $10^{-3.0}$ and $10^{-0.7}$ atm respectively. The

rationale for the oxygen partial pressure is that it is equivalent to that in the atmosphere (Weast 1977, p. F-210). The rationale for choosing the carbon dioxide pressure is to reflect the observation that J-13 well water appears to be in equilibrium with above-atmospheric carbon dioxide levels (Yang 1996, Tables 7 and 8).

2.3.4.9 It is assumed that precipitated solids remain in place and are not mechanically eroded or entrained as colloids in the advected water. The rationale for this assumption is that since dissolved fissile material (U) may be absorbed on colloids (clays, iron oxides) or may be precipitated as colloids during WP degradation, it is conservative, for internal criticality, to assume that all precipitated solids, including mobile colloids, will be deposited inside the WP rather than transported out of the WP.

2.3.4.10 It is assumed that the most insoluble solids for a fissile radionuclide will form. The rationale for this assumption is that the approach is conservative with respect to internal criticality since it will lead to the maximum retention of fissile material within the WP during EQ6 runs.

2.3.4.11 In the EQ6 calculations for the FSVR WP it is assumed that the graphite block holding the fuel compacts in place is chemically inert, therefore it was not used in the calculations except for use in calculations of volumes. The rationale for this is that graphite degrades very slowly (Propp 1998) and during the time period investigated the degradation of graphite would be negligible.

2.3.5 Intact and Degraded Component Criticality

The assumptions in this section are used throughout Section 7.

2.3.5.1 For the degraded component criticality calculations, it is assumed that the iron in the stainless steel degrades to goethite (FeOOH) rather than hematite (Fe_2O_3). The rationale for this assumption is that it is conservative to consider goethite rather than hematite since hydrogen (moderator) is a component of goethite. All the other constituents of steel are neglected since they are neutron absorbers, and, hence, their absence provides a conservative (higher) value of the k_{eff} of the system.

2.3.5.2 The length of the fuel in the fuel elements is assumed to be the same as the length of the fuel elements rather than the actual length of the fuel holes, which is slightly smaller. This gives a larger void fraction and thus the potential for more water in the fuel. This is a conservative assumption since it is shown (Section 7.3, Table 7-2) that it is more reactive to have more water in the fuel, i.e., this gives a higher value of the k_{eff} for the system.

2.3.5.3 A most reactive fissile concentration is used for the FSVR fuel that is shown (BSC 2001e, Table 12) to bound fuel compositions for actual fuel elements. These selected fuel compositions use the larger fissile masses from either the beginning-of-life (BOL) or end-of-life (EOL), neglect any U-238 and use EOL values for Th-232. These selected compositions are conservative since they maximize the fissile isotope content while minimizing the effect of neutron absorbers. Therefore, the fuel composition used for the

FSVR fuel is even more conservative since it bounds these actual (conservative) compositions.

2.3.6 General

The assumptions in this section are used in Section 2 through 7.

2.3.6.1 It is assumed that the limits for Th/U carbide fuel group, which are established by the technical information related to the FSVR SNF (Taylor 2001), are bounding. The rationale for this assumption is that the technical information for a representative fuel type was supplied for criticality and related design calculations as a bounding case within each fuel group. The fuel grouping is the activity in which the DOE SNF program has evaluated the parameters and properties of the DOE SNF important to criticality, design events, and performance assessment, and categorized the DOE SNF into fuel groups. Therefore, the burden is placed on the custodian of the SNF to demonstrate, before acceptance of SNF by BSC that SNF characteristics identified as important to criticality control or other analyses herein are not exceeded.

2.3.6.2 It is assumed that the high-level radioactive waste glass that fills the 4.5-m-long glass pour canisters is the SRS Design-Basis DHLW glass. The rationale for this assumption is that the Hanford HLW glass composition is not known at this time and the characteristics of the two types of glass are expected to be similar. The composition of SRS Design-Basis DHLW glass is taken from CRWMS M&O (1999a, p. 7). Also, radiation source terms of the SRS Design-Basis DHLW glass bound the source terms of all projected high-level radioactive waste glass forms (CRWMS 2000c, Attachments V and VI), and generates conservative (higher) dose rates at the external surfaces of the WP.

2.4 BIAS AND UNCERTAINTY IN CRITICALITY CALCULATIONS

The purpose of this section is to document the MCNP (Monte Carlo particle transport code, Version 4B2LV, CRWMS M&O 1998c; used in the criticality and shielding analyses supporting this document) evaluations of laboratory critical experiments performed as part of the Disposal Criticality Analysis Methodology program. Only laboratory critical experiments relevant to FSVR SNF were studied. Laboratory Critical Experiment results listed in this section are given in CRWMS M&O (1999c) for the high enriched uranium systems typical of FSVR fuel and in CRWMS M&O (1997b and 1999f) for the high enriched uranium solution systems. The objective of this analysis is to quantify the ability of the MCNP Version 4B2LV code system to accurately calculate the k_{eff} for various configurations. Continuous-energy cross sections processed from the evaluated nuclear data files ENDF/B-V were used in the MCNP calculations (Briesmeister 1997, Appendix G). These cross section libraries are part of the MCNP code system that has been obtained from the Software Configuration Management in accordance with appropriate procedures. Each of the critical core configurations was simulated, and the results reported from the MCNP calculations are the combined average values of k_{eff} from the three estimates (collision, absorption, and track length) and the standard deviation (σ) of these results listed in the final summary in the MCNP output. When MCNP underpredicts the experimental k_{eff}, the experimental uncertainty is added to the uncertainty at 95% confidence from the MCNP

calculation to obtain the bias. This bias along with the 5% margin (see Section 2.2.5) is used to determine the interim critical limit for all MCNP calculations of the WP with FSVR SNF in the DOE SNF canister.

2.4.1 Benchmarks Related to Intact WP Configurations

Several surrogate critical experiments with highly enriched uranium fuel rods are used for the FSVR fuel with respect to intact criticality analyses: HEU-COMP-THERM-003, HEU-COMP-THERM-005, HEU-COMP-THERM-006, HEU-COMP-THERM-007, HEU-COMP-THERM-010, and HEU-MET-FAST-019 (NEA 1998).

A series of critical experiments with water-moderated hexagonally-pitched lattices of highly enriched fuel rods of cross-shaped cross section was performed over several years in the Russian Research Center "Kurchatov Institute." The twenty-two experiments analyzed under this category in this report consist of the following:

1. Fifteen critical two-zone lattice experiments corresponding to different combinations of inner and peripheral zones of cross-shaped fuel rods at two pitches. For detailed descriptions of these experimental configurations see pages 2, and 7 through 14 of NEA (1998), HEU-COMP-THERM-003 (HCT-003).

2. One critical configuration of hexagonal pitched clusters of lattices of fuel rods with copper (Cu) rods. Detailed experimental configuration descriptions are available on pages 2 through 8 of NEA (1998), HEU-COMP-THERM-005 (HCT-005).

3. Three critical configurations with uniform hexagonal lattices with pitch values of 5.6, 10.0, and 21.13 mm. Detailed experimental configuration descriptions are available on pages 2, 5, and 6 of NEA (1998), HEU-COMP-THERM-006 (HCT-006).

4. Three critical configurations with double hexagonal lattices of fuel rods and zirconium (Zr) hydride rods. Detailed experimental configuration descriptions are available on pages 2 through 8 of NEA (1998), HEU-COMP-THERM-007 (HCT-007).

The pitch and number of fuel rods were the parameters that were varied. The maximum deviation from unity for this set of calculations was 0.019 (CRWMS M&O 1999c, pp. 16 through 19, and 76).

Twenty-one critical experiments involving water-moderated lattices of Experimental Beryllium Oxide Reactor fuel pins were performed in 1967 at Oak Ridge National Laboratory. The fuel pins consisted of ceramic pellets contained in Hastelloy X-280 tubes. The pellets were a homogeneous mixture of UO_2 (enriched 62.4 wt% in U-235) and BeO. Detailed experimental configuration descriptions are available in NEA (1998, HEU-COMP-THERM-010, pp. 1 through 15). The lattice configuration, number of rods, and neutron absorber (boron) concentration were the parameters that were varied. The maximum deviation from unity for this set of calculations was 0.016 (CRWMS M&O 1999c, pp. 30, 84, and 85).

A single experiment with a graphite-reflected U-235 (enriched 90 wt%) spherical assembly was performed in 1962 at the Russian Scientific Research Institute of Experimental Physics. The detailed experimental configuration description is available in NEA (1998, HEU-MET-FAST-019, pp. 1 through 7). The maximum deviation from unity for this set of calculations was 0.010 (CRWMS M&O 1999c, pp. 53 and 97).

2.4.2 Benchmarks Related to Degraded WP Configurations

Critical experiments with highly enriched (approximately 90 wt%) uranium nitrate solutions are described in detail in NEA (1998) (HEU-SOL-THERM-001, HEU-SOL-THERM-002, HEU-SOL-THERM-003). The concentration of fissile element in the solution, enrichment, reflector type and thickness, tank diameter, and solution height were among the parameters that were varied. The maximum deviation from unity for this set of experiments was 0.020 (CRWMS M&O 1997b, pp. 26 through 32; 1999f, pp. 14-18).

Critical experiments with highly enriched U-233 (approximately 97.7 wt.%) nitrate solution are described in detail in NEA (1998) (U233-SOL-THERM-001, U233-SOL-THERM-008). The concentration of fissile and neutron absorber (boron) in the solution, and tank diameter were among the parameters that were varied. The maximum deviation from unity for this set of experiments is 0.018 (CRWMS M&O 1999f, pp. 23 and 24).

2.4.3 Interim Critical Limit

The maximum deviation from unity was used as the bias for the purpose of this report. The worst-case bias, which is the maximum bias of the MCNP simulations of the experiments described in Sections 2.4.1 and 2.4.2, was 0.020. This bias includes the bias in the method of calculation and the uncertainty in the experiments. Based on this bias, a conservative interim critical limit is determined to be 0.93 after allowance for a 5 percent margin, for the bias in the method of calculation, and the uncertainty in the experiments used to validate the method of calculation.

INTENTIONALLY LEFT BLANK

3. STRUCTURAL ANALYSIS

3.1 USE OF COMPUTER SOFTWARE

The finite element analysis computer codes used for the structural evaluations were ANSYS Version (V) 5.6.2 (CRWMS 2000k) and Livermore Software Technology Corporation (LSTC) LS-DYNA V950 (CRWMS M&O 2000j). The information regarding these codes and their uses for the structural analysis is documented in BSC (2001a).

3.2 DESIGN ANALYSIS

Finite element solutions resulted from structural analyses for the components of the 5-DHLW/DOE SNF-long WP. A detailed description of the finite element representations, the method of solution, and the results are provided in BSC (2001a). The results presented here, in terms of maximum stress intensities, were compared to the design criteria obtained from the 1995 American Society of Mechanical Engineers (ASME) Boiler and Pressure Vessel Code (BPVC) with 1997 Addenda, Section III, Appendix F (Sections F-1340 and F-1341). Conclusions can be drawn regarding the structural performance of the 5-DHLW/DOE SNF-long WP design using the stated criteria. The results of the calculation meet the criteria specified in Table 3-1. The structural performance of the DHLW canister is not evaluated in this report.

The design approach for determining the adequacy of a structural component is based on the stress limits given in the 1995 ASME BPVC with 1997 Addenda. S_u is defined as the ultimate tensile strength of the materials and is compared to the design stress intensity of the materials. Table 3-1 summarizes design criteria as obtained from appropriate sections of the 1995 ASME BPVC. All three conditions must be met.

Table 3-1. Containment Structure Allowable Stress-Limit Criteria

Category	Containment Structure Allowable Stresses Accident Conditions (ASME 1995 w/ 1997 Add., Division 1, Appendix F, Article F-1341.2)
Primary membrane stress intensity	$0.7S_u$
Maximum primary stress intensity	$0.9S_u$
Average primary shear stress across a section loaded in pure shear	$0.42S_u$

3.3 CALCULATIONS AND RESULTS

3.3.1 Description of the Finite Element Representation

A full three-dimensional finite element representation of the WP and the DOE SNF standardized canister was developed in ANSYS V5.6.2 by using the dimensions provided in Appendix A. The finite element representation was created with the largest possible radial gap of 4 mm between the inner and outer shells (CRWMS M&O 2000g, Section 8.1.8). The initial orientation of the inner shells maintains this 4-mm gap around the circumference of the shell.

The structure of the DHLW glass canister, was reduced to a cylinder of uniform mass density (Assumptions 2.3.1.2 and 2.3.1.3). The total mass and geometric dimensions of the DHLW canister define the density. The benefit of using this approach was to reduce the computer execution time while preserving all features of the problem relevant to the structural calculation.

The target surface was conservatively assumed to be unyielding with a large elastic modulus (Assumption 2.3.1.1).

The initial tip-over angle with respect to the horizontal plane was reduced to 0.1°, and the WP was given an initial angular velocity corresponding to the rigid-body motion of the WP (BSC 2001a, Section 5.5). This configuration reduces the computer execution time while preserving all features of the problem relevant to the structural calculation.

The finite element representation was solved using LS-DYNA V950 to perform the transient dynamic analysis for the 5-DHLW/DOE SNF-long WP tip-over design basis event at room temperature (20 °C), 204 °C, and 316 °C.

LS-DYNA uses true stress and true strain as material property inputs. The ASME Code reports only engineering stress and engineering strain. The material properties needed to be converted to the proper form in order for the solution to execute correctly. Table 3-2 reports the true ultimate tensile strength (σ_u) for Alloy 22 and SS 316NG. σ_u values are given in BSC (2001a, p. 14). σ_u should be substituted for S_u in Table 3-1 in order to remain consistent.

Table 3-2. True Stress of Alloy 22 and SS 316NG

Temperature	σ_u of Alloy 22 (MPa)	σ_u of SS 316 (MPa)	σ_u of SS 316L (MPa)
Room Temperature (20 °C)	971	703	575
204 °C	926	675	511
316 °C	885	673	506

3.3.2 Results of Structural Calculations

The results obtained from LS-DYNA V950 were reported in terms of maximum shear stress. Since the maximum stress intensities were desired, the results needed to be converted. The maximum shear stress is defined as one-half the difference between maximum and minimum principal stress (Shigley and Mischke 1989, p. 31). Stress intensity is defined as the difference between maximum and minimum principal stress. Therefore, the results obtained from LS-DYNA V950 were multiplied by two to obtain the corresponding stress intensities.

The maximum stresses were found by carefully examining each time step taken by LS-DYNA V950, which outputs the element with the highest magnitude of stress, at each step, for each defined part. Table 3-3 lists the maximum stress intensities in the outer shell and inner shell at room temperature, 204 °C, and 316 °C.

Table 3-3. Maximum Stress Intensities Comparison

Temperature	Maximum Stress Intensity in the WP Outer Shell (MPa)	Trunnion Collars (MPa)	$0.9\sigma_u$ of Alloy 22 (MPa)	Maximum Stress Intensity in the WP Inner Shell (MPa)	$0.9\sigma_u$ of SS 316[a] (MPa)	Maximum Stress in the DOE SNF Canister (MPa)	$0.9\sigma_u$ of SS 316L[a] (MPa)	FSVR Fuel Elements
Room Temperature	575	724	874	370	633	561	518	716
204 °C	520	644	833	337	608	515	460	556
316 °C	505	632	797	325	606	504	455	572
316 °C (with modified elongation)	495	634	820	355	557	578	432	564

Source: BSC 2001a, Section 5.1 and Table 1.

NOTE: [a]The material properties of SS 316 are the same as SS 316NG.

Table 3-3 shows that for each temperature condition, the maximum stress intensity was less than the allowable for the WP outer and inner shells, and higher than the allowable for the DOE SNF canister.

Since the WP is not internally pressurized, the stress intensity consists primarily of bending stresses. In this case, the membrane stress is close to or approaches zero and meets the first criterion in Table 3-1.

During the tip-over calculation, no components were loaded in pure shear.

The ultimate tensile strength of graphite H-327 at 25 °C (which is the lowest of the two types of graphite used) is 6.481 MPa in the radial direction (Table 2-4). This value is two orders of magnitude less than the calculated value shown in Table 3-3 (669 MPa), therefore it is expected that the graphite blocks inside the DOE SNF canister will fail during a tip-over event.

3.4 SUMMARY

Table 3-1 states the applicable criteria, according to paragraph F-1341.2 of the 1995 ASME BPVC with 1997 Addenda, Section III, Appendix F.

The primary membrane stress intensity is at or near zero (therefore lower than $0.7\sigma_u$) since the WP is not pressurized. Therefore, the first criterion in Table 3-1 is met.

Table 3-3 clearly shows the highest stress calculated during tip-over is lower than $0.9\sigma_u$ for the WP outer shell, inner shell, and the DOE SNF canister. Therefore, the second criterion in Table 3-1 is met.

None of the components are loaded in pure shear during tip-over. The third and final criterion in Table 3-1 is met. Therefore, the WP meets the safety standards stated in Appendix F of the 1995 ASME BPVC with 1997 Addenda.

The 5-DHLW/DOE SNF-long WP internal design with a DOE SNF canister loaded with FSVR SNF meets the SDD Criterion 1.2.2.1.6 (Section 2.2.1.4) if the DOE SNF canister loaded mass limit (2,721 kg) and the DHLW glass canisters mass limit (4200 kg) are not exceeded.

4. THERMAL ANALYSIS

4.1 USE OF COMPUTER SOFTWARE

The finite element analysis computer code used for the thermal evaluations was ANSYS Version (V) 5.4 (CRWMS M&O 1998b). The information regarding the code and its use for the thermal analysis is documented in BSC (2001b). Version 5.4 was used because Version 5.6.2 could not be used for times past 60 years from WP emplacement in the monitored geologic repository.

4.2 THERMAL DESIGN ANALYSIS

A detailed description of the finite element representations, the method of solution, and the results are provided in BSC (2001b). The finite element representations were created as a 2-D representation. The 2-D method was chosen because it was assumed that radial heat transfer will dominate the solution and that axial heat transfer will be minor (see Assumption 2.3.2.2).

The boundary conditions on the outer surface of the WP were taken from CRWMS M&O (2000a, Table 6-18). The actual numbers are from an initial 50-year forced ventilation period with 0.1 m spacing between WPs and no backfill. The WP is loaded with five Hanford 4.5-m- (15-ft-) long DHLW glass canisters and one DOE SNF canister containing FSVR SNF. The WP cross section was modeled (taking advantage of symmetry) and the boundary conditions were applied. However, the detail of the FSVR fuel element in the center of the WP required too many elements to make a feasible finite element representation. Therefore, the FSVR fuel element was given distributed properties in the large model. The boundary temperatures were saved and applied to a second finite element representation of the FSVR fuel element only, to obtain an accurate, continuous temperature profile from the center of the WP to the edge of its outer shell.

The time period covered by the thermal analysis was from the time of WP emplacement in the monitored geologic repository to 1,000 years after emplacement. This ensures that the time when the maximum temperatures inside the WP will be experienced, is covered.

4.3 CALCULATIONS AND RESULTS

The maximum thermal output of the 5-DHLW/DOE SNF-long WP loaded with FSVR SNF is 1,037 W. This value was calculated using the thermal outputs of the Hanford DHLW canister and DOE SNF canister containing FSVR SNF at the time of WP emplacement in the monitored geologic repository ($5 \cdot 52.21$ W + 776 W = 1,037 W; the values were taken from Tables 2-7 and 2-8).

Figure 4-1 shows the plot of temperature versus time for three positions across the DHLW glass canisters. The location nearest the center of the WP is labeled "inner". The location farthest from the center of the WP is labeled "outer". The location labeled "middle" is between "inner" and "outer" locations.

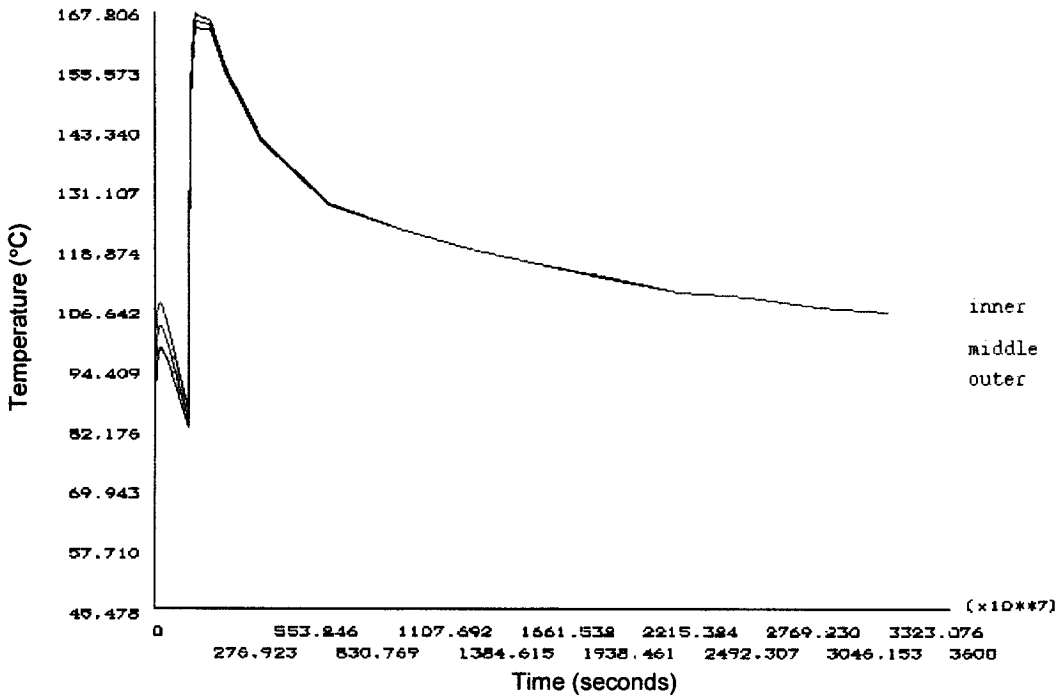

Source: BSC 2001b, p. 22.

Figure 4-1. Plot of Temperature Versus Time at Points along WP Radius

Figure 4-2 shows the plot of temperature versus time for the maximum and minimum values for the FSVR fuel element. In Figure 4-2 the two plots are indistinguishable, therefore they can be seen as only one curve.

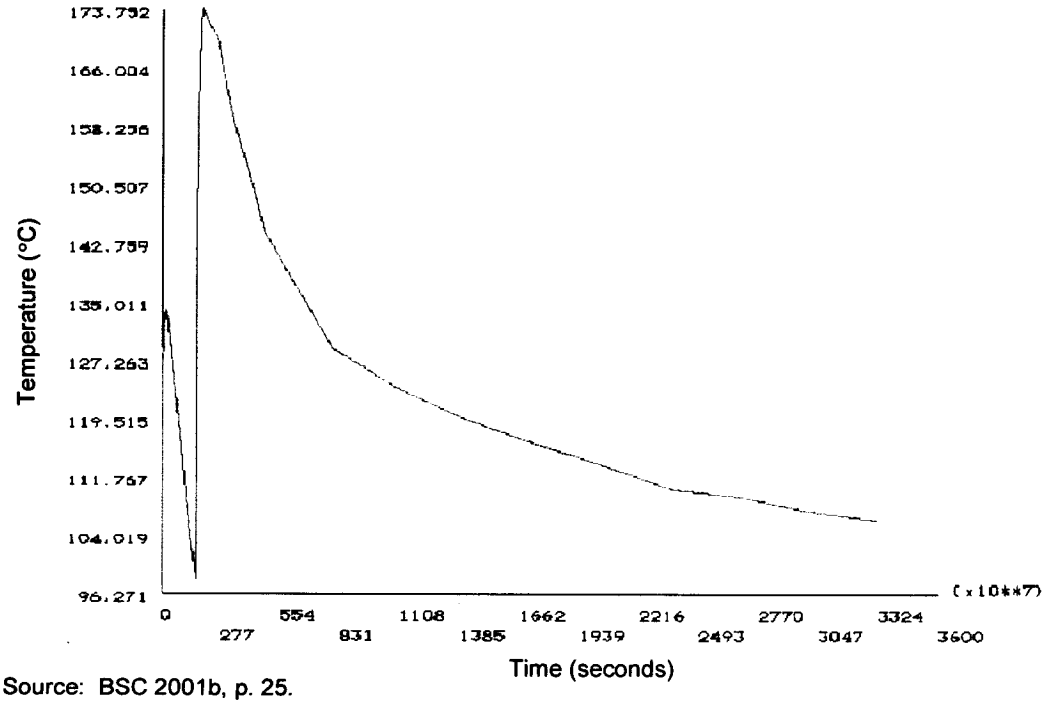

Source: BSC 2001b, p. 25.

Figure 4-2. Plot of Temperature Versus Time for the FSVR SNF Element

Figures 4-1 and 4-2 show a rapid temperature increase immediately after WP emplacement, followed by a drop that continues until the 50 years (i.e., $1.578 \cdot 10^9$ seconds) forced ventilation period ends. Then another rapid increase and peaking of the temperature is followed by a slow decrease as the fission products in the FSVR SNF continue to decay.

4.4 SUMMARY

The temperature between any two points in the FSVR SNF element did not vary by more than 1 °C at any time (see Figure 4-2). The maximum temperature in the FSVR SNF element was 173.8 °C and was attained at 59 years after WP emplacement.

The maximum DHLW glass temperature for the 5-DHLW/DOE SNF-long WP loaded with FSVR SNF was 167.4 °C at 59 years after WP emplacement. This temperature is less than the SDD criterion of 400 °C (Section 2.2.2.1). The maximum thermal output of the 5-DHLW/DOE SNF-long WP loaded with FSVR SNF is 1,037 W, which is less than the SDD criterion of 11,800 W (Section 2.2.2.2).

INTENTIONALLY LEFT BLANK

5. SHIELDING ANALYSIS

5.1 USE OF COMPUTER SOFTWARE

The Monte Carlo particle transport code, MCNP, Version 4B2LV (CRWMS M&O 1998c), was used to calculate average dose rates at the external surfaces of the WP. The information regarding the code and its use for the shielding analysis is documented in BSC (2001c).

5.2 DESIGN ANALYSIS

The Monte Carlo method for solving the integral radiation transport equation, which is implemented in the MCNP computer program, is used to calculate radiation dose rates for the WPs. MCNP uses continuous-energy cross sections processed from the evaluated nuclear data files ENDF/B-V (Briesmeister 1997, Appendix G). These cross-section libraries are part of the qualified MCNP code. The flux averaged over a surface tally is specified in calculations and the neutron and gamma flux-to-dose rate conversion factors, which were extracted from the American National Standard Institute/American Nuclear Society (ANSI/ANS) Standard 6.1.1-1977, are applied to obtain surface dose rates.

5.3 CALCULATIONS AND RESULTS

BSC (2001c) gives the details of the calculations and the results. The geometric representation of the WP used in the MCNP calculations is shown in Figure 5-1. The WP contains two different radiation sources (see Section 2.1.7), which are volumetric sources uniformly distributed inside the FSVR element stack (see Assumption 2.3.3.3) and the glass volume, respectively.

In the calculation, the external surfaces of the WP are divided into segments and the dose rate is averaged over each segment to evaluate the spatial distribution of the dose rate. Figures 5-2 and 5-3 show the radial and axial segments used in the dose-rate calculations. The radial surface, between the bottom and top planes of DHLW glass, is equally divided into five segments, each of which is 73.61-cm high. The first radial segment (segment 1), 93.65-cm high, corresponds to the empty portion of the DHLW canister, which is between the top of the WP cavity and the top of the DHLW glass. The WP top and bottom axial surfaces are divided into two radial segments of 0-30 cm (segment 7) and 30-101.5 cm (segment 8). For this WP, the DOE canister is positioned in the center of the WP and the gamma source intensity of the FSVR SNF is approximately half of that of each individual DHLW glass canister. Therefore, it is expected that the gamma radiation generated inside the DHLW glass canisters are the primary contributors to the doses on the axial segments of the WP external surface between the bottom and top planes of the glass canisters (segments 2 through 6). To evaluate any angular dependence of the WP radial dose, the radial surface is divided into ten equal angular segments, as shown in Figure 5-3. The angular segments adjacent to the DHLW glass canister are denoted by "Segment B" and the other segments are denoted as "Segment A" since only statistical variations of the dose rate averaged over each of these two angular segments are expected.

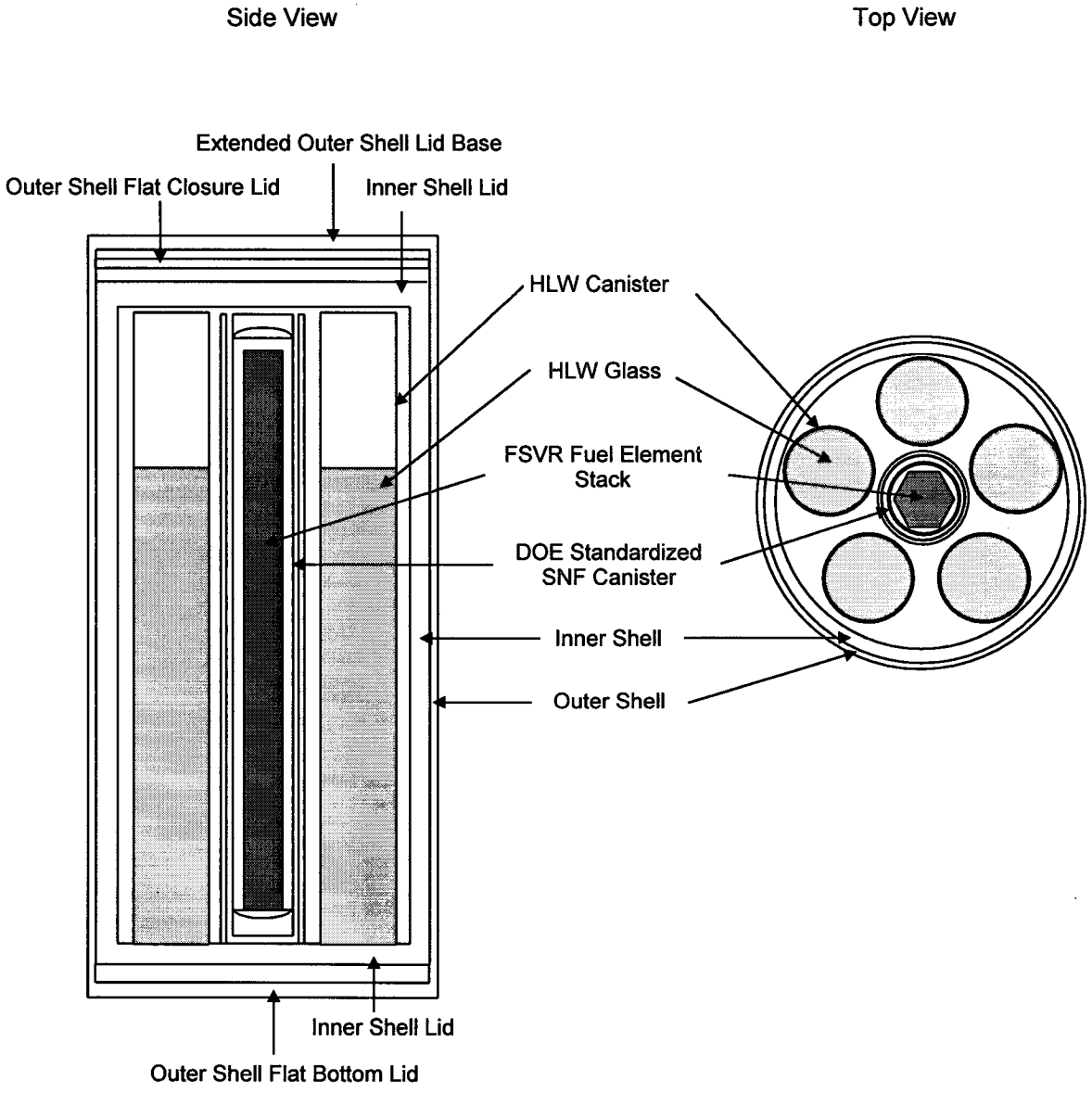

Figure 5-1. Vertical and Horizontal Cross Sections of MCNP Geometry Representation

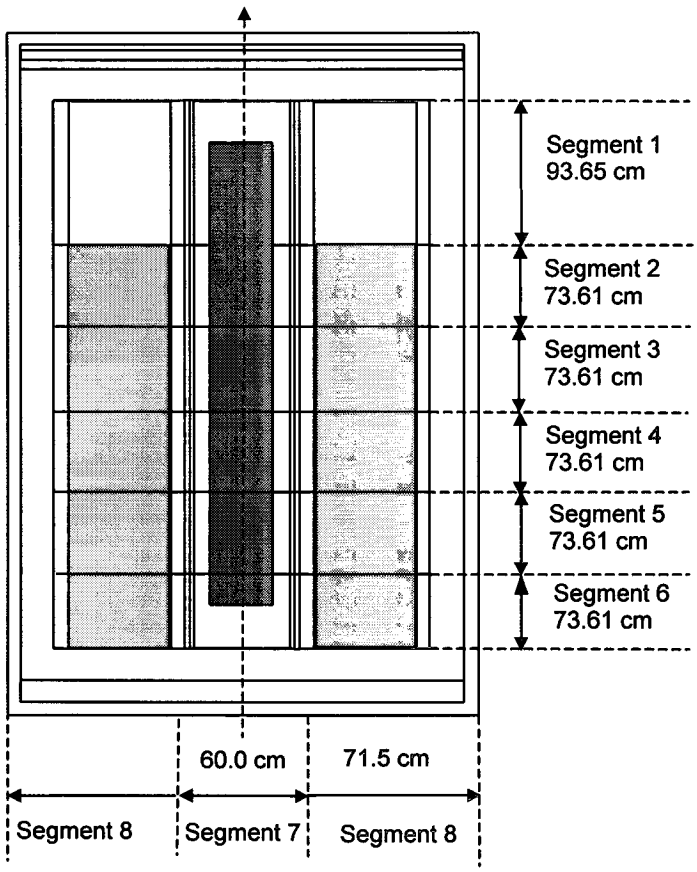

Figure 5-2. Surfaces and Segments (axial and radial) Used for Dose Rate Calculations

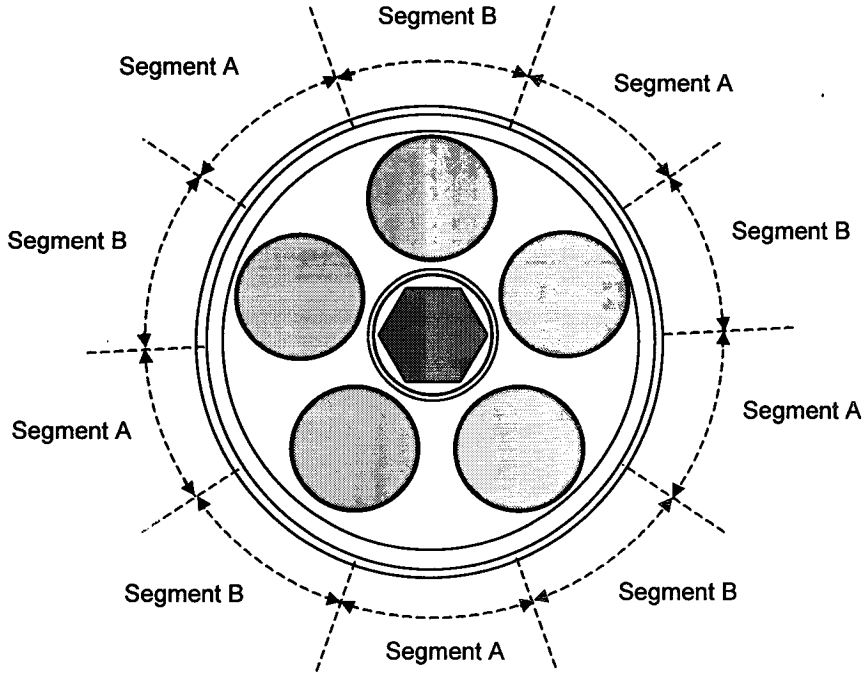

Figure 5-3. Angular Segments of the WP Outer Radial Surface Used in Dose Rate Calculations

Tables 5-1 and 5-2 provide the radial and axial dose rates on the outer surface of the WP containing the five 4.5-m-long DHLW glass canisters and the DOE SNF canister loaded with FSVR SNF. The dose rates listed in both tables are the upper limits of the 95% confidence intervals of the Monte Carlo dose rate calculations.

Table 5-1. Dose Rates Averaged over Axial and Radial Segments of the WP Outer-Radial and Axial Surfaces

Location	Gamma Dose Rate (rem/h)	Neutron Dose Rate (rem/h)	Total Dose Rate (rem/h)
Radial surface: Segment 1	20.639	0.029	20.668
Radial surface: Segment 2	88.732	0.081	88.812
Radial surface: Segment 3	94.363	0.095	94.458
Radial surface: Segment 4	95.214	0.096	95.309
Radial surface: Segment 5	94.346	0.095	94.440
Radial surface: Segment 6	84.535	0.083	84.616
Bottom surface: Segment 7	2.841	0.046	2.886
Bottom surface: Segment 8	3.632	0.038	3.670
Top surface: Segment 7	1.071	0.012	1.083
Top surface: Segment 8	0.681	0.012	0.693

Source: BSC 2001c, Tables 19 and 22.

Table 5-2. Dose Rates Averaged Over Angular Segments of the WP Outer-Radial Surface

Axial Location	Angular Segment A			Angular Segment B		
	Gamma Dose Rate (rem/h)	Neutron Dose Rate (rem/h)	Total Dose Rate (rem/h)	Gamma Dose Rate (rem/h)	Neutron Dose Rate (rem/h)	Total Dose Rate (rem/h)
Segment 1	23.11	0.03	23.14	20.32	0.03	20.35
Segment 2	88.31	0.08	88.39	96.23	0.08	96.32
Segment 3	93.18	0.10	93.28	100.82	0.10	100.91
Segment 4	94.59	0.10	94.69	101.36	0.10	101.46
Segment 5	93.84	0.10	93.93	101.87	0.10	101.97
Segment 6	80.28	0.09	80.36	93.67	0.09	93.75

Source: BSC 2001c, Table 23.

5.4 SUMMARY

A maximum dose rate of 101.97 rem/h occurs at the external radial surface, which is approximately 14 times lower than the maximum dose rate of 1,450 rem/h specified by the design criterion (Section 2.2.3). Axially over the length of the DHLW glass canisters, the dose rate at the outer WP radial surface is approximately uniform. The radial dose rate shows a weak angular dependence. Thus, over the length of the glass canisters (segments 2 through 6), the dose rates on segments B are approximately ten percent higher than those on segments A. For the axial segment corresponding to the empty portion of the glass canister (segment 10), the dose rate on segments A is approximately fifteen percent higher than that on segments B. The dose rates on the bottom and top surfaces of the WP are about four percent, and about one percent of the maximum dose rate on the outer radial surface, respectively. The dose rates in rem/h and rad/h are basically the same due to the insignificant contribution of the neutron dose rate to the total dose rate (less than 0.2%).

6. DEGRADATION AND GEOCHEMISTRY ANALYSIS

6.1 USE OF COMPUTER SOFTWARE

The EQ3/6 geochemistry software package, Version 7.2bLV (CRWMS M&O 1998d, 1999e), was used for the geochemistry evaluations. The information regarding the code and its use for the degradation and geochemistry analysis is documented in BSC (2001d).

6.2 DESIGN ANALYSIS

6.2.1 Systematic Investigation of Degradation Scenarios and Configurations

Degradation scenarios comprise a combination of features, events, and processes that result in degraded configurations to be evaluated for criticality. A configuration is defined by a set of parameters characterizing the amount and physical arrangement, at a specific location, of the materials that can significantly affect criticality (e.g., fissile materials, neutron absorbing materials, reflecting materials, and moderators). The variety of possible configurations is best understood by grouping them into classes. A configuration class is a set of similar configurations whose composition and geometry is defined by specific parameters that distinguish one class from another. Within a configuration class, the values of configuration parameters may vary over a given range.

A master scenario list and set of configuration classes relating to internal criticality is given in the *Disposal Criticality Analysis Methodology Topical Report* (YMP 2000, pp. 3-12 through 3-14) and also shown in Figures 6-1 and 6-2. This list was developed through a process that involved workshops and peer review. The comprehensive evaluation of disposal criticality for any waste form must include variations of the standard scenarios and configurations to ensure that no credible degradation scenario is neglected. All of the scenarios that can lead to criticality begin with the breaching of the WP, followed by entry of water, which eventually leads to degradation of the SNF and/or other internal components (OIC) of the WP.

The standard scenarios for internal criticality divide into two groups:

1. When the WP is breached only on the top, water flowing into the WP collects and fills the WP. This water provides moderation to potentially increase the possibility of criticality. Further, after a few hundred years of steady dripping, the water can overflow through the hole on the top of the WP and flush out any dissolved degradation products.

2. When the WP breach occurs on the bottom as well as the top, the water can flow through the WP. This group of scenarios allows the soluble degradation products to be removed more quickly but does not directly provide water for moderation. Criticality is possible, however, if the WP fills with corrosion products that can retain water and/or plug any holes in the bottom of the WP while fissile material is retained.

The standard scenarios for the first group shown in Figure 6-1, which have the WP breached only at the top, are designated IP-1, -2, and -3 (IP stands for internal to the package) according to whether the waste form degrades before the WP OIC, at approximately the same time (but not

necessarily at the same rate) or later than the WP OIC. The standard scenarios for the second group shown in Figure 6-2, which have the WP breached at both the top and the bottom, are designated IP-4, -5, or -6 based on the same criteria. The internal criticality configurations resulting from these scenarios fall into six generic configuration classes described below (YMP 2000, pp. 3-13 through 3-14). These configuration classes are intended to comprehensively represent the configurations that can result from physically realizable scenarios. As presented here, the configuration classes do not distinguish between WP internal components inside versus outside the DOE SNF canister. It should be noted that the WP studied in this technical report has no added neutron absorbers, no basket structure inside the DOE SNF canister, and no credit is taken for SNF burnup (or fission product neutron absorbers).

1. Basket is degraded but waste form is relatively intact and sits on the bottom of the WP (or the DOE SNF canister) surrounded by, and/or beneath, the basket corrosion products. This configuration class is reached from scenario IP-3.

2. Both basket and waste form are degraded. The sludge at the bottom of the WP is a mixture consisting of fissile material, corrosion products, and iron oxides and may contain clay. It is more complex than for configuration class 1 and is determined by geochemistry calculations as described in BSC (2001d). This configuration class is most directly reached from standard scenario IP-2 in which all the WP components degrade at the same time. However, after many tens of thousands of years the scenarios IP-1 and IP-3, in which the waste form degrades before or after the other components, also lead to this configuration.

3. Fissile material is moved some distance from the neutron absorber, but both remain in the WP. This configuration class can be reached from IP-1.

4. Fissile material accumulates at the bottom of the WP (or the DOE SNF canister), together with moderator provided by water trapped in clay. The clay composition is determined by geochemistry calculations (BSC 2001d). This configuration class can be reached by any of the scenarios, although IP-2 and IP-5 lead to this configuration by the most direct path; the only requirement is that there be a large amount of glass in the WP (as in the codisposal WP) to form the clay.

5. Fissile material is incorporated into the clay, similar to configuration class 4, but with the fissile material not at the bottom of the WP. Generally, the mixture is spread throughout most of the WP volume but could vary in composition so that the fissile material is confined to one or more layers within the clay. Generally, the variations of this configuration are less reactive than for configuration class 4. Either standard scenario IP-1 or IP-4 can reach this configuration class.

6. Fissile material is degraded and spread into a more reactive configuration. This configuration class can be reached by scenario IP-1.

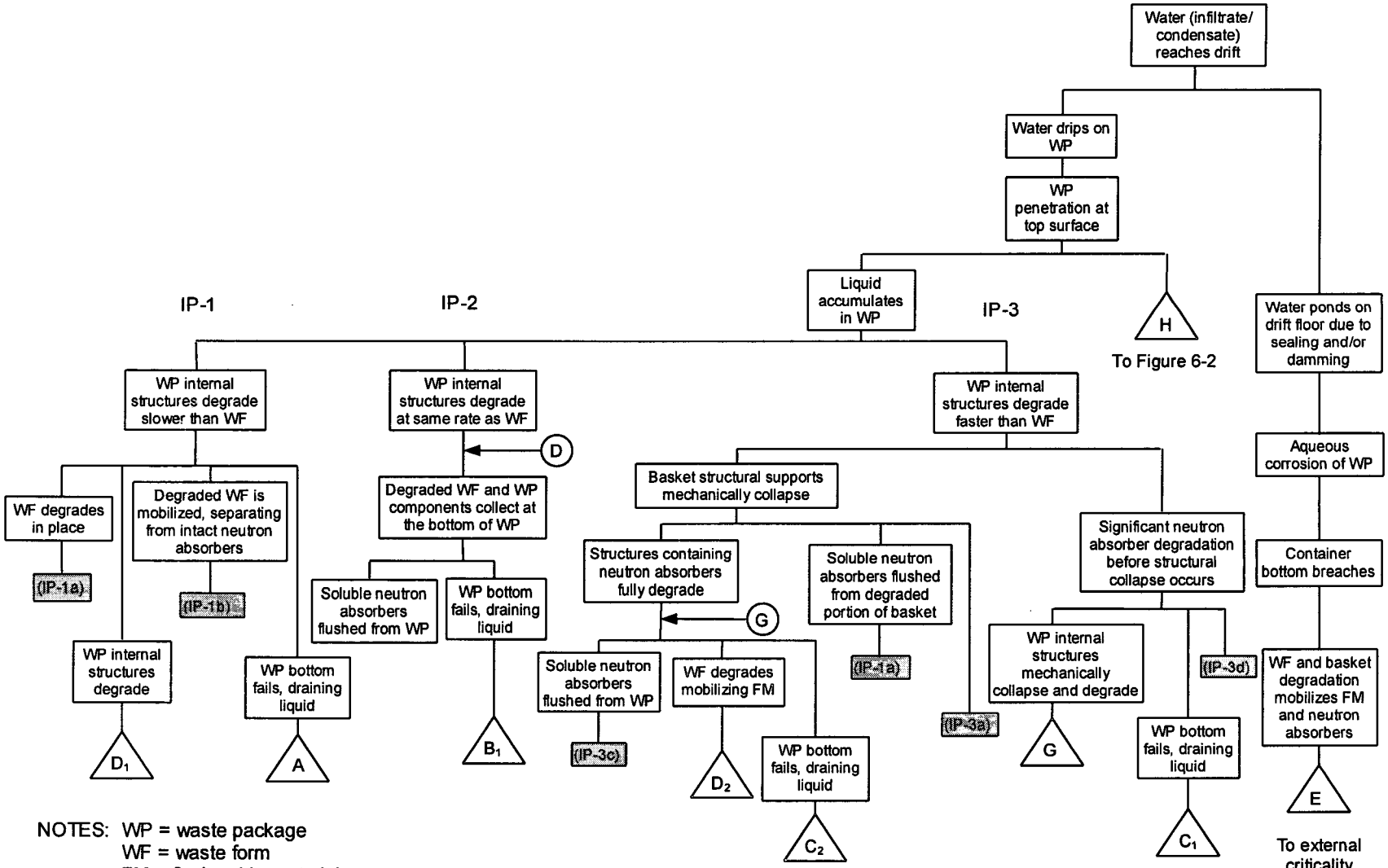

NOTES: WP = waste package
WF = waste form
FM = fissionable material

Source: YMP 2000, p. 3-8.

Figure 6-1. Internal Criticality Master Scenarios, Part 1

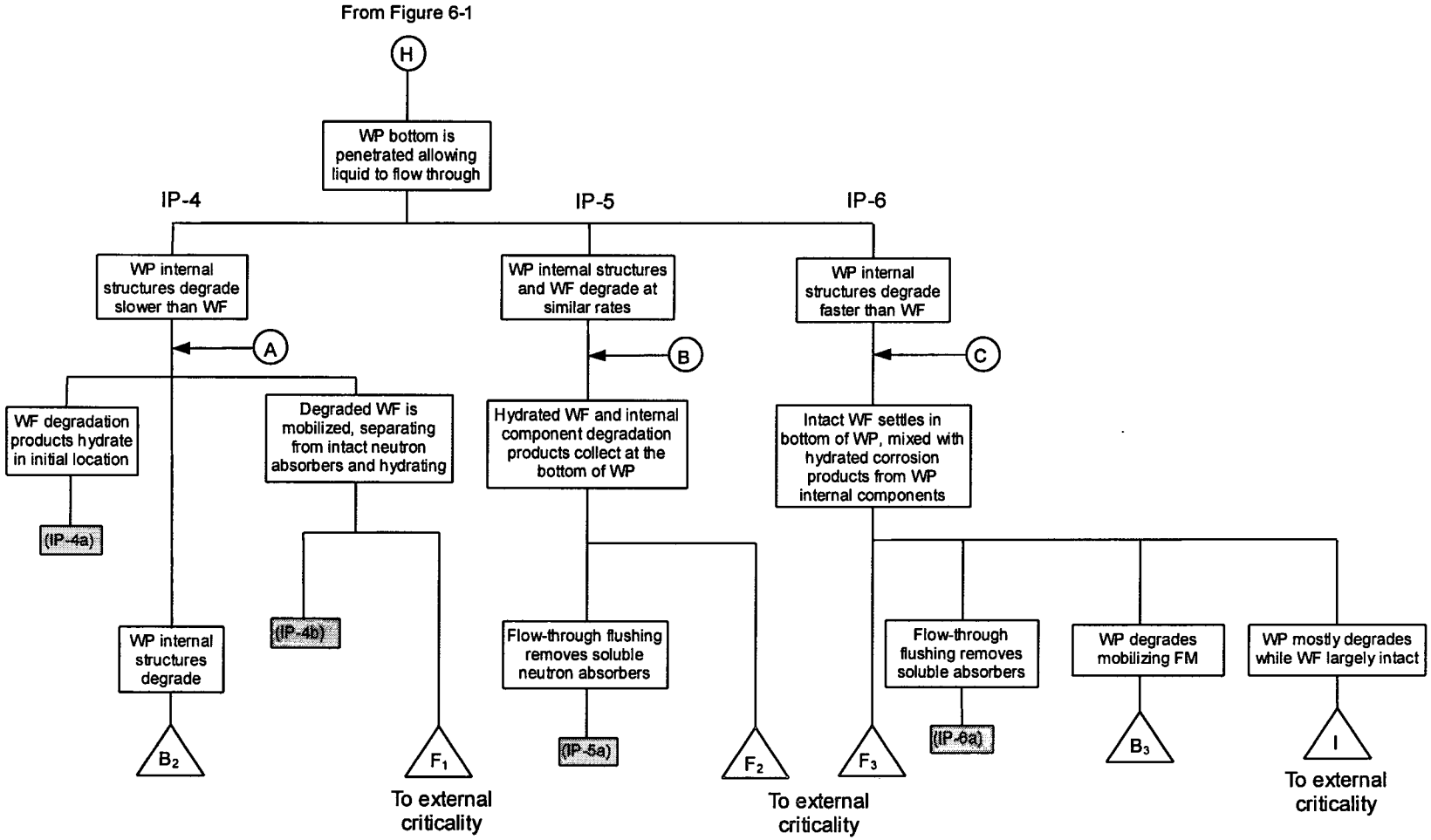

NOTE: Hydrated degradation products may include hydrated metal oxides, metal hydroxides, and clayey materials

Source: YMP 2000, p. 3-9.

Figure 6-2. Internal Criticality Master Scenarios, Part 2

The report titled *Generic Degradation Scenario and Configuration Analysis for DOE Codisposal Waste Package* (CRWMS M&O 1999d) serves as the basis for the specific degraded WP criticality analysis to be performed for any type of DOE SNF that will be codisposed with the high-level radioactive waste in a codisposal WP. Starting from these guidelines, a set of degradation scenarios and resultant configurations has been developed for the codisposal WP containing FSVR SNF. The following description focuses on the correspondence between different classes of configurations and their refinements. This approach allows a systematic treatment of the degraded internal criticality analysis, taking into account all possible configurations with potential for internal criticality. In Sections 6.3 and 6.4, the scenarios and the resulting configuration classes that are applicable to a codisposal WP with a DOE standardized SNF canister containing FSVR SNF are discussed.

6.2.2 Generic Degraded Configuration Classes

Configuration classes resulting from degradation scenario IP-1, in which the SNF degraded before the OICs:

IP-1-A: SNF degraded, DOE SNF canister and internal supporting structure not degraded.

IP-1-B: SNF degraded, DOE SNF canister and supporting structure partially degraded.

IP-1-C: All WP components degraded.

Configuration classes resulting from degradation scenario IP-2, in which WP components degrade concurrently with the SNF:

IP-2-A: All WP components degraded.

Configuration classes resulting from degradation scenario IP-3, in which the SNF degrades after the OICs:

IP-3-A: Degraded DOE SNF canister internal structure; intact SNF and DOE SNF canister shell; degraded WP basket structure and DHLW glass canister(s).

IP-3-B: Degraded WP basket structure, DHLW glass canister(s), and DOE SNF canister; intact SNF.

IP-3-C: All WP components degraded.

Configuration classes resulting from flow-through degradation scenario IP-4, in which the SNF degrades before the OICs:

IP-4-A: SNF degraded, DOE SNF canister shell not fully degraded.

IP-4-B: All WP components degraded.

Configuration classes resulting from flow-through degradation scenario IP-5, in which the WP components including the SNF, are degrading concurrently:

IP-5-A: All WP components degraded.

Configuration classes resulting from flow-through degradation scenarios of IP-6, in which the SNF degrades after the OICs:

IP-6-A: All WP components degraded.

6.3 APPLICATION OF STANDARD SCENARIOS TO FSVR SNF

There is no internal structure inside the DOE SNF canister. The FSVR fuel elements fill most of the space inside the DOE SNF canister and thus do not need a support structure. This implies that configurations following from degradation of DOE SNF canister basket structure are not valid for the FSVR SNF disposal. Taking into consideration this characteristic, the application of the standard scenarios follows based on the sequence discussed in Section 6.2.1.

IP-1: The configurations resulting from IP-1 scenario involve the FSVR fuel compacts degrading before other internal components and depends on the degradation rates of the various materials that make up the OICs as compared to the degradation rate of the fuel compacts. Figure 6-3 is an example. The degradation rates show that the FSVR fuel high degradation rates are in the $2.78 \cdot 10^{-10}$ to $1.50 \cdot 10^{-8}$ $mol \cdot cm^{-2} \cdot s^{-1}$ (see Table 2-19) while the low rate of the SS components is $2.53 \cdot 10^{-14}$ $mol \cdot cm^{-2} \cdot s^{-1}$ (see Table 2-18). The carbon steel has a degradation rate of $1.79 \cdot 10^{-11}$ $mol \cdot cm^{-2} \cdot s^{-1}$. Therefore, the degradation of the carbon steel basket and the FSVR fuel, with the stainless steel and DHLW glass components intact, is possible. Since there is no basket structure in the DOE SNF canister associated with the FSVR SNF, configuration variations within the DOE SNF canister are limited. Possible variations are configurations with partial or total degradations of the components outside the DOE SNF canister and the DOE SNF canister falling to the bottom of the WP. Near the end of this sequence, layers of degradation products in the WP might result surrounding a partially degraded DOE SNF canister shell.

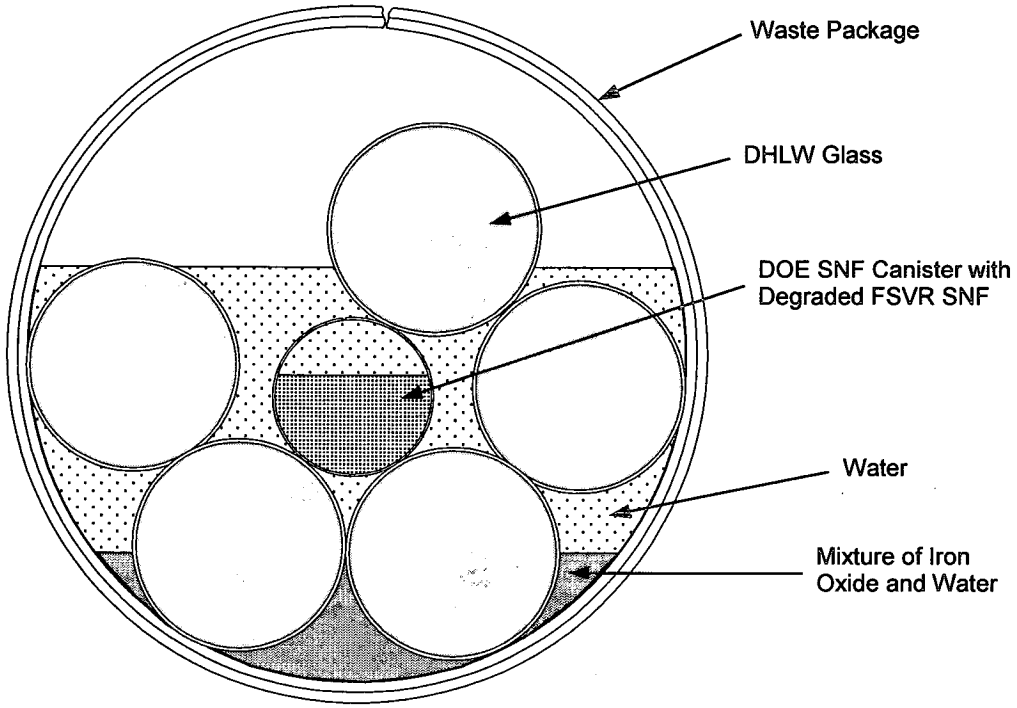

Figure 6-3. Conceptual Sketch of WP for Degradation Scenario IP-1

IP-2: In the configurations resulting from IP-2 scenario the SNF may degrade simultaneously with the other components in the WP if the environmental conditions favor DHLW glass degradation rates that are comparable to SNF and steel degradation rates. Figure 6-4 is an example. In this scenario the gradual degradation of the various constituents could result in a configuration where higher density material collects at the bottom of the WP while lower density material stays on top.

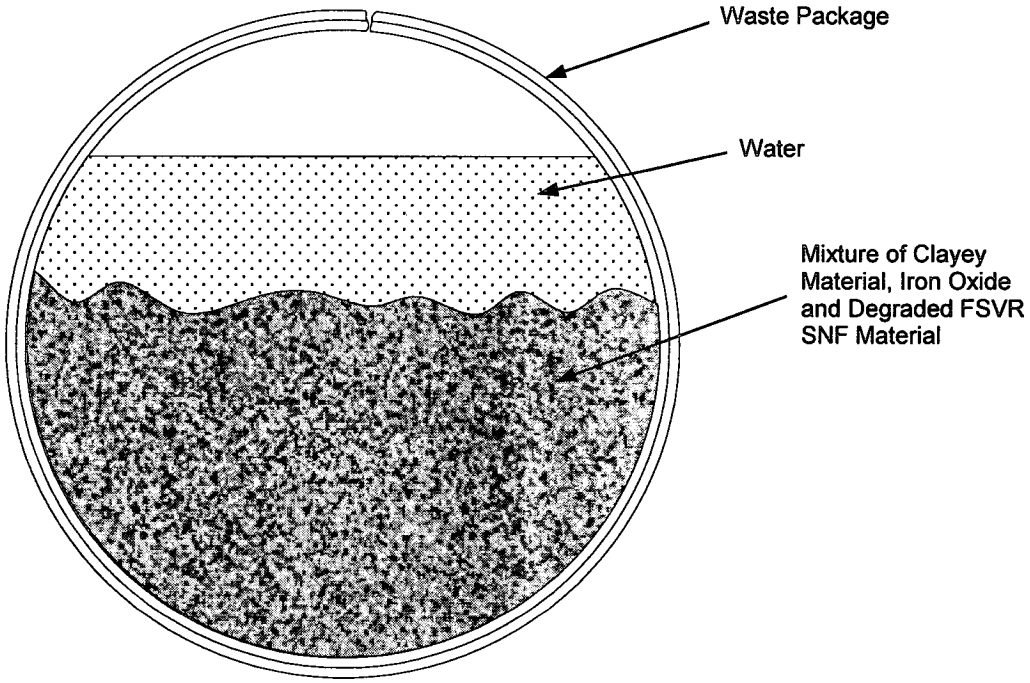

Figure 6-4. Conceptual Sketch of WP for Degradation Scenario IP-2

IP-3: The configurations resulting from IP-3 scenario for SNF degrading after OIC would require that the SNF has a low degradation rate and the SS 316L of the DOE SNF canister has substantially lower rates than the SS 304L of the DHLW canisters, along with high degradation rates for the DHLW glass. In this configuration the FSVR fuel elements collect at the bottom of the WP while surrounded by degradation products (e.g., clayey material). Figure 6-5 is an example. Possible variations are configurations with DOE SNF canister degraded and intact SNF accumulated at the WP bottom with partial or total degradation of WP components.

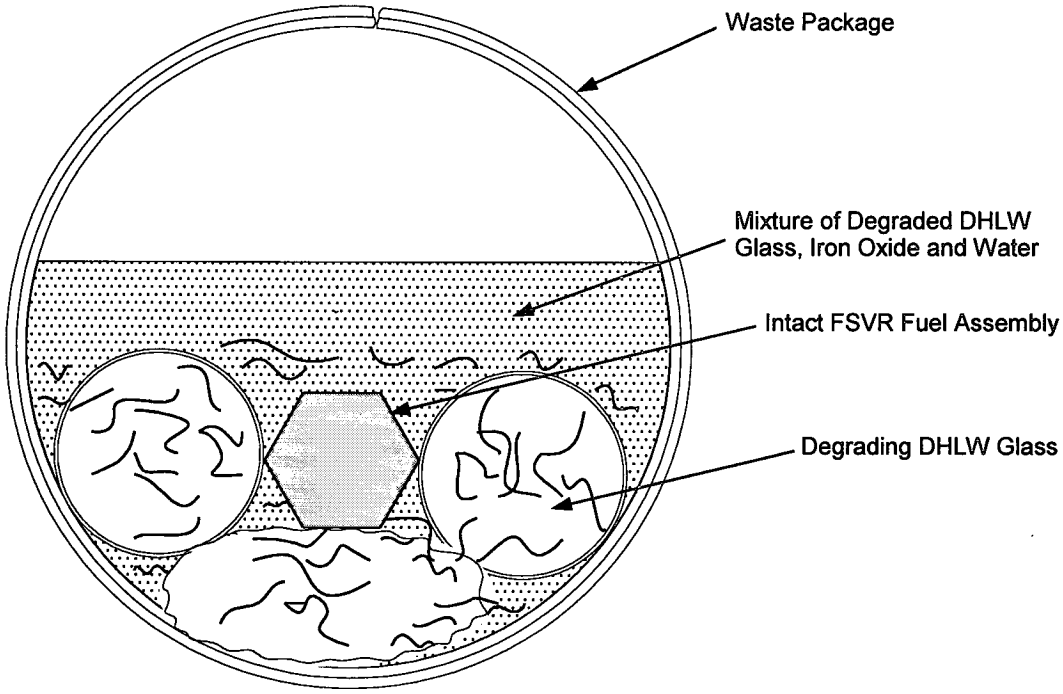

Figure 6-5. Conceptual Sketch of WP for Degradation Scenario IP-3

The standard scenarios for the flow through cases, IP-4, IP-5 and IP-6 require a top and bottom breach of the WP in order to occur. However, for these scenarios to lead to potential critical configurations there must be some plugging of the hole(s) in the bottom, so that water can accumulate to provide neutron moderation. In addition, geochemistry calculations assume that a material does not get flushed out unless it is in solution. In that case the resulting configurations are the same as the configurations for the top breach only cases (IP-1, IP-2 and IP-3).

6.4 MOST LIKELY DEGRADED COMPONENT CONFIGURATIONS FOR FSVR SNF

The parameters that need to be considered to develop the most probable degradation scenario/configuration for the codisposal WP with FSVR SNF are: the materials of the components associated with the WP; the DOE SNF canister and the fuel; the thicknesses of the materials; and the associated corrosion rates. The sequence of degradation can then be developed and the most probable degradation scenario/configuration can be identified by using these parameters, which are discussed below.

6.4.1 Corrosion Rates

The material corrosion rates are presented in Tables 2-18 and 2-19 of this report. The carbon steel (Type A 516) degrades more rapidly than the SS 304L. The silicon carbide degradation rate is the lowest among all materials listed, except only graphite, which is considered chemically inert. The fuel kernels have the highest degradation rate, however this is applicable only if all the layers are breached, thus allowing water to reach the kernels.

6.4.2 Most Probable Degradation Path

Based on the corrosion rates and the material thicknesses given in Tables 2-18, 2-19 and 6-1, the most probable degradation path for the WP, the DOE SNF canister, and the FSVR SNF follows the sequence below:

1. WP is penetrated and flooded internally. Water has not yet penetrated the DOE SNF canister.

2. The WP separation plates and DOE SNF canister support cylinder degrade first because of the high corrosion rate of A516 carbon steel. Degraded steel product (iron oxide) accumulates at the bottom of the WP.

3. DHLW glass canister shell degrades and exposes the DHLW glass. The DHLW glass degrades at a much lower rate than the stainless steel components and only a small percentage degrades while the stainless steel degrades as demonstrated in the geochemistry calculations (BSC 2001d). There are two possible degradation paths:

   3a. DOE SNF canister stays intact. Intact DOE SNF canister with intact FSVR SNF fall and are surrounded by the iron-rich degradation products near the bottom of the WP.

   3b. DOE SNF canister starts to degrade.

4. Following 3b above, DOE SNF canister shell is penetrated but remains intact and DOE SNF canister interior is flooded.

5. DOE SNF canister shell completely degrades. The degraded iron oxide mixes with the degraded glass and iron oxide clay at the bottom of the WP. The intact FSVR fuel elements fall on top of the clay.

6. Given a very long period of time, it is postulated that everything will degrade including the FSVR fuel compacts and graphite block. However, it is very unlikely to attain complete degradation of the graphite block and fuel particles within the time period covered by the geochemistry and criticality analyses (up to $6.34 \cdot 10^5$ years from emplacement) due to very low degradation rates of SiC and graphite. It is expected that rock fall and seismic events could break the graphite blocks and fuel compacts into pieces, but the number of pieces is rather small. The degraded SNF, other degradation products, and water mix and accumulate at the bottom of the WP.

Table 6-1. Materials and Thicknesses

Components	Material	Thickness (mm)
WP divider plate	A516 Carbon Steel	12.7
WP support tube	A516 Carbon Steel	31.75
DHLW glass canister shell	SS 304L	10.5
DHLW glass	Glass	N/A
DOE SNF canister shell	SS 316L	9.525
Fuel particles layer	SiC	0.020

Source: Section 2.1 and Appendix A.

6.4.3 Most Probable Degradation Scenario/Configuration

According to the analysis in *Generic Degradation Scenario and Configuration Analysis for DOE Codisposal Waste Package* (CRWMS M&O 1999d), the above degradation sequences match with the degradation scenario/configurations of IP-3-A to IP-3-C (equivalent to IP-2). The details of these degradation scenario/configurations are discussed in Section 7.4.1. The most likely scenario begins with the localized degradation of the canisters inside the WP followed by the degradation of the DOE SNF canister and, given enough time, the SNF degrades by breaching into small pieces (rather than being chemically transformed since the SiC has a very low degradation rate). The degradation scenario of IP-1, i.e., SNF degrades faster than the other materials, is not probable, since the corrosion rate of the FSVR SNF (specifically of the SiC layer surrounding the fuel kernels) is the lowest among all of the materials, except graphite, which was considered inert. However, for completeness, configurations associated with scenario group IP-1 have been analyzed as presented in Sections 6.4.3.3 and 6.4.3.4.

The final degraded configurations that were used for criticality calculations presented in Section 7.4 are characterized by location of the fissile material and possible displacement from any material that can act as neutron absorber. The assignment of such locations has been consistent with a conservative interpretation of possible physical processes. At this time, there is no detailed calculation of transport processes to support this. Such a calculation could significantly reduce the conservatism in the present method, and, consequently, reduce the resulting k_{eff}. However, such a calculation would require considerable resources and still not resolve the issue of alternative physical pathways for such transport processes. Since none of the likely degraded configurations that can be reached through plausible physical mechanisms that are found to be critical, the additional effort of the more detailed calculations is not necessary.

Since none of the configurations that can be reached through plausible physical mechanisms and have been found to be critical, probability calculations will not be needed. Nevertheless, the configurations described in Sections 6.4.3.1 and 6.4.3.2 are believed to be the most likely, since the FSVR SNF is the slowest degrading material in the WP.

6.4.3.1 Intact DOE SNF Canister and Degraded WP Internals

In this case, the SNF is intact or partially degraded. This configuration is a variation of configuration class 1 and can be reached from standard scenario IP-3. The results of criticality calculations for this configuration are given in Section 7.4.2.1.

6.4.3.2 Degraded DOE SNF Canister and WP Internals, Intact SNF

In this case, the DOE SNF canister, WP internals, and DHLW canisters are degraded. The fuel element is intact. The degradation scenarios and configuration classes are applied to the entire WP. As a variation, there could be partial degradation of the SNF. This configuration is a variation of configuration class 1 and can be reached from standard scenario IP-3. The results of the criticality calculations for this configuration are given in Section 7.4.2.2.

6.4.3.3 Degraded SNF with Intact DOE SNF Canister or WP

In this case, the SNF could be partially or fully degraded. This configuration is a variation of configuration class 6 and can be reached from standard scenario IP-1. The results of the criticality calculations for this configuration are given in Section 7.4.1.

6.4.3.4 Partially or Completely Degraded DOE SNF Canister and WP Internals

In this case, the degradation scenario and configuration are applied to the entire WP including the SNF. Degradation products from the DOE SNF canister, SNF and the OIC mix uniformly inside the WP. This configuration is a variation of configuration class 2 and can be reached from standard scenario IP-1, IP-2, or IP-3. The results of the criticality calculations for this configuration are given in Section 7.4.3.

6.4.4 Tilting of DOE Canister Inside WP

Tilt angle influences distributions of degraded products inside the WP. Tilting has the potential to change the concentrations of the fissile materials and the neutron absorber and may result in a more favorable geometry for criticality. The maximum tilt angle of the DOE SNF canister inside the WP can be calculated by fixing one endpoint of the canister while moving the other end to the bottom. The value of the maximum tilt angle is approximately 9°. This value is calculated using the design parameters in Table 2-1 and Section 2.1.3. Maximum tilt angle = $\sin^{-1}$([WP inner radius - support tube inner radius]/DOE SNF canister length) = $\sin^{-1}$(68.925/456.9).

Tilting of the DOE SNF canister would physically require that the space beneath does allow for movement of the canister. This condition is unrealistic since the DHLW glass and the degradation products from the steel components (WP basket and support tube) would collect at the bottom of the WP and fill the available space. A second factor is that the degradation rate of the stainless steel is higher than that of the DHLW glass and as such the canister shell would most probably be gone at the time when DHLW glass degradation would make the DOE SNF canister tilting a possibility.

6.4.5 Tilting of WP

Tilting of the WP in the emplacement drift is not a concern for the time period of interest (from emplacement to $6.34 \cdot 10^5$ years). The WP is placed in the drift horizontally and will stay in that position unless an external event, such as a seismic event occurs. In addition, the WP is emplaced in the drift by means of an Alloy 22 pallet which rests on cross-connected carbon steel I-beams which are embedded in the ballast (gravel) inside the drift (see Figures 5 and 6 of

CRWMS M&O 2000d) and the distance between the WPs inside the drift is less than half the length of the WP so that sliding of the WP over the pallet edge is not possible (CRWMS M&O 2000d).

6.5 BASIC DESIGN APPROACH FOR GEOCHEMISTRY ANALYSIS

The method used for this analysis involves eight steps as described below:

- Use of the modified and qualified version of the EQ3/6 reaction-path code to trace the progress of reactions as the chemistry evolves, including estimating the concentrations of materials remaining in solution as well as the composition of precipitated minerals. EQ3NR is used to determine a starting fluid composition for EQ6 reaction-path calculations.

- Evaluate available data on the range of dissolution rates for the materials involved, to be used as material/species input for each time step.

- Use the "solid-centered flow-through" mode in EQ6. In this mode, an increment of aqueous "feed" solution is added continuously to the WP system, and a like volume of the existing solution is removed. This mode simulates a continuously stirred tank reactor.

- Determine the concentrations of fissile material in solution as a function of time (from the output of EQ6 simulated reaction times up to $6.34 \cdot 10^5$ years).

- Calculate the amount of fissile material released from the WP as a function of time (fissile material loss reduces the chance of criticality within the WP).

- Determine the concentrations of neutron absorbers (most importantly Th) in solution as a function of time (from the output of EQ6 over times up to $6.34 \cdot 10^5$ years).

- Calculate the amount of neutron absorber retained within the WP as a function of time.

- Calculate the composition and amounts of solids (precipitated minerals or corrosion products and unreacted WP materials).

6.6 CALCULATIONS AND RESULTS

The calculations begin using selected representative values from known ranges for composition, amounts, surface areas, and reaction rates of the various components of the FSVR SNF WP. The input to EQ6 includes the composition of J-13 well water, a rate of influx to the WP that corresponds to suitably chosen percolation rates into a drift, and a drip rate into the WP (Section 2.1.9.3), which is also the flow rate out of the WP. In some cases, the degradation of the WP is divided into stages (e.g., degradation of the DHLW glass before breach of the DOE SNF canister and exposure of the fuel material to the water). The source of the results presented in this section is BSC (2001d).

6.6.1 Cases with Simultaneous Degradation of All WP Internal Components

The losses for U, Pu, and Th from the FSVR WP are summarized in Sections 6.6.1.1 and 6.6.1.2. Several characteristics of the WP internal component degradation process with all components within the WP exposed to simultaneous degradation are:

- In all cases, all Pu released from the fuel is lost from the WP. In the rare instances that the solid PuO_2 formed, it was short lived and of minimal concentration. Pu decay was conservatively not included in any of the runs.

- Retention of U in the WP ranged from 99.4% to 0%. Retention was due primarily to the formation of three major U-bearing minerals including $(UO_2)_3(PO_4)_2 \cdot 6H_2O$, α-uranophane $[Ca(UO_2SiO_3OH)_2 \cdot 5H_2O]$, and Na-boltwoodite $(NaUO_2SiO_3OH \cdot 1.5H_2O)$. Other U minerals formed were schoepite $(UO_3 \cdot 2H_2O)$ and $CaUO_4$, but these were minimal and short lived in the system. In all cases that simulated a high DHLW glass degradation rate, all of the U was lost from the WP. For runs with a low DHLW glass degradation rate, U retention decreased with increasing steel degradation rate since the steels last for a shorter time, therefore the pH remains high in the WP for extended periods of time.

- Retention of Th in the system ranged from 100% to 70.2%. Similar to U, Th showed greater retention with lower steel degradation rates. The bulk of Th minerals formed in the WP include ThO_2 (am), $Th_{0.75}PO_4$, and $ThF_4 \cdot 2.5H_2O$. The mineral $Th(SO_4)_2$ also formed but was usually of minimal concentration and short lived in the system.

- Allowing goethite rather than hematite to form in the WP has little effect on the results. In cases 17, 18, and 21 the formation of hematite was suppressed, allowing goethite to form instead. The results show that the percentages of U, Pu, and Th retained in the WP at the end of runs in cases 17, 18, and 21 are very similar to those in cases 6, 15, and 19, where hematite was allowed to form (see Tables 6-3 and 6-4).

6.6.1.1 Cases with 1% of the Fuel Particles Having Damaged Coatings

Table 6-2 indicates the retention of U, Pu and Th in the cases where 1% of the fuel particles have damaged coatings. For these cases, 1% of the fuel was assigned the degradation rate of Th/U carbide. The remaining 99% was assigned the degradation rate of silicon carbide. Since the rates differ by six orders of magnitude, the initial chemistry in the WP is effected primarily by the damaged fuel particles. However, this state is short lived and the U released from the 1% of the quickly degrading fuel is lost from the WP. The remainder of the fuel requires an additional 320,000 years to degrade completely.

Table 6-2. Cases with 1% of the Fuel Particles Having Damaged Coatings

Case #	Time Run (years)	U Retained (%)	Pu Retained (%)	Th Retained (%)
1	634,000	99.4	0	100
2	634,000	63.4	0	81.2
3	634,000	0	0	85.0
4	634,000	9.9	0	70.2
5	634,000	0	0	73.0

In cases where a slow steel degradation is combined with slow DHLW glass degradation, the pH in the WP decreases due to the Cr and Mo released into solution from the degradation of the stainless steels. It is assumed that Cr and Mo completely oxidize causing acidic conditions. A slight increase in pH occurs when the SS 316L from the DOE SNF canister and the SS 304L from the DHLW canisters are exhausted. Since the DHLW glass is degrading slowly, the alkalinity from the DHLW glass is insufficient to neutralize the pH until all of the steel is consumed (after approximately 600,000 years, when the SS 316NG liner is exhausted). The Mg and Ca carbonate minerals formed from the DHLW glass dissolution do not fully neutralize the acid produced from steel degradation until this point. The low drip rate also causes these ions to remain in the WP instead of being flushed out, helping to maintain the lower pH conditions. If the drip rate is increased, pH will rise since acidic ions will be flushed from the WP. As the pH increases, the degradation of the DHLW glass also increases, allowing for a basic (rather than an acidic) solution within the WP. Once all of the glass is degraded, pH will decrease until all of the steel is degraded. At this point, pH will return to a value of approximately 8.1.

The U and Th phosphates dominate the U- and Th-bearing minerals in this analysis because of the higher levels of phosphorus from the degradation of the SS 316NG liner. 100% of the Pu is lost because of the lack of formation of Pu minerals. U retention remains high at lower pH values since U-bearing minerals can form. If pH rises, U lost from the WP increases because U stays in solution as stable carbonate and hydroxyl complexes. More Th may be lost at these higher pH values but overall, since Th compounds are more stable at higher pH values than U compounds, most of the Th is retained.

In the cases with a fast DHLW glass degradation rate, the solution in the WP is basic until all the DHLW glass is exhausted. As the steel continues to degrade after this point, the pH will decrease substantially until the DOE SNF canister and DHLW canisters are exhausted. The pH will then increase to around neutral due to continued degradation of the SS 316NG liner. As soon as the liner is exhausted, the pH will return to approximately 8.1. Because of the high initial pH, most (if not all) of the U is flushed out of the WP due to the high solubility of U and U-minerals at high pH values.

In the cases where the steels are degrading quickly, the pH of the system is acidic (independent of the glass degradation rate) until all the steel within the WP is exhausted. Since the pH in the system is high for long periods of time, most or all of the U is lost from the WP. Some U is retained in the runs simulating low glass degradation and high drip rate since these two parameters keep the pH from spiking above 8.5. In the runs where DHLW glass degrades quickly, most of the U stays in solution as stable carbonate and hydroxyl complexes causing 100% loss of U from the WP.

6.6.1.2 Cases with Intact Fuel Particles

Table 6-3 indicates the retention of U, Pu, and Th in the cases where all the fuel particles are intact. For these cases, all the fuel is assigned the degradation rate of silicon carbide.

Table 6-3. Cases with Intact Fuel Particles

Case #	Time Run (years)	U Retained (%)	Pu Retained (%)	Th Retained (%)
6	634,000	99.4	0	100
7	634,000	94.9	0	99.9
8	608,000	64.7	0	81.5
9	634,000	0	0	97.5
10	609,000	0	0	86.4
11	634,000	0	0	91.8
12	634,000	13.6	0	71.6
13	634,000	0	0	75.2
14	609,000	0	0	76.7
15	609,000	11.6	0	71.2
16	609,000	0	0	73.9
17	634,000	99.1	0	100
18	634,000	10.7	0	70.4

For these cases, the results follow the same pattern as indicated in Section 6.6.1.1. Since all of the fuel is degrading at the slow (silicon carbide) rate, slightly more (up to 1.7% total) U and Th is retained in the WP as compared to the cases that degrade 1% of the fuel at the faster Th/U carbide rate.

6.6.2 Cases with Degradation of WP Internal Components in Stages

Sections 6.6.2.1 and 6.6.2.2 explore the cases where the degradation of the WP is as follows:

1. Separated into stages, with each stage representing certain sections of the WP that are exposed to degradation.

2. Degradation within the DOE SNF canister only.

6.6.2.1 Separation of Degradation Process into Two Stages

Table 6-4 summarizes the U, Pu, and Th retention in the WP when the degradation process is divided into several stages. The first stage includes degradation of WP internals, exclusive of those inside the DOE SNF canister. The second stage assumes that the DOE SNF canister, after approximately 35,000 years, was breached and the DOE SNF canister internals are now degrading along with the rest of the WP.

For the two stage runs, the U contained within the DHLW glass is completely lost from the WP in the first stage. The high drip rate is sufficient to flush most of the alkalinity (from DHLW glass dissolution) from the package so that the second stage begins at a pH of approximately 6.5.

The pH for the second stage of case 19 remains low for the entire run since only the degrading steels are adding to the pH of the system. Total U retention is low (2.50%) since all U from the DHLW glass was flushed from the WP in the first stage. However, U retention from the FSVR fuel remains high (91% of U from degraded fuel) due to the low pH of the system allowing formation of U-bearing minerals.

Table 6-4. Cases with WP Degradation in Stages

Case #	Time Run (years)	U Retained (%)	Pu Retained (%)	Th Retained (%)
19	53,200	0	N/A	N/A
	634,000	2.50 (91.6)	0 (0)	100 (100)
20	53,200	0	N/A	N/A
	634,000	2.71 (24.8)	99 (0.00)	100 (100)
21	53,200	0	N/A	N/A
	634,000	1.61 (58.9)	0 (100)	100 (100)

NOTE: Retention values presented are for total U, Pu, and Th in both degraded and intact fuel (U also accounts for DHLW glass). Values in parentheses represent the retention of these elements from degraded fuel.

Case 20 investigates the possibility that the silicon carbide layer surrounding the Th/U carbide fuel kernels is inert. For this type of scenario, 1% of the fuel particles were considered damaged and subject to degradation at the fast Th/U carbide degradation rate. The other 99% of the fuel is considered inert due to the integrity of the silicon carbide layer.

The pH of the second stage of case 20 also remains low for the entirety of the run. Once again the total U retention is low (2.71%), but retention of U from degraded fuel is 24.8%. A larger percentage of the U was lost from this run as compared to case 19 because there was not enough U in solution at any one time to form U phosphate. Instead of the U phosphate forming, other phosphates (such as $Ni_3[PO_4]_2$) were formed.

Case 21 is similar to case 19, the only difference being that goethite was allowed to form instead of hematite. A larger percentage of the U was lost from this run as compared to case 19.

6.6.2.2 Cases with Degradation of DOE SNF Canister Contents Only

Similar to the cases that expose all the WP internal components to degradation (cases 1 through 21), the same characteristics of the U, Pu, and Th retention process can be seen here.

- All Pu released from the fuel is subsequently lost from the WP.
- For cases with the slow (silicon carbide) rate (cases 22-24), U retention ranges from 90.1% to 0% and is highly dependent on the drip rate. This may be due to the steadily increasing pH of the system as the drip rate increases. As pH increases, the solubility of U also increases, allowing the U carbonate and hydroxyl complexes to be washed from the DOE SNF canister. Also, at higher pH, minerals such as fluorapatite precipitate more profusely, removing the phosphorous from the system making it unavailable to form U phosphate minerals.

For cases simulating that silicon carbide is inert (cases 25-27, 99% of fuel unavailable for degradation), the same trends are present but loss from the DOE SNF canister occurs much faster. This is because the elements from the 1% degraded, damaged fuel kernels are released into solution very quickly (from UC_2 degradation rate).

- Thorium loss from the DOE SNF canister is minimal and ranges from 0% to 11%. Unlike U, Th minerals are more stable at higher pH values, therefore more are retained in the DOE SNF canister even as pH increases.

  For runs simulating that silicon carbide is inert (cases 25-27, 99% of the fuel unavailable for degradation), Th retention from degraded portion of the fuel ranges from 100% to 0%. The 0% retention was predicted for the fastest drip rate.

Table 6-5 summarizes the total percentage of U, Pu, and Th retained in the DOE SNF canister after 65,000 years. These runs simulate a first stage where only the DOE SNF canister floods leaving the rest of the WP essentially "dry." This configuration can be reached by water filling the WP and DOE SNF canister, then the WP being breached near its bottom and releasing only the water inside the WP. A second stage was never run since this configuration is more conservative with regard to criticality.

Table 6-5. Summary of U, Pu, and Th Retention for Cases Simulating the DOE SNF Canister Degradation Only

Case #	Time Run (years)	U Retained (%)	Pu Retained (%)	Th Retained (%)
22	65,100	98.0 (90.1)	80.2 (0.00)	100 (100)
23	65,000	89.0 (44.9)	80.0 (0.00)	100 (100)
24	65,000	80.0 (0.00)	80.0 (0.00)	97.8 (89.0)
25	65,200	99.1 (14.8)	99.0 (0.00)	100 (100)
26	65,000	99.0 (0.00)	99.0 (0.00)	100 (98.0)
27	65,000	99.0 (0.00)	99.0 (0.00)	99.0 (0.00)

NOTE: Values of retention presented are for all U, Pu, and Th in both degraded and intact fuel. The values in parentheses represent the retention of these elements from degraded fuel only.

6.7 SUMMARY

Based on the generic degradation scenarios and configuration classes discussed in YMP (2000) and CRWMS M&O (1999d), specific degradation configurations for FSVR SNF WP have been developed. These degraded configurations include the application of the generic scenario groups of IP-1, IP-2, and IP-3. Variations of the generic groups specific to FSVR SNF are discussed. The most probable degradation path based on the material corrosion rates and thicknesses has also been identified in Section 6.4.3. The maximum angle of tilt for the DOE SNF canister inside the WP has been calculated to be 9°. Tilt of WP is not physically possible due to the emplacement design.

A principal objective of the geochemistry calculations was to estimate the chemical composition of the degradation products remaining in a WP containing FSVR SNF and DHLW glass. Twenty-seven EQ6 reaction path calculations were carried out to span the range of possible

system behavior and to assess the specific and coupled effects of SNF degradation, steel corrosion, DHLW glass degradation, and fluid influx rate on U, Pu, and Th mobilization. Corrosion product accumulation and U, Pu and Th mobilization were examined as well. The results presented in BSC (2001d), and summarized in this section, have been used as inputs to the criticality calculations described in Section 7 of this document.

7. INTACT AND DEGRADED COMPONENT CRITICALITY ANALYSES

7.1 USE OF COMPUTER SOFTWARE

The Monte Carlo particle transport code, MCNP, Version 4B2LV (CRWMS M&O 1998c), was used to estimate the effective neutron-multiplication factor (k_{eff}) of the codisposal WP. The information regarding the code and its use for the criticality analyses is documented in BSC (2001e).

7.2 DESIGN ANALYSIS

The MCNP Version 4B2LV was used to estimate the k_{eff} values for various geometrical configurations of the FSVR SNF in the 5-DHLW/DOE SNF-long WP. The k_{eff} results represent the average combined collision, absorption, and track-length estimator from the MCNP calculations. The standard deviation (σ) represents the standard deviation of k_{eff} related to the average combined collision, absorption, and track-length estimate of the Monte Carlo calculation statistics. The calculations are performed using ENDF/B-V continuous energy cross-section libraries that are part of the qualified MCNP code system.

BSC (2001e) describes the Monte Carlo representations, the method of solution, and the results for nuclear criticality evaluations that were performed for intact and degraded components of the WP. The intact component cases are described in Section 7.3 and the degraded component cases are described in Section 7.4.

The MCNP results are presented in the following section in order to demonstrate that all foreseeable intact and degraded configurations inside the codisposal WP (see Section 6) have been investigated and the values of k_{eff} are below the interim critical limit of 0.93 (Section 2.4). Each of the configurations presented in Section 6 is addressed, but many are bounded by results in subsequent configurations, and are not, therefore, fully parameterized.

7.3 CALCULATIONS AND RESULTS-PART I: INTACT-MODE CRITICALITY ANALYSIS

This section presents the results of the intact-mode criticality analysis. These configurations represent a WP, which has been breached allowing the inflow of water, but the internal components of the WP are intact (see Figure 7-1). For most of the MCNP representations the WP was reflected by water, but in order to investigate the effect of different reflective conditions on criticality, the mirror reflection boundary condition was also considered. Use of a mirror reflective boundary condition is conservative since no neutrons leak (escape) from the system. The graphite block type was H-327 unless otherwise specified. The DOE SNF canister is represented as loaded with five FSVR fuel elements axially aligned. Variations of the intact configurations were examined to identify the configuration that results in the highest calculated k_{eff} value within the range of possible conditions.

The base case is shown in Figure 7-1. The water reflected WP is in a horizontal storage position where the effect of gravity on the DHLW and DOE SNF canisters is evident. All the voids and porosities in the fuel and graphite block were represented as completely filled with water, the

fuel length is considered to be the same as the element length, and the DOE SNF canister is completely flooded. The fourth fuel composition from Section 2.1.4.2 was used with an additional 2.59 g of Pu per fuel element (which is equal to the maximum amount of Pu at EOL and was added for conservatism). The amount of Th in the fuel is reduced (arbitrarily) by 5% to show the sensitivity of the results to Th content. Other modeling details such as whether the fuel has the same length as the element (neglecting the plugs at the end of the fuel holes) or the slightly smaller length of the actual fuel holes and reflector boundary conditions were also investigated. The results of the MCNP cases are presented in Table 7-1.

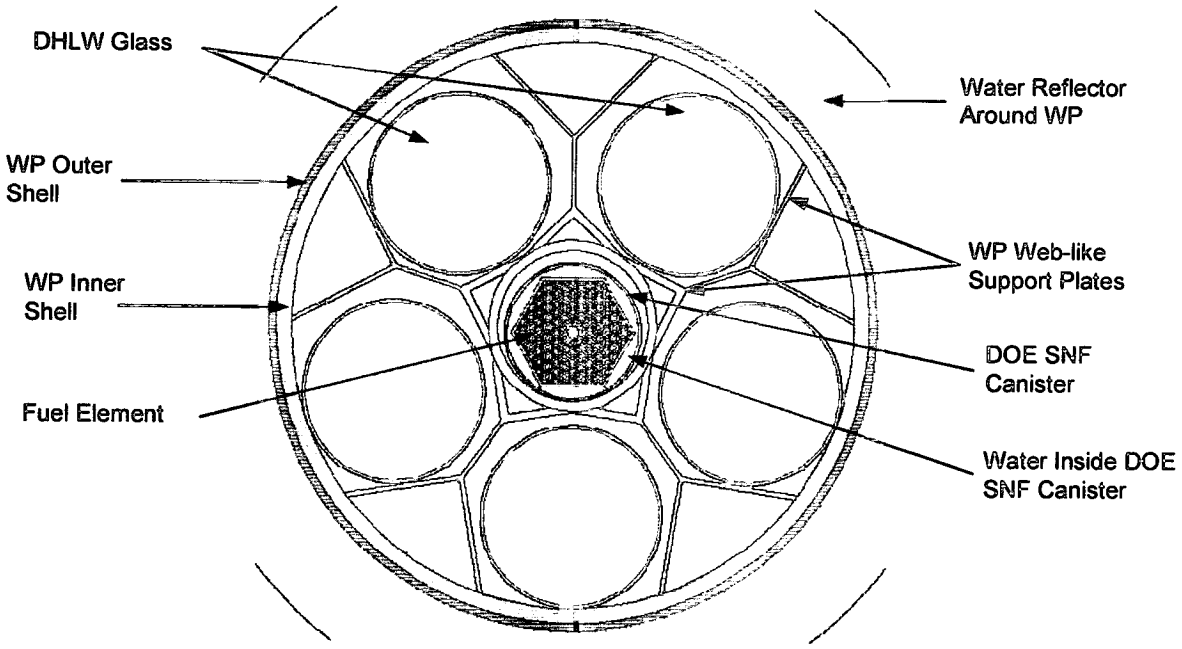

Figure 7-1. Cross-section View of the 5-DHLW/DOE WP Intact Configuration

Table 7-1. Results for Intact Mode Configuration with Several Changes in the Modeling Details

Case Description	$k_{off} + 2\sigma$
Base case (see Figure 7-1)	0.9149
Base case, but the second composition in Section 2.1.4.2	0.9035
Base case, but the third composition in Section 2.1.4.2	0.9112
Base case, but the fourth composition in Section 2.1.4.2	0.9109
Base case, but actual fuel length modeled	0.9144
Base case, but mirror reflective WP boundary conditions	0.9162
Base case, but water replaces graphite in neutron absorber holes	0.9167
The case above, but with mirror reflective WP boundary conditions	0.9176
Base case, but no (EOL) Pu in fuel	0.9158
Base case, but uses the other type of (saturated) graphite (H-451)	0.9157
Base case, but 5% of the Th is neglected	0.9196

The results in Table 7-1 indicate that the intact configuration of the FSVR WP has a $k_{eff}+2\sigma$ below 0.93 and the fourth fuel composition from Section 2.1.4.2 is the most reactive among the four compositions evaluated, therefore conservatively selected for further use in the analysis. The variations applied to the intact configuration show a statistically insignificant change in

results from the base case (for all cases σ is less than 0.0010), except the last case where a 5% reduction of the Th amount results in an increase of about 0.5% in $k_{eff}+2\sigma$.

In the next set of results, presented in Table 7-2, the amount of water saturation is varied in the fuel compacts and in the graphite block. The same base case from Table 7-1 is used here, with 100% saturated voids in the fuel and graphite block, whereas the last case in the table is for a completely dry (0% saturated) element. Saturation values greater than 100% are not physically possible, but are considered here to investigate the effect of increasing water content.

Table 7-2. Amount of Water Saturation in Fuel Compacts and Graphite Block

% Water Saturation in Fuel Compacts	% Water Saturation in Graphite Block	$k_{eff} + 2\sigma$
100	100	0.9149
95	100	0.9144
85	100	0.9095
75	100	0.9026
105	100	0.9182
110	100	0.9210
120	100	0.9234
100	95	0.9142
100	90	0.9147
100	85	0.9134
100	105	0.9154
100	110	0.9198
100	125	0.9212
0	0	0.7796

Examination of Table 7-2 shows that the FSVR WP system is under-moderated, and the absence of water in the fuel and graphite block voids significantly reduces the k_{eff}.

Cases with variations in the positioning of the WP internal components and other cases are presented in Table 7-3.

Table 7-3. Variations in Positioning of the Various Components in the WP and Other Results

Case #	Case Description	$k_{eff} + 2\sigma$
1	Base case (see Figure 7-1); the WP is in a horizontal storage position, therefore the DHLW canisters and DOE SNF canister have the lowest (down) position; the FSVR fuel element stack is represented as centered inside the DOE SNF canister	0.9149
2	DHLW canisters down; DOE SNF canister centered; FSVR fuel element stack centered	0.9146
3	DHLW canisters down; DOE SNF canister down; FSVR fuel element stack down	0.9139
4	Similar to the case above, but FSVR fuel elements rotated 30°	0.9169
5	Similar to the case above, but water replaced with mirror reflective WP boundary conditions	0.9173
6	DHLW canisters centered; DOE SNF canister centered; FSVR fuel element centered	0.9165
7	Base case, but water fills support tube of WP	0.9063
8	Base case, but water fills entire WP	0.9021
9	Base case, but DOE SNF canister contains 4 FSVR fuel elements	0.9145
10	Base case, but DOE SNF canister contains 3 FSVR fuel elements	0.9133
11	Base case, but DOE SNF canister contains 2 FSVR fuel elements	0.9029
12	Base case, but DOE SNF canister contains 1 FSVR fuel element	0.8692

Cases 1 through 6 in Table 7-3 demonstrate that changing the positions of internal WP components has no statistical significance for the $k_{eff}+2\sigma$ results (in all cases in Table 7-3, σ is less than 0.0010). Also, there is no statistical difference between water and a perfect (mirror) reflector at the outer boundary of the WP.

In cases 7 and 8 in Table 7-3, the results identify the most reactive configuration with regards to flooding in the WP. As seen, the dry WP (external to the DOE SNF canister) is more reactive. Unless otherwise specified, in the following cases of this report, the DOE SNF canister was represented as flooded with the empty spaces in the WP (outside the DOE SNF canister) represented as voids.

Cases 9 through 12 in Table 7-3 are for a DOE SNF canister containing a reduced number of FSVR fuel elements. Values of $k_{eff}+2\sigma$ are statistically unchanged for a canister containing at least three fuel elements and axially stacking more elements does not make the canister more reactive, i.e., the fuel is essentially infinitely long for these cases. The values of $k_{eff}+2\sigma$ reduce by slightly more than 1% and 5% for two and one fuel elements, respectively.

The results in this section show that the most reactive composition of the four considered (see Section 2.1.4.2) is that using 1,485 g U-235 per fuel element. On the basis of conservatism, this is the composition used further in the criticality safety analyses.

7.4 CALCULATIONS AND RESULTS-PART II: DEGRADED MODE

The criticality calculations conducted for the degraded cases are discussed in the following sections. Several configurations were considered. Short descriptions of these general configurations are given in Section 6.4.3. Section 7.4.1 presents the results where the waste form inside the DOE SNF canister degrades before the DHLW canisters, the DOE SNF canister, and the WP basket. Section 7.4.2 gives the results where the internal components of the WP (but external to the DOE SNF canister) degrade first. In the configurations studied in this section, the DHLW canisters and the WP basket degrade before the inner components (FSVR fuel elements) of the DOE SNF canister. Section 7.4.3 presents the results for a WP with its internal components fully degraded. Unless otherwise noted, the WP was reflected by water, the graphite in the fuel element block is type H-327, and empty spaces in the WP were represented as voids (for cases where the externals in the WP are intact).

7.4.1 Waste Form Degrades Before the Internal Components of the WP

In this section, cases where the waste form degrades before any other internal components of the WP were investigated. This corresponds to configuration IP-1-A/B discussed in Sections 6.2.2 and 6.3 (shown in Figure 6-3). This configuration assumes a rapid degradation of the FSVR fuel elements inside the DOE SNF canister while the rest of the WP internals remain intact.

7.4.1.1 Partial Degradation of Fuel Compacts Before the Graphite Block

In this scenario the graphite blocks are intact, but some portion of the fuel compacts have degraded. This degradation is due to either some amount of the fissile material in the fuel having dissolved into solution and only reentering the fuel elements, or some portion of the fuel compact has fallen out of the graphite block and settles at the bottom of the canister. In the first case,

where the fissile material has dissolved, only the uranium is considered to dissolve and is redistributed in the coolant channels and voids of the fuel elements. This is conservative since otherwise the uranium would redistribute in all the water throughout the entire DOE SNF canister and not just inside the fuel elements. Variations are considered where the water level in the DOE SNF canister is such that only a portion of the fuel elements is submerged and the dissolved fissile material only fills the portion of the fuel elements below the water level. This configuration is shown in Figure 7-2 where the water level is at half of the fuel elements' height and dissolved fissile material fills the coolant channels and voids below the water level. Although physically not possible, in several cases water was conservatively considered to fill the coolant channels and voids above the water level. Water fills the remainder of the DOE SNF canister and fuel elements for all cases except those where the DOE SNF canister is only partially filled with water. The results of the MCNP cases are presented in Table 7-4.

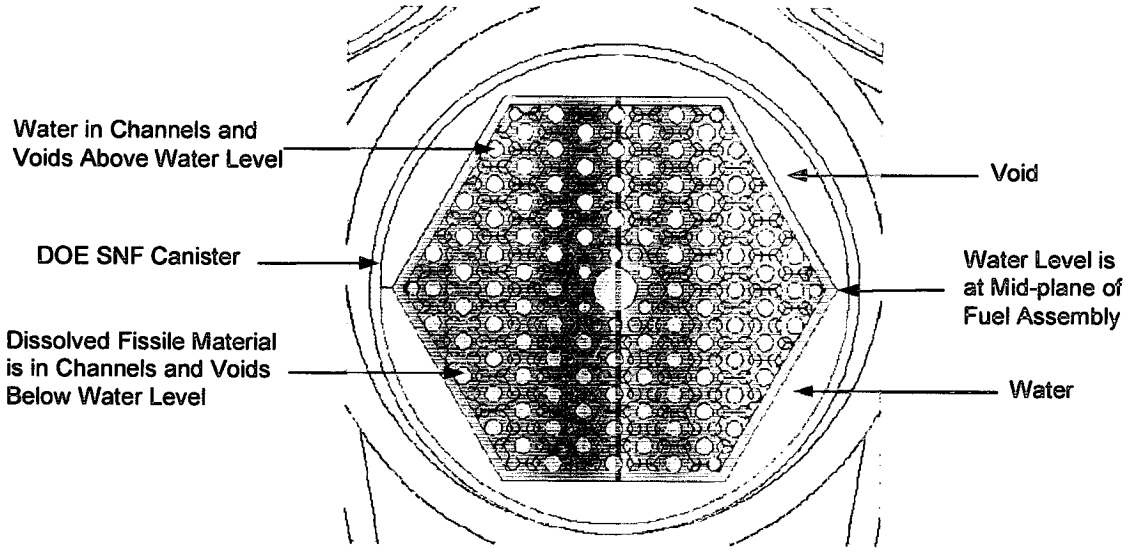

Figure 7-2. Configuration with Fissile Material in Solution in the Lower Half of the Coolant Channels and Voids of the Fuel Element

Table 7-4. Results of Cases with Dissolved Fuel Redistributed in Coolant Channels and Voids of Fuel Element

Case Description	$k_{eff} + 2\sigma$	% of U Dissolved
Cases Where the DOE SNF Canister is Completely Filled with Water		
No fuel removed from fuel elements	0.9264	2
Fuel uniformly removed from fuel elements	0.9195	2
No fuel removed from fuel elements	0.9284	3
Similar to the case above, but mirror reflective boundary conditions	0.9299	3
Fuel uniformly removed from fuel elements	0.9223	3
No fuel removed from fuel elements	0.9345	4
Fuel uniformly removed from fuel elements	0.9208	4
No fuel removed from fuel elements	0.9398	5
Fuel uniformly removed from fuel elements	0.9256	5
Similar to the case above, but mirror reflective boundary conditions	0.9226	5
No fuel removed from fuel elements	0.9587	10
Fuel uniformly removed from fuel elements	0.9291	10

Table 7-4. Results of Cases with Dissolved Fuel Redistributed in Coolant Channels and Voids of Fuel Element (Continued)

Case Description	$k_{eff} + 2\sigma$	% of U Dissolved
Cases Where the DOE SNF Canister is Partially Filled with Water		
No fuel removed from fuel elements; water level at 3/4 of fuel elements' height[a]	0.9494	10
No fuel removed from fuel elements; water level at 3/4 of fuel elements' height	0.9339	10
No fuel removed from fuel elements; water level at 1/2 of fuel elements' height[a]	0.9431	10
No fuel removed from fuel elements; water level at 1/2 of fuel elements' height	0.9015	10

NOTE: [a]Water fills coolant/void channels above water level in canister.

In Table 7-4 values of $k_{eff}+2\sigma$ are given for configurations where some fraction of the fuel, as indicated in the table, has dissolved and has been redistributed in the coolant channels and voids of the fuel elements. Only the uranium content of the fuel is assumed to dissolve, leaving the fuel compacts unchanged in every other way. Since the dissolved fuel can originate from anywhere in the fuel elements, e.g., the ends of the fuel elements or uniformly from the entire length of the fuel channels, two types of cases were investigated. In one type, the fuel is assumed to be uniformly removed from the entire length of the fuel elements, whereas in the other type, the fuel is added to the fuel elements channels but no fuel is removed from the fuel compacts, i.e., the total fuel in the canister is greater than that from the five fuel elements. This is done since the five fuel elements in the DOE SNF canister are essentially infinitely long (see Table 7-1) and reducing the amount of fuel at an end of the stack would have no effect on the reactivity of the system. In other words, removing fuel from an end of the fuel element stack and redistributing it in all the fuel elements increases the fuel linear loading in the other fuel elements. If this same linear loading were achieved by adding additional fuel to the intact fuel elements, then the results would be statistically identical. For the cases where the canister is completely filled with water, the dissolved fuel is distributed in the coolant channels and voids. In the remaining cases the DOE SNF canister is only partially filled with water. For these cases the water level is adjusted to fill the DOE SNF canister up to the half-height (see Figure 7-1) and ¾-height of the fuel elements. Here the dissolved fuel fills those channels and voids below the water level while the channels and voids above the water level are either treated as void or filled with water as indicated in the table. Completely filling the channels above the water level with water is clearly unphysical but conservative as seen in the table. Also, it should be noted that $k_{eff}+2\sigma$ decreases as the water level decreases in the canister.

For the most conservative configuration, i.e., no fuel is removed from the intact fuel elements, the results in Table 7-4 indicate that the interim critical limit of 0.93 is exceeded only if 4% or more additional uranium is added to the channels and voids. In cases where fuel is uniformly removed from the fuel elements, at least 10% of the uranium must be redistributed into the channels in order to exceed the interim critical limit. Both these amounts of dissolved uranium are significantly greater than approximately 0.3% - the upper bound of the failure rate for all fuel particles (see Section 2.1.4.3). It should be noted that failure of fuel particles that expose the kernel to water is the only known mechanism resulting in fissile material being dissolved in the surrounding water.

For the cases shown in Table 7-5, a portion of the fuel, as indicated in the table, degrades, is removed from an end element in the fuel element stack, and is re-deposited at the bottom of the

canister along its entire length. The carbonaceous matrix binder is neglected for this re-deposited fuel since it is assumed to wash away. This situation is represented in Figures 7-3 and 7-4, where depending on the orientation of the fuel elements, a space is formed either directly under the fuel elements from the chord formed by the fuel elements resting on the inside canister walls (see Figure 7-4), or to the sides of a point of the fuel elements (see Figure 7-3). This space can fill with fuel and water. For cases 1 through 7 in the table, the amount of water in the degraded fuel is the same as that of the intact fuel elements. Additional water was added to the fuel to give different volume fractions of water for the remaining cases in the table.

Table 7-5. Results of Cases with Degraded Fuel from an End Fuel Element that Re-deposits at Bottom of DOE SNF Canister

Case #	Case Description	$k_{eff} + 2\sigma$	% of Fuel Removed from Fuel Elements	% Additional Water in Degraded Fuel
1	Base case	0.9263	10	0
2	Fraction of fuel removed increased to 15%	0.9270	15	0
3	Previous case, but reflective bc	0.9296	15	0
4	Chord below fuel elements just filled	0.9323	19.7	0
5	Fraction of fuel removed increased to 20%	0.9324	20	0
6	Fraction of fuel removed increased to 25%	0.9342	25	0
7	Fuel elements partially submerged	0.9357	25	0
8	Variation of base case	0.9240	10	10
9	Variation of base case	0.9257	10	20
10	Variation of base case	0.9271	10	30
11	Variation of base case	0.9276	10	40
12	Similar to case above, but mirror reflective WP boundary conditions	0.9296	10	40
13	Variation of second case	0.9299	15	10
14	Variation of second case	0.9290	15	20
15	Variation of second case	0.9311	15	24
16	Similar to case above, but fuel elements rotated 30° and partially submerged (see Figure 7-4)	0.9320	15	24

Results in Table 7-5 indicate that $k_{eff}+2\sigma$ is greater than 0.93 in cases where more than 10% of fuel is removed from fuel elements in the configuration investigated. There are two known mechanisms through which the fuel could be removed from the fuel elements: the failure of fuel particles that expose the kernel to water, and the fuel particles separating from the compacts. As mentioned before, the first mechanism, which results in fissile material being dissolved in the surrounding water, is limited to approximately 0.3% failed fuel particles - significantly less than the 10% minimum needed to obtain $k_{eff}+2\sigma$ greater than 0.93. The second mechanism could result in fuel particles accumulating at the bottom of the DOE SNF canister only if the graphite blocks break into a large number of pieces, which is not possible through known degradation processes.

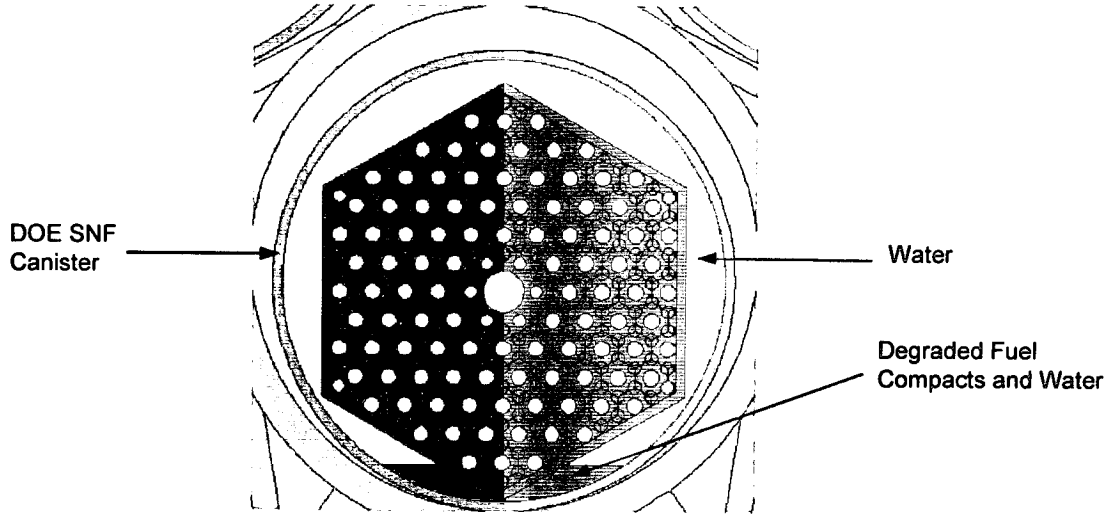

Figure 7-3. Configuration with a Portion of the Fuel at the Bottom of the DOE SNF Canister

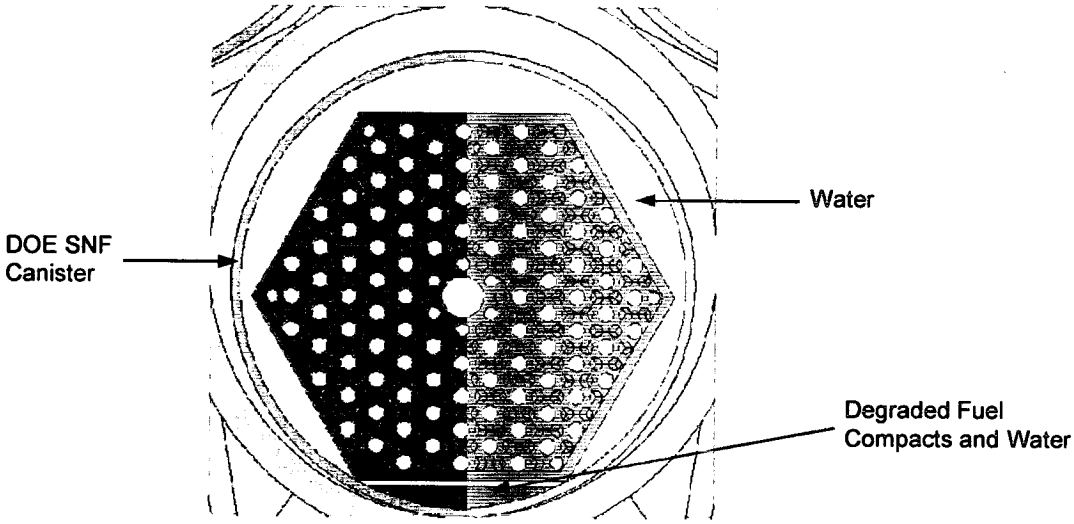

Figure 7-4. Configuration Similar to that Shown in Figure 7-3 but the Fuel Elements are Rotated 30°

As a simple variation of the cases presented in Table 7-4, some portion of the fuel degrades, is removed uniformly from the entire length of the fuel elements and re-deposits at the bottom of the DOE SNF canister. The fuel remaining in the fuel channels were treated in one of two ways. The first would be to homogenize the remaining fuel with water to completely fill the fuel channels, while the second would be to fill the annulus between the remaining fuel and graphite block with water. Results for these and other cases with different volume fractions of additional water in the degraded fuel are presented in BSC (2001e, Table 17). These results show that as the amount of fuel removed from the fuel elements (and redistributed at the bottom of the canister) increases, k_{eff} decreases. Cases with goethite added to the degraded fuel and water mixture at the bottom of the DOE SNF canister show that the addition of goethite has a statistically negligible effect on the results. All the variations covered (up to 50% fuel removed from assemblies and up to 40% water mixed with degraded fuel) result in $k_{eff}+2\sigma$ less than 0.91.

A group of cases also investigated the effect of tilting the DOE SNF canister. The fuel was removed from some portion of a fuel element and re-deposited either in the volume between the end of the fuel element stack and the canister or in the volume between the second and third element of the stack. The re-deposited fuel was composed of degraded fuel compacts homogenized with water. The volume left in the fuel holes by removing fuel was filled either by water or by axially homogenizing the remaining fuel with water over the entire length of the fuel hole. The volume fraction of water in the displaced fuel was also varied. Any unfilled spaces in the canister were filled by water. The results, presented in BSC (2001e, Table 18) show that $k_{eff}+2\sigma$ was below 0.93 for all physically possible cases.

7.4.1.2 Degraded Graphite Block with Intact Fuel Compacts

Cases were treated for various degrees of degradation ranging from the graphite block broken into a few pieces to a completely rubblized block. For the cases where the block has broken into pieces the separation between pieces was varied. An example of a fuel element that has broken into 6 pieces is shown in Figure 7-5.

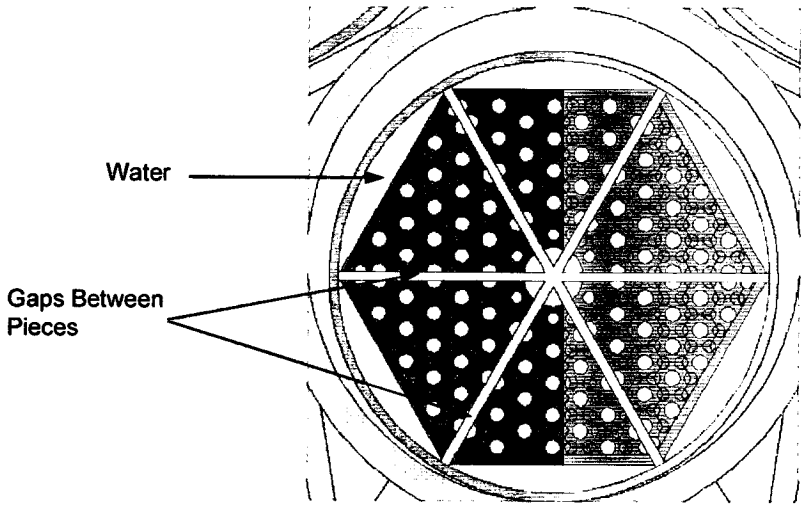

Figure 7-5. Configuration with the Fuel Elements Broken into Six Pieces

The results for this configuration are presented in BSC (2001e, Table 19). The $k_{eff}+2\sigma$ was below 0.93 for all variations covered (two, four, six or more pieces, moved outward in the radial direction up to 1 cm).

For the cases where the block was treated as rubble, the fuel compacts are represented axially aligned and radially separated so as to form fictitious "fuel rods," which are surrounded by the graphite from the fuel elements mixed with water. In these cases the radial separation (pitch) between "fuel rods" is varied from touching to just greater than that for the intact fuel elements. Figure 7-6 shows a configuration of these "fuel rods" in the DOE SNF canister. In this configuration the "fuel rods" have settled into the canister with a pitch of 2.0 cm and uniformly fill the DOE SNF canister to an approximately leveled arrangement across the canister. This configuration is considered to be more probable than that shown in Figure 7-7, where the "fuel rods" form a pile heaped at the center of the DOE SNF canister. The average pitch between "fuel rods" for the configuration shown in Figure 7-7 is the kept the same as for the

configuration in Figure 7-6. The configuration in Figure 7-7 is shown to be the more reactive of the two in BSC (2001e, Section 6.2.1.2). The effect of varying the volume fraction of water in the rubble was also investigated, as well as the axial separation between the fuel compacts in the "fuel rods." For this scenario any unoccupied space in the canister was filled with water. The results for these cases are presented in BSC (2001e, Table 20). Examination of the results shows that k_{eff} increases for increasing pitch and volume fraction of water in the carbon rubble, but decreases slightly for increasing axial separation between fuel compacts. Also, the most reactive cases for a given pitch, volume fraction of water in the rubble, and axial separation occurs for configurations that are more tightly compacted and less spread out in the canister (see Figure 7-7). However, the compacted configurations are less probable since any disturbance of the WP would tend to spread out the rods and also decrease the pitch. For all cases analyzed, the calculated $k_{eff}+2\sigma$ was below 0.93.

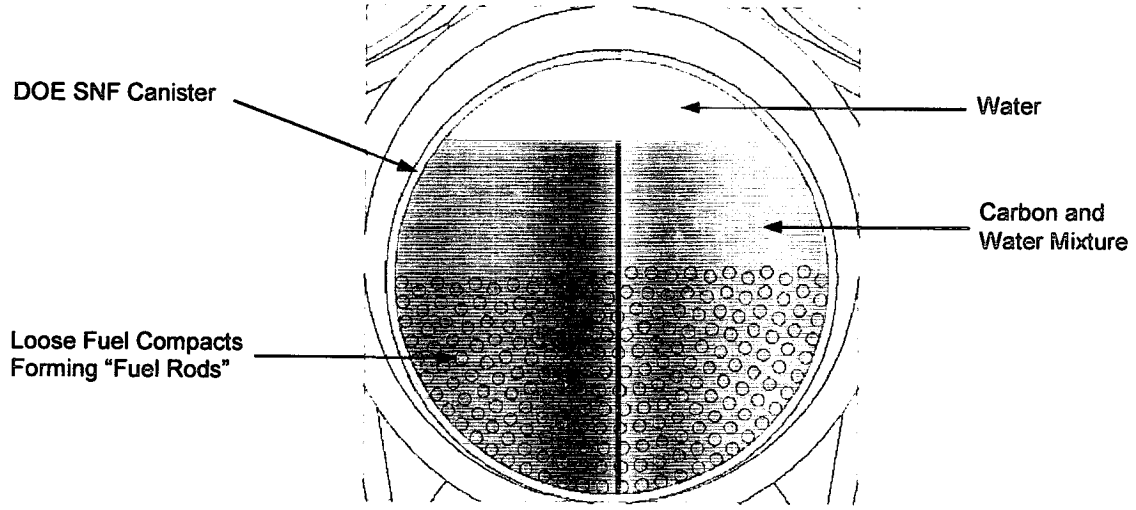

Figure 7-6. Configuration with Graphite Block Broken into Rubble and Fuel Compacts Axially Aligned Forming "Fuel Rods" (level arrangement)

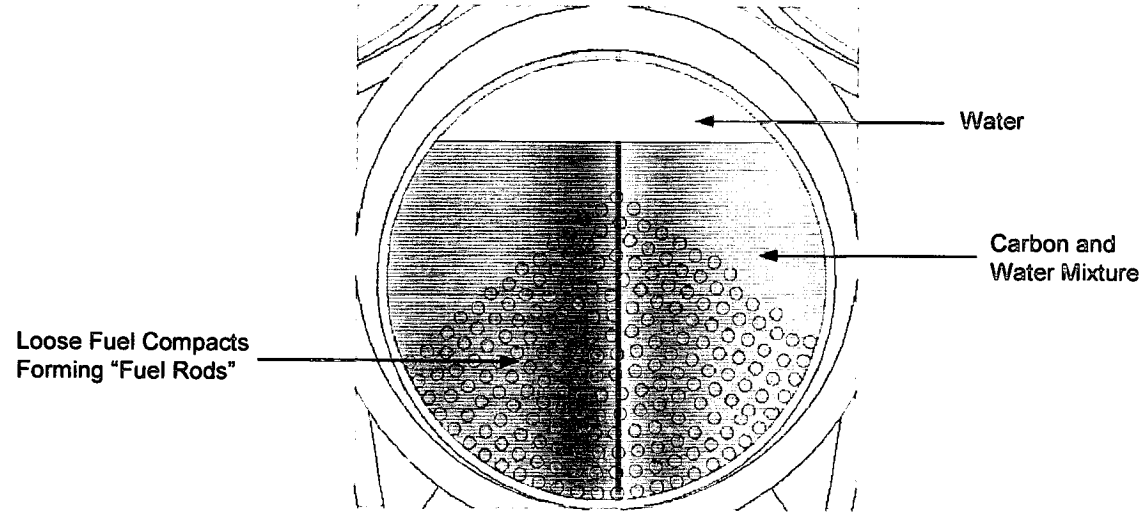

Figure 7-7. Configuration with Graphite Block Broken into Rubble and Fuel Compacts Axially Aligned Forming "Fuel Rods" (mound arrangement)

7.4.1.3 Degraded Graphite Block and Degraded Fuel Compacts

For this scenario both the graphite block and the fuel compacts have degraded to rubble. These degraded materials would in general mix together, but cases are presented where these are treated as layers of separate materials to investigate the effect of their segregation on $k_{eff}+2\sigma$. Such a case is shown in Figure 7-8 where the remnants of the fuel compacts mixed with carbon from the graphite block and water are below a layer of carbon and water. A set of cases where the carbon from the graphite block is neglected and another set where the fuel and varying amounts of carbon are mixed together were also investigated. When mixed together the materials are treated as homogeneous. The volume fraction of water in these materials was varied from zero up to the point where the volume of the DOE SNF canister is completely filled with material. Any unoccupied space in the canister was filled with water. These cases and the $k_{eff}+2\sigma$ results are presented in BSC (2001e, Tables 21 and 22).

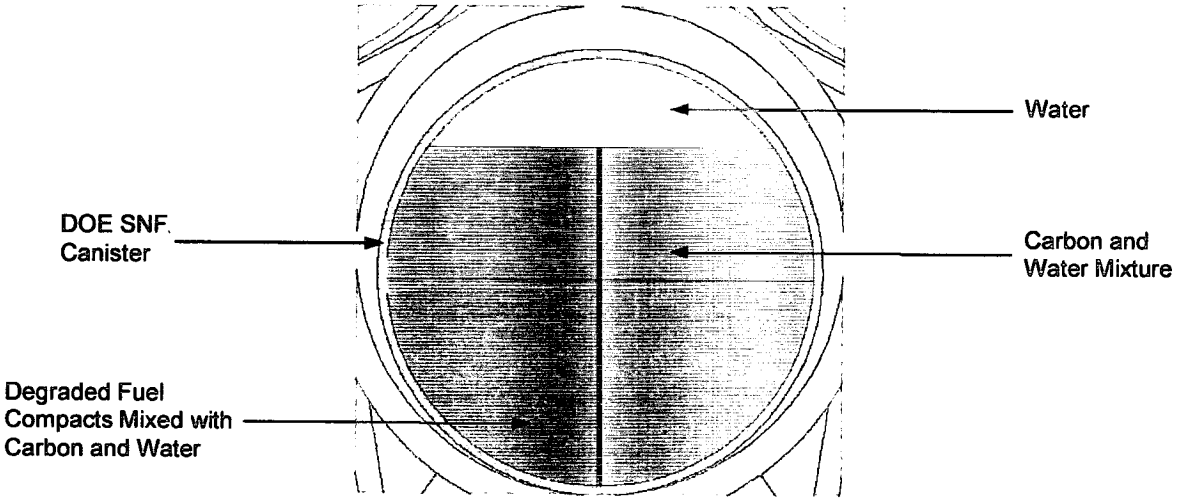

Figure 7-8. Configuration with Degraded Contents of DOE SNF Canister Forming Separate Layers

The highest $k_{eff}+2\sigma$ value obtained was 0.96. The values above 0.93 were obtained for cases with fuel content between 30 and 60 volume % (vol%) in the bottom layer, and at least 60 vol% carbon in the layer above (for both layers, the difference up to 100% is water).

A set of cases was also investigated where some portion of the carbon from the degraded graphite blocks was mixed with the fuel layer. The remaining carbon is represented in a layer above the fuel mixture. These cases consider varying amounts of carbon and use a water volume percent that gives the same hydrogen to fissile atom (H/X) ratio as some of most reactive cases in the previous paragraphs of this section (BSC 2001e, Table 21). The results for these cases, which also include four cases with all the degraded carbon and fuel mixed together, and varying amounts of water are presented in BSC (2001e, Table 22). The cases in this set are more likely, since it is more probable that all the degradation products would mix together rather than separate in layers. The highest $k_{eff}+2\sigma$ value obtained for this set of cases was 0.952.

It should be noted that all fuel elements are loaded into the DOE SNF canister and the canister is then loaded into the WP. The fuel elements are then assumed to be emplaced into the monitored geologic repository in an intact condition, i.e., without any significant cracks and chips in the

graphite blocks. At and after emplacement, there is no degradation mechanism to break the graphite blocks into a large number of pieces.

7.4.2 Other Internal Components of the WP Degraded

This section describes configurations resulting from scenario IP-3. The OICs of the WP (outside the DOE SNF canister) are represented as completely degraded. The compositions of the slurry resulting from this degradation are given in BSC (2001d, Table 6-12) and is referred to as the pre-breach clay. The amount of water mixed in this clay varies. There is U-238 present in the slurry from the degraded glass, but was conservatively neglected (U-238 is a neutron absorber) in these cases. The cases in this section are divided into two categories depending upon whether the DOE SNF canister is treated as being intact or degraded. In the first category (Section 7.4.2.1), the DOE SNF canister is intact and its contents can be either intact or degraded. In the second category (Section 7.4.2.2), the DOE SNF canister is degraded, but the canister and its contents have not chemically reacted with the pre-breach clay.

7.4.2.1 Intact DOE SNF Canister

The DOE SNF canister configurations investigated include intact and degraded cases and are derived from the most reactive cases identified in the previous sections. For these cases the intact canister containing the intact or degraded fuel was surrounded by pre-breach clay. The location of the DOE SNF canister in the clay was varied from just under the surface of pre-breach clay to the bottom of WP. Figure 7-9 shows a configuration where the DOE SNF canister containing an intact fuel element is centered in the clay formed from the degraded contents of the WP.

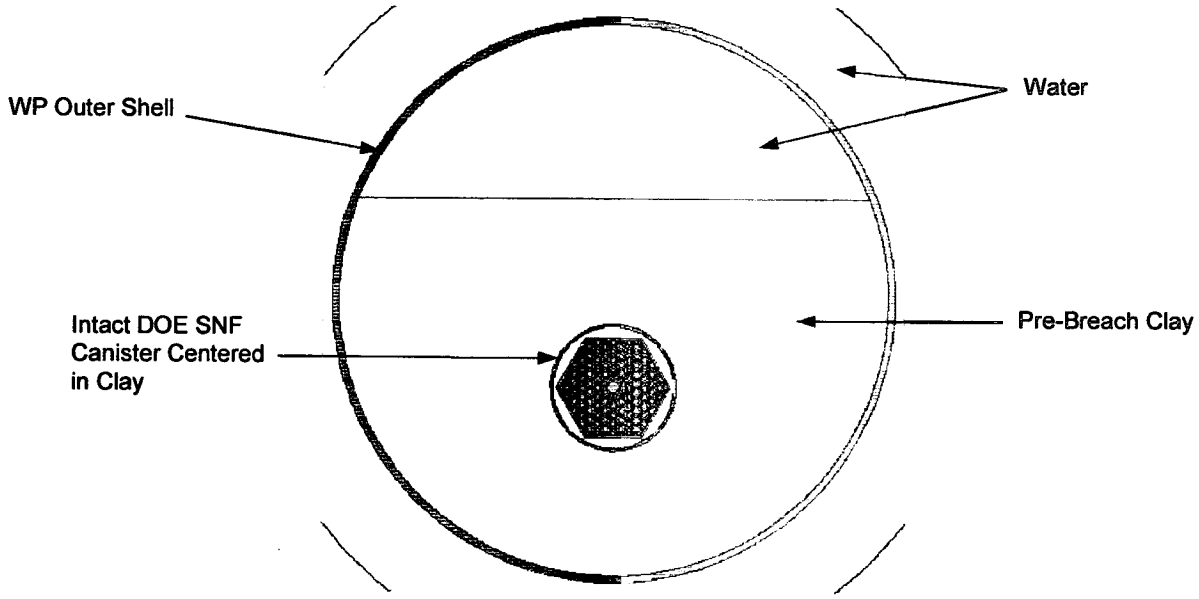

Figure 7-9. Cross-sectional View of an Intact SNF Canister Centered in Clay Formed from the Degradation of the Contents of the WP

The results of the MCNP cases are given in BSC (2001e, Table 23). For all cases with intact fuel elements the $k_{eff}+2\sigma$ values were below 0.93. The set of cases that have partially or completely

degraded fuel components (based on the most reactive configurations inside the DOE SNF canister that were taken from Section 7.4.1 - those with degraded graphite block) had several $k_{eff}+2\sigma$ values above 0.93. However, as mentioned also in Section 7.4.1.3, at and after emplacement of FSVR SNF in the monitored geologic repository, there is no degradation mechanism to break the graphite blocks in a large number of pieces, therefore the configurations with $k_{eff}+2\sigma$ values above 0.93 are not physically attainable.

7.4.2.2 Degraded DOE SNF Canister with Non-reacted Pre-breach Clay

For these configurations the DOE SNF canister has degraded to goethite, but the fuel elements may be intact, partially, or fully degraded. The fuel components and the goethite formed from the canister walls have not chemically reacted with each other or the pre-breach clay. The configurations in this section are similar to those in Sections 7.3 and 7.4.1, but now pre-breach clay and goethite either mixed together or forming separate layers can surround or be mixed with the fuel component from the fuel elements. These configurations were positioned in the WP with any unoccupied space in the WP being filled with water.

7.4.2.2.1 Intact Fuel Elements with Degraded DOE SNF Canister and OICs

In these configurations the fuel elements are intact and surrounded by pre-breach clay and goethite either mixed together or in separate layers. When mixed together, the composition of the mixture was varied to determine how reactive the configuration is. Also, the water volume fraction of the materials in the various layers was varied. For most cases the coolant channels and voids of the fuel elements were filled with water, but for some of the more reactive cases a mixture of clay and water was used to fill the coolant channels and voids of the fuel elements. This type of configuration is partially shown in Figure 7-10 (goethite at the bottom of the WP is not seen). The depth of the fuel elements in the clay layer was also varied.

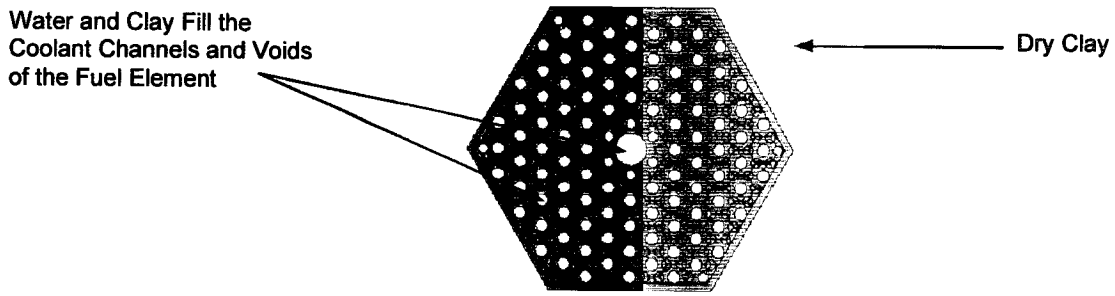

Figure 7-10. Intact Fuel Element Surrounded by Clay in the WP

A possibly more realistic configuration is partially shown in Figure 7-11 where goethite surrounds the intact fuel elements, which in turn are surrounded by clay. This configuration could occur if the canister degrades to goethite after it is trapped in the clay formed from the degraded contents of the WP. Variations of this case were investigated by changing the volume

fraction of water in the goethite surrounding the fuel elements, varying the volume fraction of goethite in the coolant channels and voids, and by assuming the goethite forms a hexagonal shaped layer around the fuel elements. The results for these cases are given in BSC (2001e, Table 24). The values of $k_{eff}+2\sigma$ were below 0.93 for all cases.

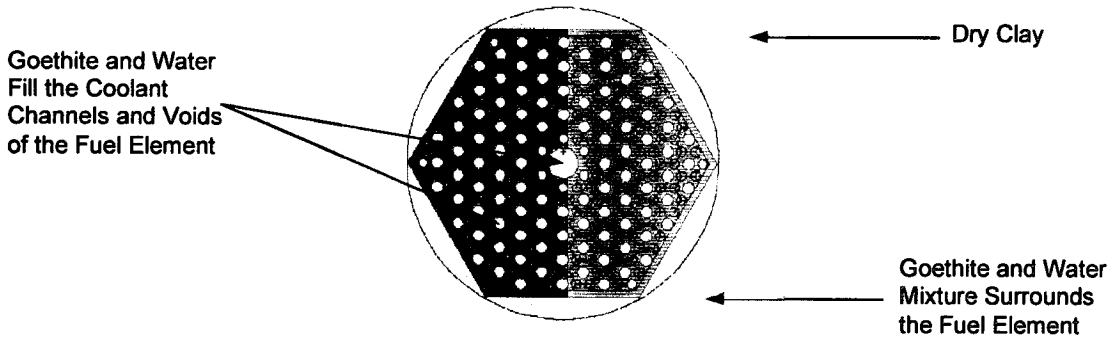

Figure 7-11. Intact Fuel Element Surrounded by Goethite Trapped in Pre-breach Clay in the WP

7.4.2.2.2 Intact Fuel Compacts with Degraded Graphite Block, DOE SNF Canister and OICs of WP

These cases are similar to those presented in Section 7.4.2.2.1, but the graphite block has been degraded to rubble and the fuel compacts are assumed to remain axially aligned and form "fuel rods" in the WP. The "fuel rods" can now be surrounded by goethite and clay in addition to the carbon from the degraded graphite block. Variations of these materials and the water volume fraction for the layers surrounding the fuel were investigated. The pitch of the "fuel rods" was also varied. An example of this type of configuration is shown in Figure 7-12. Here the loose "rods" are heaped at the bottom of the WP and are surrounded by a mixture of goethite, carbon, water, and clay. These cases and the results of the MCNP cases are presented in BSC (2001e, Table 25). The maximum value of $k_{eff}+2\sigma$ was 0.841 for this set of cases.

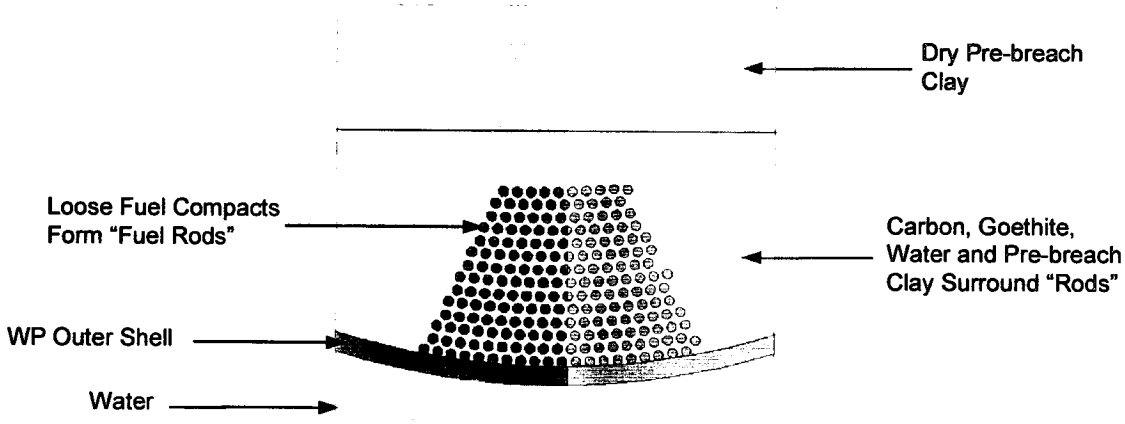

Figure 7-12. Loose "Fuel Rods" at the bottom of the WP Surrounded by a Mixture of Goethite, Carbon, Water, and Pre-breach Clay

Configurations similar to those in Section 7.4.2.2.1 where the rods surrounded by goethite and carbon have been trapped in the clay layer were also investigated. Such a configuration is shown in Figure 7-13 where the pins form an array with a circular cross-section (henceforth referred to as a "circular" array). Here, a mixture of goethite, carbon, and water surrounds the pins that are positioned in the pre-breach clay layer. Different compositions, volume fractions of water and pitches were investigated. Also, cases were considered where the "fuel pins" are assumed to be in the same position as in the intact fuel elements and are surrounded by goethite, and the volume fraction of water in the surrounding carbon is varied. All of these cases and the results of the MCNP runs are presented in BSC (2001e, Table 27). Several of the $k_{eff}+2\sigma$ values are between 0.93 and 0.96. However, the breach of the graphite block in a large number of pieces is non-physical, therefore the configurations described in this set of cases are not attainable.

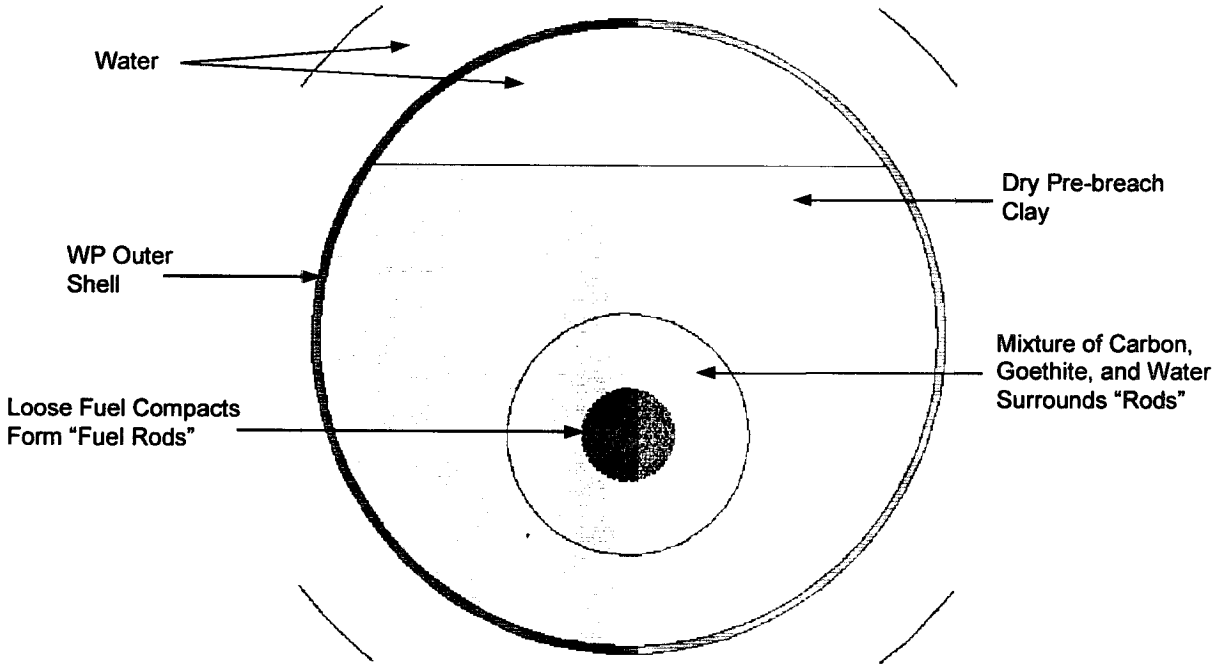

Figure 7-13. Cylinder of Loose "Fuel Rods" Surrounded by Goethite, Carbon, and Water Trapped in the Pre-breach Clay in the WP

7.4.2.2.3 Degraded Fuel Compacts, Graphite Block, DOE SNF Canister and OIC

These configurations are similar to those in Section 7.4.2.2.2, but now the fuel can be mixed with goethite and clay in addition to carbon and water in the WP. Different cases with single and mixed materials in the layers were investigated. The volume fraction of water was also varied for these different compositions. The materials in each layer were always represented as homogeneously mixed. Figure 7-14 shows an improbable example of these materials forming different layers in the WP. Degraded fuel compacts mixed with water and carbon from the graphite block form the bottom layer, which is covered by layers of carbon, goethite, pre-breach clay, and a layer of water filling the remaining space at the top of the WP. These cases and the results of MCNP cases are presented in BSC (2001e, Table 28). All the values of $k_{eff}+2\sigma$ were below 0.76.

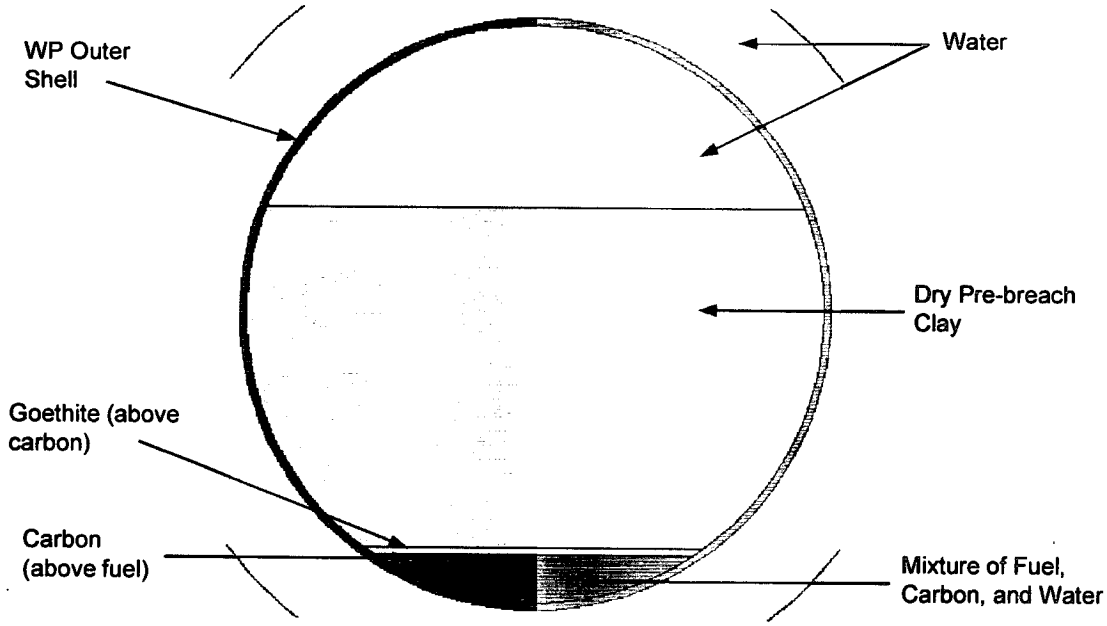

Figure 7-14. Layers of Completely Degraded Fuel Compacts, Goethite, Carbon, and Pre-breach Clay in the WP

7.4.3 All Components Degrade Concurrently

These configurations represent the final stage of degradation for the two previous scenarios, discussed in Sections 7.4.1 and 7.4.2 (where the waste form degrades before/after the OIC of the WP) and correspond to IP-1-C, IP-2-A, IP-3-C, IP-4-B, IP-5-A, and IP-6-A configurations as defined in Section 6.2.2. The composition of the clay resulting from the degradation of all components inside the WP is given in BSC (2001d, Table 6-14). This clay is referred to as post-breach clay. The amount of water in the clay was varied to determine the most reactive compositions. These cases and the results of the MCNP cases are presented in BSC (2001e, Tables 28 and 29). All the values of $k_{eff}+2\sigma$ were below 0.93, except one case where $k_{eff}+2\sigma$ was 0.938. However, this case, like all the others in this set is based on the breaking of the graphite block into a large number of pieces. This configuration cannot be attained by any known degradation mechanism.

7.5 SUMMARY

The results of the 3-D Monte Carlo criticality calculations for all anticipated intact- and degraded-mode configurations developed through the degradation analysis, and which are physically possible, show that the requirement of $k_{eff}+2\sigma$ values less than or equal to the interim critical limit of 0.93 is satisfied for the FSVR SNF codisposal WP. No neutron absorber material is required as long as the U-235 mass for codisposal is within the specified limit as described in Section 2 of this report.

The highest k_{eff} values resulted from the configurations assuming that approximately 10% of the fuel contained in the compacts inside the FSVR fuel elements is degraded and leaves the compacts, while the DOE SNF canister is still intact. However, these configurations are not possible because the carbonaceous matrix of the fuel compacts is similar to graphite, therefore

chemically inert. Additionally, there is no known degradation mechanism that can remove 10% or more of the fuel particles from the compacts. The highest $k_{eff}+2\sigma$ values also resulted from the configurations that assume either the breaking of the graphite block into a large number of pieces or complete degradation. Neither configuration is attainable through any known degradation mechanism. All possible degraded configurations (intact and degraded) are bounded by the intact configuration with water inside the DOE SNF canister but no water outside the DOE SNF canister (WP is still reflected with 30 cm of water). In this case the $k_{eff}+2\sigma$ is just below 0.92.

Table 7-6 summarizes the criticality calculation input parameters and results for the intact configurations.

Table 7-6. Summary for the Intact Configurations

Parameter		Range	$(k_{eff}+2\sigma)_{max}$	Comments
Neutron reflection		Water or mirror reflection at the outer boundaries of the WP	0.92	$(k_{eff}+2\sigma)_{max}$ <0.93
Moderation	DOE SNF canister	Fuel elements' channels, voids and porosities are up to 100% filled with water		
		Both types of graphite (H-327 and H-451) were used		
	WP	Dry, partially, or completely water filled WP		
Geometry		FSVR fuel element stack centered in the DOE SNF canister, rotated 30°, and reduced to 4, 3, 2, or 1 elements		
Composition		5% of initial content of Th neglected		
		No Pu in fuel composition		

Table 7-7 summarizes the criticality calculation input parameters and results for degraded component configurations. The connectivity among the master scenario list and set of configuration classes relating to internal criticality (discussed in Sections 6.2 and 6.3), the geochemistry analysis results, and the criticality calculations results are also outlined in the table.

Table 7-7. Summary for Degraded Configurations

Master Scenarios	Description		Configuration Classes (see Sections 6.2 and 6.3)	Geochemistry Results	Criticality Results		Comments
					Reference	$(k_{eff}+2\sigma)_{max}$	
IP-1	Liquid accumulates in WP	FSVR fuel degrades before OICs	IP-1-A/B: FSVR fuel partially or fully degraded; DOE SNF canister intact (Figure 6-3)	For most conditions and variations of parameters the geochemistry results indicated that the WP retention ranges were 99.4% to 0% for U and 100% to 70.2% for Th. In all cases the U loss was more severe than Th loss.	Section 7.4.1 Figures 7-2 through 7-8 Tables 7-4 and 7-5	0.960	All cases where $k_{eff}+2\sigma$ > 0.93 were based on 10% or more of the fuel degraded. Post-irradiation data indicate that approximately 0.3% of the fuel particles degraded. There is no mechanism that can increase this number significantly after emplacement (SiC has a very low degradation rate). Therefore, for all possible cases $(k_{eff}+2\sigma)_{max}$ < 0.93.
			IP-1-C: All WP components degraded		Sections 7.4.2.2.2, 7.4.2.2.3 and 7.4.3 Figures 7-12 through 7-14	0.959	All cases where $k_{eff}+2\sigma$ > 0.93 were based on partial or complete degradation of the graphite block. However, there is no mechanism that can cause this. Therefore, for all possible cases $(k_{eff}+2\sigma)_{max}$ < 0.93.
IP-2		FSVR fuel degrades concurrently with OICs	IP-2-A: All WP components degraded (see Figure 6-4)				
IP-3		FSVR fuel degrades after OICs	IP-3-C: All WP components degraded				
			IP-3-A: FSVR fuel and DOE SNF canister intact; WP basket degraded		Section 7.4.2.1 Figure 7-9	0.952	
			IP-3-B: FSVR fuel elements intact; WP basket, DHLW glass and DOE SNF canister degraded (see Figure 6-5)		Section 7.4.2.2.1 Figures 7-10 and 7-11	0.921	$(k_{eff}+2\sigma)_{max}$ < 0.93
IP-4	WP bottom is penetrated allowing liquid to flow through	FSVR fuel degrades before OICs	These classes were not discussed in Sections 6.2 and 6.4 (see the explanation in the second cell at right)	The geochemistry calculation does not address this group of scenarios (see explanation in the next cell at right).	All cases are bounded by IP-1, IP-2 and IP-3 as the latter have better moderation (water is pooling inside WP), and more favorable conditions for neutron absorber loss (mainly Th).		-
IP-5		FSVR fuel degrades concurrently with OICs					
IP-6		FSVR fuel degrades after OICs					

8. CONCLUSIONS

This document may be affected by technical product input information that requires confirmation. Any changes to the document that may occur as a result of completing the confirmation activities will be reflected in subsequent revisions. The status of the technical product information quality may be confirmed by review of the DIRS database.

8.1 STRUCTURAL ANALYSIS

Table 3-1 states the applicable design criteria for the structural performance of the 5-DHLW/DOE SNF-long WP. The results of the 3-D finite element analysis calculations for the 5-DHLW/DOE SNF-long WP tip over design basis event at room temperature (20°C), 204°C, and 316°C are presented in Section 3.3. The results meet all the design criteria for each temperature condition considered for the steel components.

It is concluded that the performance of the 5-DHLW/DOE SNF-long WP internal design is structurally acceptable when exposed to a tip over event and, therefore, meets SDD Criterion 1.2.2.1.6 (Section 2.2.1.4) as long as the DOE SNF canister loaded mass limit (2,721 kg) and the DHLW glass canisters mass limit (4,200 kg) are not exceeded. However, the FSVR fuel elements will probably be broken as a result of a tip over design basis event, since the maximum stress intensity during such an event in the FSVR fuel elements is higher than the maximum allowed stress intensity for graphite.

8.2 THERMAL ANALYSIS

The results of the thermal analysis using a 2-D finite element representation presented in Section 4, indicate that the maximum DHLW glass temperature for the 5-DHLW/DOE SNF-long WP containing FSVR SNF is 167.4 °C (reached 59 years after emplacement), which is less than the SDD criterion of 400 °C (BSC 2001f, Criterion 1.2.1.6). The maximum temperature in the FSVR SNF elements is 173.8 °C, reached at 59 years after emplacement. The maximum thermal output of the 5-DHLW/DOE SNF-long WP loaded with FSVR SNF is 1,037 W, which is less than the SDD criterion of 11,800 W (BSC 2001f, Criterion 1.2.4.2).

8.3 SHIELDING ANALYSIS

The maximum dose rate at the external surfaces of the WP occurs on the radial surface and is calculated to be 101.97 rem/h. Axially, over the length of the DHLW glass canisters, the dose rate at the outer WP radial surface is approximately uniform. The radial dose rate shows a weak angular distribution, with dose rates on segments B differing from those on segments A by less than 15 percent (see Figure 5-3 and Table 5-2). The dose rates on the bottom and top surfaces of the WP are approximately four percent, and one percent of the maximum dose rate on the outer radial surface, respectively. The dose rates in rem/h and rad/h are practically the same due to the insignificant contribution of the neutron dose rate to the total dose rate (less than 0.2%).

The SDD criterion for WP design (BSC 2001f, Criterion 1.2.4.1), cited in Section 2.2.3, specifies a maximum dose rate of 1,450 rem/h at the external surface of the WP. This analysis shows that the maximum dose rate at the external surfaces of the WP is 101.97 rem/h, which is

approximately 14 times lower than the criterion value. This demonstrates that the WP design complies with SDD Criterion 1.2.4.1, and that there is a large margin to the maximum allowable dose rate specified in SDD Criterion 1.2.4.1.

8.4 DEGRADATION AND GEOCHEMISTRY ANALYSIS

Based on the generic degradation scenarios and configuration classes discussed in YMP (2000) and CRWMS M&O (1999d), specific degradation configurations for the FSVR SNF WP have been developed. These degraded configurations include the application of the generic scenario groups of IP-1, IP-2, and IP-3. Variations of the generic groups specific to FSVR SNF were discussed. The most probable degradation path based on the material corrosion rates and thicknesses has also been identified (Section 6.4.2). The maximum angle of tilt for the DOE SNF canister inside the WP has been calculated to be 9°. Tilting of the DOE SNF canister would physically require that the space beneath does allow for movement of the canister. This condition is unrealistic since the DHLW glass and the degradation products from the steel components (WP basket and support tube) would collect at the bottom of the WP and fill the available space. A second factor is that the degradation rate of the stainless steel is higher than that of the DHLW glass and as such the canister shell would most probably be completely degraded at the time when DHLW glass degradation would make the DOE SNF canister tilting a possibility. Tilt of WP is not physically possible due to the emplacement design.

A principal objective of the geochemistry calculations was to estimate the chemical composition of the degradation products remaining in a WP containing FSVR SNF and DHLW glass. Twenty-seven EQ6 reaction path calculations were carried out to span the range of possible system behavior and to assess the specific and coupled effects of SNF degradation, steel corrosion, DHLW glass degradation, and fluid influx rate on U, Pu, and Th mobilization. Corrosion product accumulation and U, Pu, and Th mobilization were examined as well. The results presented in BSC (2001d), have been used as inputs to the criticality calculations described in Section 7 of this document.

In all cases investigated, all Pu released from the fuel was lost from the WP faster than U and Th. Retention of U in the WP ranged from 99.4% to 0%. Retention of Th in the system ranged from 100% to 70.2% and was always higher than for U and Pu.

8.5 INTACT AND DEGRADED COMPONENT CRITICALITY ANALYSES

The criticality analyses considered all aspects of intact and degraded configurations of the codisposal WP containing FSVR SNF, including optimum moderation conditions, optimum reflection, geometry, and composition. The results of the 3-D Monte Carlo criticality calculations for all anticipated intact and degraded configurations developed through the degradation analysis, and physically attainable, show that the requirement of $k_{eff}+2\sigma$ values be less than or equal to the interim critical limit of 0.93 is satisfied. No neutron absorber material is required as long as the U-235 mass for codisposal is within the specified limit as described in Section 2 of this report.

A number of parametric analyses were run to address or bound the configuration classes discussed in Sections 6.2 and 7.4. These parametric analyses identified conditions of optimum

moderation, optimum spacing between fuel compacts, and optimum neutron reflection. The highest $k_{eff}+2\sigma$ values resulted from the configurations assuming that approximately 10% of the fuel contained in the compacts inside the FSVR fuel elements is degraded and leaves the compacts, while the DOE SNF canister is still intact. However, these configurations are not possible due to the fact that the carbonaceous matrix of the fuel compacts is similar to graphite, therefore chemically inert. Additionally, there is no known degradation mechanism that can remove 10% or more of the fuel particles from the compacts. The highest $k_{eff}+2\sigma$ values also resulted from the configurations assuming either the breakage of the graphite block into a large number of pieces or complete degradation, which are not attainable through any known degradation mechanism. All possible degraded configurations (intact and degraded) are bounded by the intact configuration with water inside the DOE SNF canister but no water outside the DOE SNF canister (WP still reflected with 30 cm of water). In this case the $k_{eff}+2\sigma$ is just below 0.92.

8.6 ITEMS IMPORTANT TO CRITICALITY CONTROL AND ACCEPTANCE

As part of the criticality licensing strategy, items that are important to criticality control will be identified during evaluation of the representative fuel types designated by the National Spent Nuclear Fuel Program. As a result of the analyses performed for the evaluation of the codisposal viability of Th/U carbide DOE-owned fuel, several items are identified as important to criticality control. The DOE SNF canister shell is naturally an item that is important to criticality control since it initially confines the fissile elements to a specific geometry and location within the WP. The fissile mass limit in the canister, the linear density of the U-235 in the DOE SNF canister, and the fuel enrichment are also important to criticality control.

All calculations were based on a maximum of 7.425 kg U-235 per DOE SNF canister. This amount is calculated using the maximum number of FSVR fuel elements that can be loaded into the DOE SNF canister, which is five. The degraded configurations of the FSVR SNF bound the other types of Th/U carbide DOE-owned SNF, as long as the limits on mass of uranium and its linear density are not exceeded.

Hence, the total mass of fissile element (U-235) should not exceed the mass used in deriving the conclusions of this report, which is 7.425 kg of U-235 per DOE SNF canister. The maximum U-235 enrichment is 100 wt%. The linear density of the U-235 should not exceed 20.0 g/cm in the DOE SNF canister. This value is calculated by dividing the total mass of fuel (7.425 kg U-235) by the active fuel length of the five FSVR fuel elements stack (369.57 cm).

INTENTIONALLY LEFT BLANK

9. REFERENCES

9.1 DOCUMENTS CITED

Bird, R.B.; Stewart, W.E.; and Lightfoot, E.N. 1960. *Transport Phenomena.* New York, New York: John Wiley & Sons. TIC: 208957.

Briesmeister, J.F., ed. 1997. *MCNP-A General Monte Carlo N-Particle Transport Code.* LA-12625-M, Version 4B. Los Alamos, New Mexico: Los Alamos National Laboratory. ACC: MOL.19980624.0328.

BSC (Bechtel SAIC Company) 2001a. *Tip-Over of the 5 DHLW/DOE SNF - Long Waste Package Containing Fort Saint Vrain HTGR Fuel onto an Unyielding Surface.* CAL-DDC-ME-000006 REV 00. Las Vegas, Nevada: Bechtel SAIC Company. URN-0936

BSC (Bechtel SAIC Company) 2001b. *Thermal Evaluation of the Fort Saint Vrain Codisposal Waste Package.* CAL-WIS-TH-000012 REV 00. Las Vegas, Nevada: Bechtel SAIC Company. ACC: MOL.20010718.0263.

BSC (Bechtel SAIC Company) 2001c. *Dose Rate Calculation for the Codisposal Waste Package of HLW Glass and the FSVR Fuel.* CAL-DDC-NU-000003 REV 00. Las Vegas, Nevada: Bechtel SAIC Company. ACC: MOL.20010924.004.

BSC (Bechtel SAIC Company) 2001d. *EQ6 Calculation for Chemical Degradation of Fort St. Vrain (Th/U Carbide) Waste Packages.* CAL-EDC-MD-000011 REV 00. Las Vegas, Nevada: Bechtel SAIC Company. ACC: MOL.20010831.0300.

BSC (Bechtel SAIC Company) 2001e. *Intact and Degraded Mode Criticality Calculations for the Codisposal of Fort Saint Vrain Spent Nuclear Fuel in a Waste Package.* CAL-EDC-NU-000007 REV 00. Las Vegas, Nevada: Bechtel SAIC Company. URN-0937

BSC (Bechtel SAIC Company) 2001f. *Defense High Level Waste Disposal Container System Description Document.* SDD-DDC-SE-000001 REV 01 ICN 01. Las Vegas, Nevada: Bechtel SAIC Company. URN-0921

BSC (Bechtel SAIC Company) 2001g. *DSNF and Other Waste Form Degradation Abstraction.* ANL-WIS-MD-000004 REV 01 ICN 01. Las Vegas, Nevada: Bechtel SAIC Company. ACC: MOL.20010316.0002.

CRWMS M&O 1995. *Analysis of Degradation Due to Water and Gases in MPC.* BB0000000-01717-0200-00005 REV 01. Las Vegas, Nevada: CRWMS M&O. ACC: MOL.19960419.0202.

CRWMS M&O 1996. *Second Waste Package Probabilistic Criticality Analysis: Generation and Evaluation of Internal Criticality Configurations.* BBA000000-01717-2200-00005 REV 00. Las Vegas, Nevada: CRWMS M&O. ACC: MOL.19960924.0193.

CRWMS M&O 1997a. *Thermal Evaluation of the Codisposal Canister in the 5-Pack DHLW Waste Package.* BBAA00000-01717-0200-00021 REV 01. Las Vegas, Nevada: CRWMS M&O. ACC: MOL.19971210.0413.

CRWMS M&O 1997b. *MCNP Evaluation of Laboratory Critical Experiments: Homogeneous Mixture Criticals.* BBA000000-01717-0200-00045 REV 00. Las Vegas, Nevada: CRWMS M&O. ACC: MOL.19971230.0134.

CRWMS M&O 1998a. *EQ6 Calculations for Chemical Degradation of Fast Flux Test Facility (FFTF) Waste Packages.* BBA000000-01717-0210-00028 REV 00. Las Vegas, Nevada: CRWMS M&O. ACC: MOL.19981229.0081.

CRWMS M&O 1998b. *ANSYS.* V5.4. HP-UX 10.20. 30040 5.4.

CRWMS M&O 1998c. *Software Code: MCNP.* 4B2LV. HP. 30033 V4B2LV.

CRWMS M&O 1998d. *Software Code: EQ3/6.* V7.2b. LLNL: UCRL-MA-110662.

CRWMS M&O 1998e. *Calculation of the Effect of Source Geometry on the 21-PWR WP Dose Rates.* BBAC00000-01717-0210-00004 REV 00. Las Vegas, Nevada: CRWMS M&O. ACC: MOL.19990222.0059.

CRWMS M&O 1999a. *DOE SRS HLW Glass Chemical Composition.* BBA000000-01717-0210-00038 REV 00. Las Vegas, Nevada: CRWMS M&O. ACC: MOL.19990215.0397.

CRWMS M&O 1999b. *EQ6 Calculation for Chemical Degradation of Pu-Ceramic Waste Packages: Effects of Updated Materials Composition and Rates.* CAL-EDC-MD-000003 REV 00. Las Vegas, Nevada: CRWMS M&O. ACC: MOL.19990928.0235.

CRWMS M&O 1999c. *LCE for Research Reactor Benchmark Calculations.* B00000000-01717-0210-00034 REV 00. Las Vegas, Nevada: CRWMS M&O. ACC: MOL.19990329.0394.

CRWMS M&O 1999d. *Generic Degradation Scenario and Configuration Analysis for DOE Codisposal Waste Package.* BBA000000-01717-0200-00071 REV 00. Las Vegas, Nevada: CRWMS M&O. ACC: MOL.19991118.0180.

CRWMS M&O 1999e. *Software Code: EQ6, Version 7.2bLV.* V7.2bLV. 10075-7.2bLV-00.

CRWMS M&O 1999f. *Laboratory Critical Experiment Reactivity Calculations.* B00000000-01717-0210-00018 REV 01. Las Vegas, Nevada: CRWMS M&O. ACC: MOL.19990526.0294.

CRWMS M&O 2000a. *Drift Scale Thermal Analysis.* CAL-WIS-TH-000002 REV 00. Las Vegas, Nevada: CRWMS M&O. ACC: MOL.20000420.0401.

CRWMS M&O 2000b. *Design Analysis for the Defense High-Level Waste Disposal Container.* ANL-DDC-ME-000001 REV 00. Las Vegas, Nevada: CRWMS M&O. ACC: MOL.20000627.0254.

CRWMS M&O 2000c. *Source Terms for HLW Glass Canisters.* CAL-MGR-NU-000002 REV 01. Las Vegas, Nevada: CRWMS M&O. ACC: MOL.20000823.0004.

CRWMS M&O 2000d. *Invert Configuration and Drip Shield Interface.* TDR-EDS-ST-000001 REV 00. Las Vegas, Nevada: CRWMS M&O. ACC: MOL.20000505.0232.

CRWMS M&O 2000e. Not used.

CRWMS M&O 2000f. *Waste Form Degradation Process Model Report.* TDR-WIS-MD-000001 REV 00 ICN 01. Las Vegas, Nevada: CRWMS M&O. ACC: MOL.20000713.0362.

CRWMS M&O 2000g. *Waste Package Operations Fabrication Process Report.* TDR-EBS-ND-000003 REV 01. Las Vegas, Nevada: CRWMS M&O. ACC: MOL.20000927.0002.

CRWMS M&O 2000h. *Total System Performance Assessment for the Site Recommendation.* TDR-WIS-PA-000001 REV 00 ICN 01. Las Vegas, Nevada: CRWMS M&O. ACC: MOL.20001220.0045.

CRWMS M&O 2000i. *Technical Work Plan for: Department of Energy Spent Nuclear Fuel Work Packages.* TWP-MGR-MD-000010 REV 00. Las Vegas, Nevada: CRWMS M&O. ACC: MOL.20001107.0305.

CRWMS M&O 2000j. *Software Code: LS-DYNA.* V950. HP 9000. 10300-950-00.

CRWMS M&O 2000k. *Software Code: ANSYS.* V5.6.2. HP-UX 10.20. 10364-5.6.2-00.

CRWMS M&O 2001a. *EQ6 Calculations for Chemical Degradation of N Reactor (U-metal) Spent Nuclear Fuel Waste Packages.* CAL-EDC-MD-000010 REV 00. Las Vegas, Nevada: CRWMS M&O. ACC: MOL.20010227.0017.

CRWMS M&O 2001b. *Defense High Level Waste Glass Degradation.* ANL-EBS-MD-000016 REV 00 ICN 01. Las Vegas, Nevada: CRWMS M&O. ACC: MOL.20010130.0004.

Curry, P.M. 2001. *Monitored Geologic Repository Project Description Document.* TDR-MGR-SE-000004 REV 02 ICN 02. Las Vegas, Nevada: Bechtel SAIC Company. ACC: MOL.20010628.0224.

DOE (U.S. Department of Energy) 1992. *Characteristics of Potential Repository Wastes.* DOE/RW-0184-R1. Volume 1. Washington, D.C.: U.S. Department of Energy, Office of Civilian Radioactive Waste Management. ACC: HQO.19920827.0001.

DOE (U.S. Department of Energy) 1998a. *Total System Performance Assessment.* Volume 3 of *Viability Assessment of a Repository at Yucca Mountain.* DOE/RW-0508. Washington, D.C.: U.S. Department of Energy, Office of Civilian Radioactive Waste Management. ACC: MOL.19981007.0030.

DOE (U.S. Department of Energy) 1998b. *Design Specification.* Volume 1 of *Preliminary Design Specification for Department of Energy Standardized Spent Nuclear Fuel Canisters.* DOE/SNF/REP-011, Rev. 1. Washington, D.C.: U.S. Department of Energy, Office of Spent Fuel Management and Special Projects. TIC: 241528.

DOE (U.S. Department of Energy) 1999a. *Waste Acceptance System Requirements Document.* DOE/RW-0351, Rev. 03. Washington, D.C.: U.S. Department of Energy, Office of Civilian Radioactive Waste Management. ACC: HQO.19990226.0001.

DOE (U.S. Department of Energy) 1999b. "Design Specification." Volume 1 of *Preliminary Design Specification for Department of Energy Standardized Spent Nuclear Fuel Canisters.* DOE/SNF/REP-011, Rev. 3. Washington, D.C.: U.S. Department of Energy, Office of Spent Fuel Management and Special Projects. TIC: 246602.

DOE (U.S. Department of Energy) 2000a. *Quality Assurance Requirements and Description.* DOE/RW-0333P, Rev. 10. Washington, D.C.: U.S. Department of Energy, Office of Civilian Radioactive Waste Management. ACC: MOL.20000427.0422.

DOE (U.S. Department of Energy) 2000b. *DOE Spent Nuclear Fuel Grouping in Support of Criticality, DBE, TSPA-LA.* DOE/SNF/REP-0046 Rev. 0. Idaho Falls, Idaho: U.S. Department of Energy, Idaho Operations Office. TIC: 248046.

Harrar, J.E.; Carley, J.F.; Isherwood, W.F.; and Raber, E. 1990. *Report of the Committee to Review the Use of J-13 Well Water in Nevada Nuclear Waste Storage Investigations.* UCID-21867. Livermore, California: Lawrence Livermore National Laboratory. ACC: NNA.19910131.0274.

Nuclear Energy Agency 1998. *International Handbook of Evaluated Criticality Safety Benchmark Experiments.* NEA/NSC/DOC(95)03. Paris, France: Nuclear Energy Agency. TIC: 243013.

Opila, E.J. 1999. "Variation of the Oxidation Rate of Silicon Carbide with Water-Vapor Pressure." *Journal of the American Ceramic Society, 82,* (3), 625-636. [Westerville, Ohio]: American Ceramic Society. TIC: 250063.

ORNL (Oak Ridge National Laboratory) 1997. *SCALE: A Modular Code System for Performing Standardized Computer Analyses for Licensing Evaluation.* NUREG/CR-0200, Rev. 5. Washington, D.C.: U.S. Nuclear Regulatory Commission. TIC: 235920.

Picha, K.G., Jr. 1997. "Response to Repository Environmental Impact Statement Data Call for High-Level Waste." Memorandum from K.G. Picha, Jr. (DOE) to W. Dixon (YMSCO), September 5, 1997, with attachments. ACC: MOL.19970917.0273.

Plodinec, M.J. and Marra, S.L. 1994. *Projected Radionuclide Inventories and Radiogenic Properties of the DWPF Product (U).* WSRC-IM-91-116-3, Rev. 0. Aiken, South Carolina: Westinghouse Savannah River Company. TIC: 242337.

Propp, W.A. 1998. *Graphite Oxidation Thermodynamics/Reactions.* DOE/SNF/REP-018, Rev. 0. Idaho Falls, Idaho: U. S. Department of Energy. TIC: 247663.

Shigley, J. E. and Mischke, C.R. 1989. *Mechanical Engineering Design.* Fifth Edition. New York, New York: McGraw-Hill. TIC: 246990.

Stout, R.B. and Leider, H.R., eds. 1991. *Preliminary Waste Form Characteristics Report.* Version 1.0. Livermore, California: Lawrence Livermore National Laboratory. ACC: MOL.19940726.0118.

Stroupe, E.P. 2000. "Approach to Implementing the Site Recommendation Design Baseline." Interoffice correspondence from E.P. Stroupe (CRWMS M&O) to D.R. Wilkins, January 26, 2000, LV.RSO.EPS.1/00-004, with attachment. ACC: MOL.20000214.0480.

Taylor, L.L. 2001. *Fort Saint Vrain HTGR (Th/U Carbide) Fuel Characteristics for Disposal Criticality Analysis.* DOE/SNF/REP-060, Rev. 0. [Washington, D.C.]: U.S. Department of Energy, Office of Environmental Management. TIC: 249783.

Taylor, W.J. 1997. "Incorporating Hanford 15 Foot (4.5 Meter) Canister into Civilian Radioactive Waste Management System (CRWMS) Baseline." Memorandum from W.J. Taylor (DOE) to J. Williams (Office of Waste Acceptance Storage and Transportation), April 2, 1997. ACC: HQP.19970609.0014.

Weast, R.C., ed. 1977. *CRC Handbook of Chemistry and Physics.* 58th Edition. Cleveland, Ohio: CRC Press. TIC: 242376.

Weast, R.C. and Astle, M.J., eds. 1979. *CRC Handbook of Chemistry and Physics.* 60th Edition. 2nd Printing 1980. Boca Raton, Florida: CRC Press. TIC: 245312.

Wolery, T.J. and Daveler, S.A. 1992. *EQ6, A Computer Program for Reaction Path Modeling of Aqueous Geochemical Systems: Theoretical Manual, User's Guide, and Related Documentation (Version 7.0).* UCRL-MA-110662 PT IV. Livermore, California: Lawrence Livermore National Laboratory. TIC: 205002.

Yang, I.C.; Rattray, G.W.; and Yu, P. 1996. *Interpretation of Chemical and Isotopic Data from Boreholes in the Unsaturated Zone at Yucca Mountain, Nevada.* Water-Resources Investigations Report 96-4058. Denver, Colorado: U.S. Geological Survey. ACC: MOL.19980528.0216.

YMP (Yucca Mountain Site Characterization Project) 2000. *Disposal Criticality Analysis Methodology Topical Report.* YMP/TR-004Q, Rev. 01. Las Vegas, Nevada: Yucca Mountain Site Characterization Office. ACC: MOL.20001214.0001.

9.2 CODES, STANDARDS, REGULATIONS, AND PROCEDURES

ANSI/ANS-6.1.1-1977. *Neutron and Gamma-Ray Flux-to-Dose-Rate Factors.* La Grange Park, Illinois: American Nuclear Society. TIC: 239401.

AP-3.11Q, Rev. 2. *Technical Reports.* Washington, D.C.: U.S. Department of Energy, Office of Civilian Radioactive Waste Management. ACC: MOL.20010405.0010.

AP-3.15Q, Rev. 3. *Managing Technical Product Inputs.* Washington, D.C.: U.S. Department of Energy, Office of Civilian Radioactive Waste Management. ACC: MOL.20010801.0318.

ASME (American Society of Mechanical Engineers) 1995. *1995 ASME Boiler and Pressure Vessel Code.* New York, New York: American Society of Mechanical Engineers. TIC: 245287.

ASTM A 20/A20M-99a. 1999. *Standard Specification for General Requirements for Steel Plates for Pressure Vessels.* West Conshohocken, Pennsylvania: American Society for Testing and Materials. TIC: 247403.

ASTM A 240/A 240M-99b. 2000. *Standard Specification for Heat-Resisting Chromium and Chromium-Nickel Stainless Steel Plate, Sheet, and Strip for Pressure Vessels.* West Conshohocken, Pennsylvania: American Society for Testing and Materials. TIC: 248529.

ASTM A 276-00. 2000. *Standard Specification for Stainless Steel Bars and Shapes.* West Conshohocken, Pennsylvania: American Society for Testing and Materials. TIC: 248098.

ASTM A 516/A 516M-90. 1991. *Standard Specification for Pressure Vessel Plates, Carbon Steel, for Moderate- and Lower-Temperature Service.* Philadelphia, Pennsylvania: American Society for Testing and Materials. TIC: 240032.

ASTM B 575-97. 1998. *Standard Specification for Low-Carbon Nickel-Molybdenum-Chromium, Low-Carbon Nickel-Chromium-Molybdenum, Low-Carbon Nickel-Chromium-Molybdenum-Copper and Low-Carbon Nickel-Chromium-Molybdenum-Tungsten Alloy Plate, Sheet, and Strip.* West Conshohocken, Pennsylvania: American Society for Testing and Materials. TIC: 241816.

ASTM G 1-90 (Reapproved 1999). 1990. *Standard Practice for Preparing, Cleaning, and Evaluating Corrosion Test Specimens.* West Conshohocken, Pennsylvania: American Society for Testing and Materials. TIC: 238771.

9.3 SOURCE DATA, LISTED BY DATA TRACKING NUMBER

MO0006J13WTRCM.000. Recommended Mean Values of Major Constituents in J-13 Well Water. Submittal date: 06/07/2000.

MO0009THRMODYN.001. Input Transmittal for Thermodynamic Data Input Files for Geochemical Calculations. Submittal date: 09/20/2000.

APPENDIX A

5-DHLW/DOE SNF - LONG WASTE PACKAGE

INTENTIONALLY LEFT BLANK

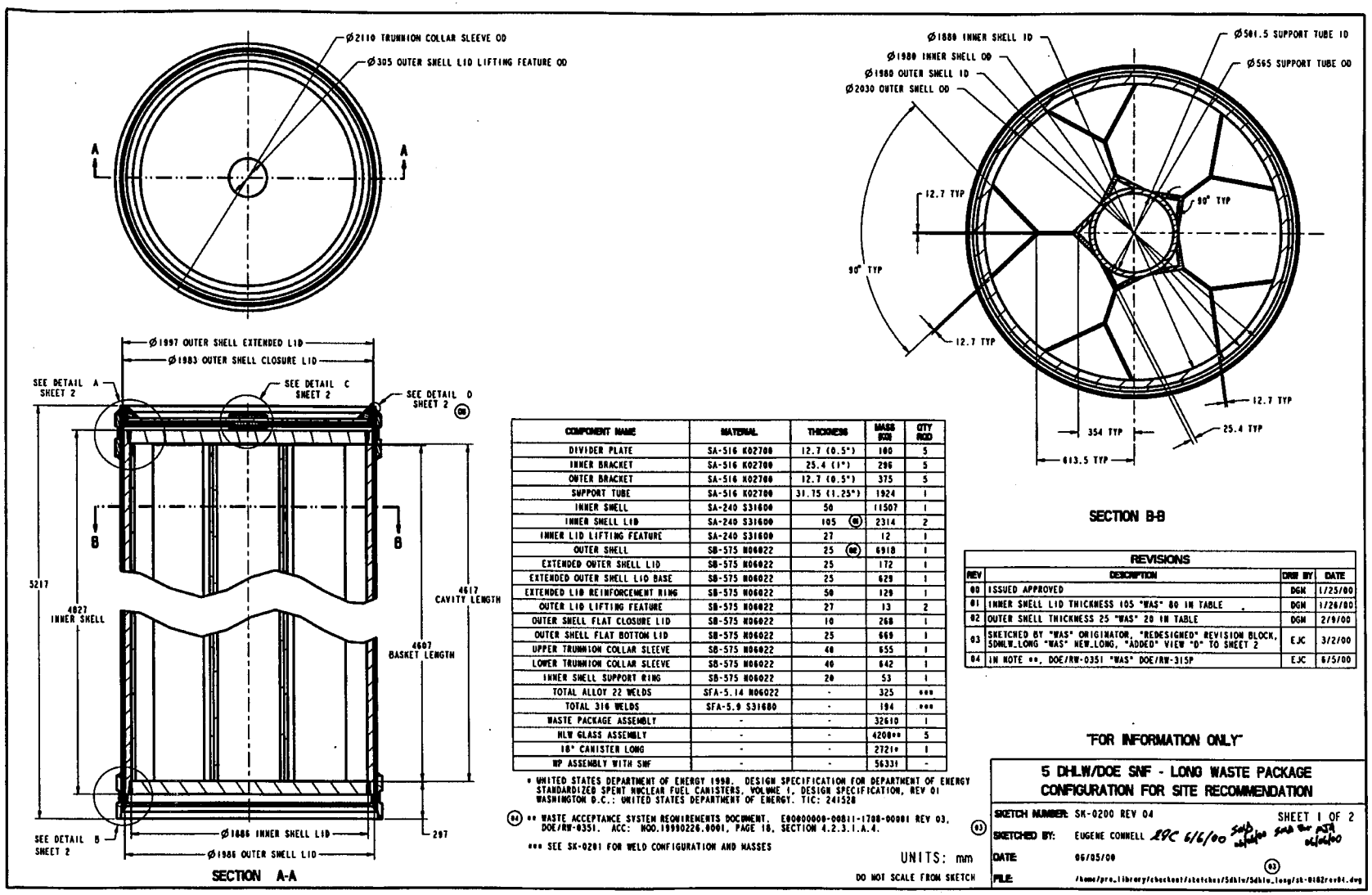

COMPONENT NAME	MATERIAL	THICKNESS	MASS (KG)	QTY /POD
DIVIDER PLATE	SA-516 K02700	12.7 (0.5")	100	5
INNER BRACKET	SA-516 K02700	25.4 (1")	296	5
OUTER BRACKET	SA-516 K02700	12.7 (0.5")	375	5
SUPPORT TUBE	SA-516 K02700	31.75 (1.25")	1924	1
INNER SHELL	SA-240 S31600	50	11507	1
INNER SHELL LID	SA-240 S31600	105 (03)	2314	2
INNER LID LIFTING FEATURE	SA-240 S31600	27	12	1
OUTER SHELL	SB-575 N06022	25 (02)	6918	1
EXTENDED OUTER SHELL LID	SB-575 N06022	25	172	1
EXTENDED OUTER SHELL LID BASE	SB-575 N06022	25	629	1
EXTENDED LID REINFORCEMENT RING	SB-575 N06022	50	129	1
OUTER LID LIFTING FEATURE	SB-575 N06022	27	13	2
OUTER SHELL FLAT CLOSURE LID	SB-575 N06022	10	268	1
OUTER SHELL FLAT BOTTOM LID	SB-575 N06022	25	669	1
UPPER TRUNNION COLLAR SLEEVE	SB-575 N06022	40	655	1
LOWER TRUNNION COLLAR SLEEVE	SB-575 N06022	40	642	1
INNER SHELL SUPPORT RING	SB-575 N06022	20	53	1
TOTAL ALLOY 22 WELDS	SFA-5.14 N06022	-	325	***
TOTAL 316 WELDS	SFA-5.9 S31680	-	194	***
WASTE PACKAGE ASSEMBLY	-	-	32610	1
HLW GLASS ASSEMBLY	-	-	4200**	5
18" CANISTER LONG	-	-	2721*	1
WP ASSEMBLY WITH SNF	-	-	56331	-

* UNITED STATES DEPARTMENT OF ENERGY 1998. DESIGN SPECIFICATION FOR DEPARTMENT OF ENERGY STANDARDIZED SPENT NUCLEAR FUEL CANISTERS, VOLUME I, DESIGN SPECIFICATION, REV 01 WASHINGTON D.C.: UNITED STATES DEPARTMENT OF ENERGY. TIC: 241528

(04) ** WASTE ACCEPTANCE SYSTEM REQUIREMENTS DOCUMENT. E00000000-00811-1708-00001 REV 03, DOE/RW-0351. ACC: MOO.19990226.0001, PAGE 18, SECTION 4.2.3.1.A.4.

*** SEE SK-0201 FOR WELD CONFIGURATION AND MASSES

UNITS: mm

DO NOT SCALE FROM SKETCH

REVISIONS			
REV	DESCRIPTION	DRW BY	DATE
00	ISSUED APPROVED	DGN	1/25/00
01	INNER SHELL LID THICKNESS 105 "WAS" 80 IN TABLE	DGN	1/26/00
02	OUTER SHELL THICKNESS 25 "WAS" 20 IN TABLE	DGN	2/9/00
03	SKETCHED BY "WAS" ORIGINATOR, "REDESIGNED" REVISION BLOCK, SDHLW_LONG "WAS" NEW_LONG, "ADDED" VIEW "D" TO SHEET 2	EJC	3/2/00
04	IN NOTE **, DOE/RW-0351 "WAS" DOE/RW-315P	EJC	6/5/00

"FOR INFORMATION ONLY"

5 DHLW/DOE SNF - LONG WASTE PACKAGE CONFIGURATION FOR SITE RECOMMENDATION

SKETCH NUMBER:	SK-0200 REV 04	SHEET 1 OF 2
SKETCHED BY:	EUGENE CONNELL EJC 6/6/00 SQA validation SQA for PSA 6/6/00	
DATE	06/05/00	
FILE	/home/pro_library/checkout/sketches/5dhlw/5dhlw_long/sk-0182rev04.dwg	

(03)

Figure A-1. 5-DHLW/DOE SNF-Long Waste Package (sheet 1)

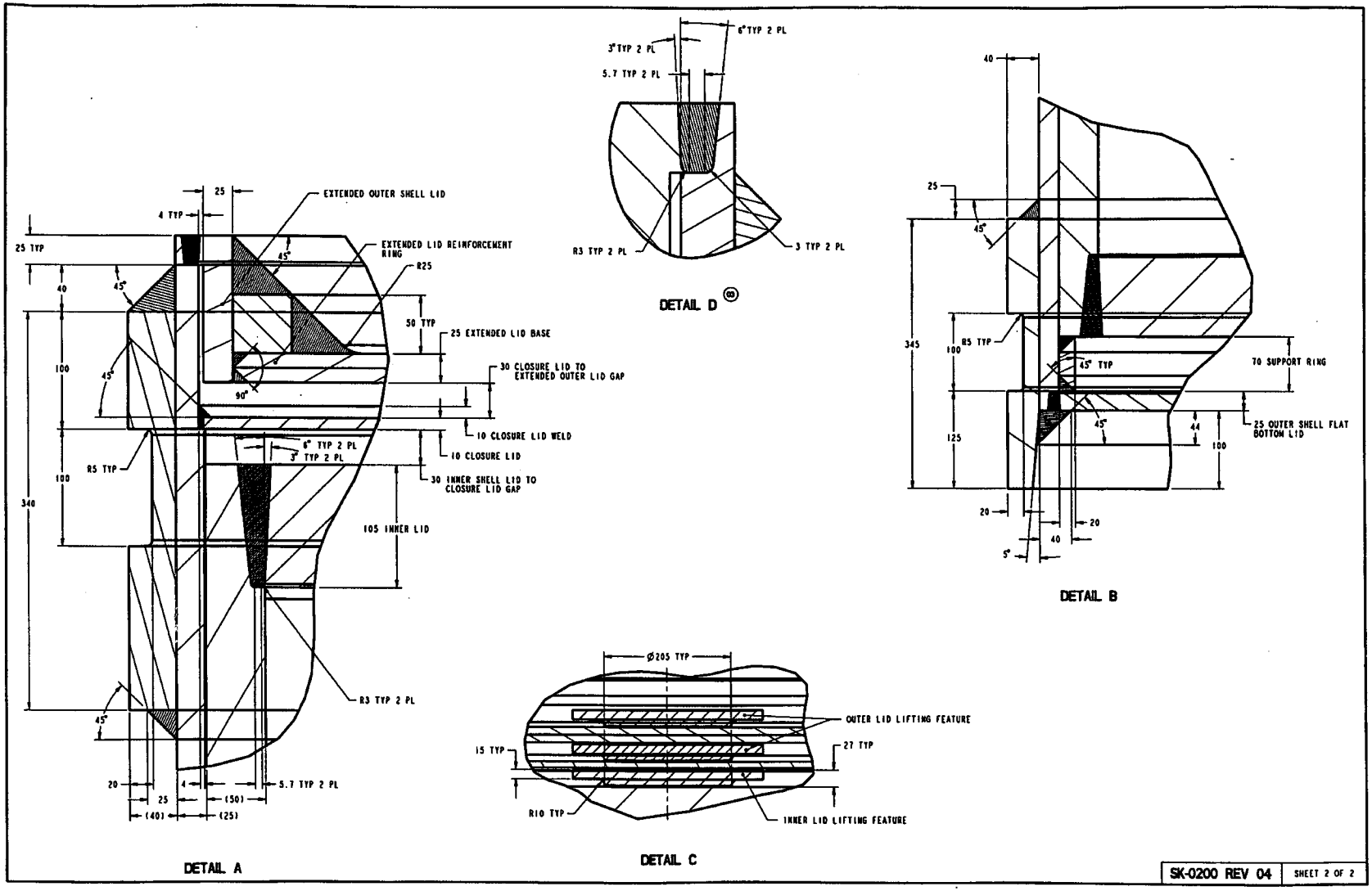

Figure A-2. 5-DHLW/DOE SNF-Long Waste Package (sheet 2)